THE UNIVERSITY OF QUEENSLAND

AUSTRALIA

Exploring mechanisms of host control and parasite growth during experimental blood-stage malaria *in vivo*

Jasmin Akter

Master of Science (M.Sc.)

A thesis submitted for the degree of Doctor of Philosophy at

The University of Queensland in 2018

Faulty of Medicine

Abstract

Malaria is an infectious disease caused by protozoan parasites of the genus *Plasmodium*. It remains a major cause of morbidity and deaths in many developing countries – an estimated 445,000 people died from malaria in 2016. The symptoms of malaria occur during the blood-stage of infection, and can vary from asymptomatic infection to life-threatening syndromes such as cerebral malaria. The disease severity often correlates with the number of blood-stage parasites in the body. It is likely that both host and parasite factors are involved in determining parasite growth kinetics *in vivo*. However, our understanding of these factors is limited. Given that an effective malaria vaccine currently remains elusive, and that resistance has emerged against the currently available anti-malarial drugs, it is important to identify new approaches for controlling the number of parasites in blood *in vivo*.

I have used experimental mouse models of blood-stage *Plasmodium* infection to directly measure parasite maturation, clearance and replication rates *in vivo*. I observed that parasite control can be achieved in a number of ways including: (i) the use of anti-malarial drugs that inhibit or arrest parasite development within a red blood cell, (ii) the use of drugs that prevent parasites from progressing from one generation of red blood cells to another, (iii) by host phagocytes actively removing parasitised red blood cells, and (iv) by host-mediated impairment of parasite maturation within red blood cells.

Next, I identified the mechanisms of antibody-mediated parasite control using *P. yoelii* 17XNL and *P. chabuadi* AS infection models. The experiments that I conducted demonstrated that the *Plasmodium*-specific antibodies in these systems provide robust protection against homologous re-challenge not by accelerating clearance of infected pRBC but by preventing asexually replicated parasites transitioning from one infected red blood cell to the others. This correlated with an inability of *Plasmodium*-specific IgG to bind to the surface of pRBC, despite showing its clear specificity for the parasite proteins. I also observed that the efficacy of antibody-mediated immunity depended on phagocytes, but not on the complement factors C3/C5.

Finally, hundreds of *Plasmodium*-exported proteins, known collectively as the "exportome", remodel host RBC, and yet the precise functions of many of these as well their ability to promote host interactions remain unclear. Using a high-throughput, barcode-based forward genetic screen in immunocompetent and immune-deficient mice, I screened 117 exportome-associated genes to understand their *in vivo* function and possible host-interaction. I demonstrated that 32 of these genes were essential for blood-stage growth, including 8 with no previous functional annotation. Further analysis revealed that 10 genes were required for growth in the presence of an intact immune system, which were not required for growth in immune-deficient mice. This study provides proof-of-principle

that although parasite genes are not essential for blood-stage growth *per se* but they are required in combating the host immune responses.

Declaration by author

This thesis *is composed of my original work, and contains* no materials previously published or written by another person except where due reference had been explicitly made in the text. I have clearly stated the contribution by others in jointly-authored works that are included in my thesis.

I have clearly stated the contribution of others to my thesis as a whole, including the study design, statistical assistance, data analysis, significant technical procedures, professional editorial advice, and any other original research work used or reported in my thesis. The content of my thesis is the result of work I have carried out since the commencement of my research higher degree candidature and does not include a substantial part of work that has been submitted *to qualify for the award of any* other degree or diploma in any university or other tertiary institution. I have clearly stated the parts of my thesis, if any, that have been submitted to qualify for another award.

I acknowledge that an electronic copy of my thesis must be lodged with the University Library and, subject to the policy and procedures of The University of Queensland, the thesis be made available for research and study in accordance with the Copyright Act 1968 unless a period of embargo has been approved by the Dean of the Graduate School.

I acknowledge that copyright of all material contained in my thesis resides with the copyright holder(s) of that material. Where appropriate I have obtained copyright permission from the copyright holder to reproduce material in this thesis.

Publications included in this thesis

No publications included

Submitted manuscripts included in this thesis

No manuscript included

Other publications during candidature

Peer-reviewed papers

- Khoury DS, Cromer D, Elliott T, Soon MSF, Thomas BS, James KR, Best SE, Aogo RA, Engel JA, Gartlan KH, **Akter J,** Sebina I, Haque A***,** Davenport MP*. (* Co-senior). Characterising the effect of antimalarial drugs on the maturation and clearance of murine blood-stage Plasmodium parasites in vivo. Int J Parasitol. 2017 Aug 31. pii: S0020-7519(17)30228-X. doi: 10.1016/j.ijpara.2017.05.009. PMID: 28864033

- Sebina I, Fogg LG, James KR, Soon MSF, **Akter J**, Thomas BS, Hill GR, Engwerda CR, **Haque A.** IL-6 promotes $CD4^+$ T-cell and B-cell activation during Plasmodium infection. Parasite Immunol. 2017 Jul 27. doi: 10.1111/pim.12455. PMID: 28748530

- Khoury, DS, Cromer, D, **Akter, J**, Sebina, I, Elliott, T, Thomas, BS, Soon, MSF, James, KR, Best, SE, **Haque A***, and Davenport, MP*. (*Co-senior). Host-mediated impairment of parasite maturation during blood-stage *Plasmodium* infection. Proc Natl Acad Sci. 2017 July 3. doi: 10.1073/pnas.1618939114.

- Aogo RA, Khoury DS, Cromer D, Elliott T, Akter J, Fogg LG, Nair AS, Liligeto UN, Soon MSF, Thomas BS, Pernold CPS, Romanczuk AS, Laohamonthonkul P, Haque A, Davenport MP. Quantification of host-mediated parasite clearance during blood-stage Plasmodium infection and anti-malarial drug treatment in mice. Int J Parasitol. 2018 Sep 1. pii: S0020-7519(18)30186-3. doi: 10.1016/j.ijpara.2018.05.010.

Conference abstracts

- **Jasmin Akter**, David S Khoury, Rosemary Aogo , Ismail Sebina, Trish Elliott, Bryce S. Thomas, Lily G. Fogg, Deborah Cromer, Megan Soon, Arya SheelaNair, Lianne Lansink, Jessica Engel[1], Kylie R. James, Miles P. Davenport and Ashraful Haque. *In vivo* mechanisms of antibody-mediated parasite control during blood-stage *Plasmodium* infection, 2017, Malaria in Melbourne conference, Melbourne, Australia (poster presentation).

- **Jasmin Akter**, David S Khoury, Rosemary Aogo , Ismail Sebina, Trish Elliott, Bryce S. Thomas, Lily G. Fogg, Deborah Cromer, Megan Soon, Arya SheelaNair, Lianne Lansink, Jessica Engel[1], Kylie R. James, Miles P. Davenport and Ashraful Haque. *In vivo* mechanisms of antibody-mediated parasite control during blood-stage *Plasmodium* infection, 2018, 1st malaria World Congress, Melbourne, Australia (poster presentation).

- **Jasmin Akter**, David S Khoury, Rosemary Aogo , Ismail Sebina, Trish Elliott, Bryce S. Thomas, Lily G. Fogg, Deborah Cromer, Megan Soon, Arya SheelaNair, Lianne Lansink, Jessica Engel[1], Kylie R. James, Miles P. Davenport and Ashraful Haque. *In vivo* mechanisms of antibody-mediated parasite control during blood-stage *Plasmodium* infection, 2018, Brisbane Immunology Group Annual Conference, Gold Coast, Australia (poster presentation).

Contributions made to the thesis by other individuals

Associate Prof. Ashraful Haque: Conceived the concept of the projects, provided inputs in designing the experiments, helped interpreting the results, and edited this thesis.

Prof. Miles Davenport: Conceived the concept of the projects, provided inputs into the experimental designs, and helped in the interpretations of the results presented in the chapters three and four.

Dr. David Khoury: Contributed to the development of the Clearance/Growth assay with mathematical model, and assisted in the analysis and interpretation of data presented in the chapters three and four.

Ms. Rosemary Aogo: Developed the mathematical model fit to analyse PTEX88 data presented in the chapter 5, and contributed to the analysis and interpretation of the results presented in the chapter five.

Dr. Oliver Bilker and his group: Contributed to the designing of *Plasmo*GEM vectors screening experiments, and in the data analysis and their interpretation presented in the chapter five.

Dr. Ellen Bushell: Contributed to the designing of and development of *Plasmo*GEM vectors screening experiments, in performing the experiments, and in data analysis and their interpretation presented in the chapter five.

Ms. Arya Sheela Nair: Assisted with routine experiments included in chapter 5.

Mr. Ismail Sebina: Assisted with ELISA

Statement of parts of the thesis submitted to qualify for the award of another degree

None

Research Involving Human or Animal Subjects

Animal use for this research was approved by the QIMR Berghofer Animal Ethics Committee (Herston, QLD, Australia; approval number:A1503-601M, Project 2085.

Acknowledgements

First, I remain thankful to Allah (S.W.T.), the almighty, for helping me in every step in my life. Next, I would like to thank my beloved spouse, Engr. Mohammad Ali Asgor, for his encouragement and continued support throughout my study periods.

I would like to thank my supervisor Associate Prof. Ashraful Haque for his guidance and support in every aspect of my doctoral studies. I would like to especially thank him for his sustained encouragement and pushing me for working hard and providing every opportunity in developing my competence and skills. I am enormously thankful for his advice and general counsel spanning my entire study period. I would also like to thank my co-supervisor, Professor James McCarthy, for his kind advice, all out support, and encouragement.

I would like to thank all the past and present members of the Malaria Immunology Laboratory, for their direct and indirect help. Many of them, namely Trish, Lily, Arya and Bryce helped me by spending tireless hours in my lab experiments. I would like to thank Prof. Christian Engwerda and members of his laboratory, especially Fiona, Marcela, Fabian and Susana for their help and support.

I would like to acknowledge the financial support of the Australian Government in the form of my Australian Postgraduate Award, and the Higher Degrees Committee of QIMRB for my travel grants. I would like to express my gratitude to my supervisor for providing some additional financial support that enabled bring my children to Australia that enormously reduced my mental stress and brought mental peace. My thanks are due to the QIMRB Core Facilities - my research would not have been possible without your help and support.

I take this opportunity to thanks all my mentors, namely Dr. Mohammed Abdus Salam and Dr. Rashidul Haque, Prof. David Sullivan, Late Dr. Hassan Ashraf, Dr. Dinesh Mondal, Dr. Wasif Ali Khan and Dr. Shafiul Alam for their encouragement, and help and assistance throughout my career.

On a particularly personal note, I would like acknowledge the support and encouragement that I received from my family. Thanks to my beautiful daughter Leuna and lovely son Hemadri for their patience and understanding of my situations. I thanks to all my brothers, Moheuddin, Salauddin, Mezbahuddin and Rokonuddin and their spouses, and sister Lizu and her husband for their love and unconditional support in perusing with my studies. My special thanks to my sister-in-law Rehana and her husband Pintu for caring for my children during the first year of my doctoral studies. I would like to thank my all relative and friends for their love, encouragement and support.

Finally, I would like to thank my parents, Al-haj Abdul Latif and Mrs. Sufia Begum, for their love and affection, and highest level of support in every regards, especially to my mom who came over to Brisbane to provide support during the final days of my thesis works. I would like to express my heartfelt respect to my father and mother-in-law; Al-haj Abdul Kader Miah and late Golapi Begum for encouraging me for further studies, and their love and support.

Financial support

This work was supported by the Australian Research Council (Grants DP120100064 & DP180103875) and the National Health and Medical Research Council (NH&MRC) (Grants 1082022, 1028634 and 1028641). The University of Queensland (UQ) provided an International Postgraduate Research scholarship to Jasmin Akter.

Keywords

Malaria, *Plasmodium* parasite, anti-malarial drugs, ACT, antibody, host-parasite, parasite proteins, *Plasmo*GEM vectors, barcode based sequencing, PTEX88.

Australian and New Zealand Standard Research Classifications (ANZSRC)

ANZSRC code: 110707 Innate Immunity, 40%

ANZSRC code: 110803 Medical Parasitology, 20%

ANZSRC code: 110309, Infectious diseases, 40%

Fields of Research (FoR) Classification

FoR code: 1107, Immunology, 50%

FoR code: 1103, Clinical Sciences, 50%

Table of contents

Table of Figures

Abbreviations

Ab	Antibody
ACT	Artemisinin Combination Therapy
ADCI	Antibody-Dependent Cellular Inhibition
AMA1	Apical Merozoite Antigen1
A-T	Adenosin-Thamine
bp	Base pair
BSA	Bovine Serum Albumin
C1	Complement component 1
CD	Cluster of Differentiation
Clod-Lip	Clodronate-liposoms
CO_2	Carbon dioxide
CSP	Circumsporite Protein
CVF	Cobra Venom Factor
DBL	Duffy Binding-like
DMSO	Dimethyl Sulfoxide
DNA	Deoxyribonucleic Acid
ECM	Experimental Cerebral Malaria
EDTA	Ethylenediaminetetraacetic Acid
FACS	Fluorescence-Activated Cell Sorting
EBL	Erythrocyte Membrane Lignad
EMPA1	Erythrocyte Membrane Associated Protein1
Gen_0	Generation 0
Gen_1	Generation 1
GFP	Green Fluorescent Protein
GIA	Growth Inhibition Assays
Hz	Haemozoin
Ig	Immunoglobulin
IFN-I	Type I Interferon
IFNγ	Interferon Gamma
iKD	induced Knock-down
IL	Interleukin
i.p.	intraperitoneal
i.v.	intravenous

KO	Knock-out
L	Litre
MAC	Membrane Attack Complexes
mAb	Monoclonal Antibody
µg	Microgram
mg	Milligram
µL	Microlitre
mL	Millilitre
MIF	Macrophage migration inhibitory factor
MO	Monocyte
MSP	Merozoite Surface Protein
n	Number
NaCl	Sodium Chloride
ng	Nanogram
NK	Natural Killer
*Pb*A	*Plasmodium berghei* ANKA
PbG	*Plasmodium berghei GFP*
PBMC	Peripheral Blood Mononuclear Cell
*Pc*AS	*Plasmodium chabaudi chabaudi* AS
PCR	Polymerase Chain Reaction
Pf	*Plasmodium falciparum*
Pv	*Plasmodium vivax*
Pm	*Plasmodium malariae*
Po	*Plasmodium ovale*
PFA	Paraformaldehyde
PfEMP1	*Plasmodium falciparum* Erythrocyte Membrane Protein 1
PfRh5	*Plasmodium falciparum* Reticulocyte binding protein 5 homologue
PfSPZ	*Plasmodium falciparum* Sporozoite
p.i.	Post-Infection
PMR	Parasite Maturation Rate
pRBC	Parasitised Red Blood Cell
PRR	Pattern Recognition Receptor
PTEX	*Plasmodium* Translocon Exported Protein
*Py*17XNL	*Plasmodium yoelii 17X* Non-Lethal
RAG	Recombination Activation Gene

RBC	Red Blood Cell
RMP	Rodent Malaria Parasite
RPMI	Roswell Park Memorial Institute medium
RT	Room Temperature
SA	Sialic Acid
SCID	Severe Combined Immunodeficiency
SEM	Standard Error of Mean
SUB1	Subtilisin-like Serine Protease
TRX2	Thioredoxin 2 Protein

Chapter One

Introduction

1.1Malaria

Malaria is a disease caused by infection with the protozoan parasites belonging to the genus *Plasmodium.* The word malaria originated from Italian words "*mal aria*" meaning "bad air" as it was believed that the disease was caused by an unknown substance in the air from swamps [1]. Today, malaria remains one of the four major life-threatening infectious diseases globally. According to the latest estimates from the World Health Organization (WHO), 216 million cases of malaria occurred in 91 countries with 445,000 deaths in 2016 (WHO report 2017). Nearly 80 % of the cases and 90 % of the deaths are reported from sub-Saharan Africa, and children under the age of 5 years and pregnant women are the most severely affected [2]. Malaria is a vector-borne disease, transmitted by female *Anopheles* mosquitoes, and different species of the parasite infect a wide range of hosts including humans, monkeys, rodents, birds and reptiles. Human malaria is caused mainly by four different species of *Plasmodium*: *Plasmodium falciparum* (*Pf*), *Plasmodium vivax* (*Pv*), *Plasmodium ovale* (*Po*) and *Plasmodium malariae* (*Pm*). A fifth species *Plasmodium knowlesi* that infects primates, has also caused human malaria but the exact mode of transmission remains unclear [3, 4].

Plasmodium falciparum causes the life-threatening disease, cerebral malaria, which prevails in Africa and accounts for the majority of global morbidity and deaths. *P. vivax* generally produces milder disease and has recently been reported among the population living in sub-tropical Africa in addition to other areas at risk, and may persist in the liver as hypnozoites forms for several months to years causing relapses; while the incidence of the other three species is currently much lower.

The clinical symptoms of malaria include fever with chills, sweating, fatigue, nausea, and anemia. However, the severe form of malaria due to *P. falciparum* can lead to life-threatening conditions including respiratory distress, metabolic acidosis, seizures and unconsciousness/ coma, and rapid death. The complex life cycle of *Plasmodium spp.* alternating between female *Anopheles* mosquitoes and vertebrate hosts has made understanding of the host-parasite interactions and infection control difficult. *Plasmodium* parasites enter the host through the bite of an infected *Anopheles* mosquito injecting sporozoites present in their saliva into the dermis, followed by infection of the hepatocytes and undergoing a pre-erythrocytic liver stage that lasts for 1-2 weeks before entry of the parasite into the blood stage [5]. In the hepatocytes the sprozoite undergo asexual development releasing merozoites in the hepatic circulation to invade erythrocytes in a rapid, dynamic and multi-

step process - pre-invasion, active invasion and echinocytosis. Pre-invasion involves robust interaction between merozoite and erythrocyte through actomyosin motor causing deformation of the erythrocytes. A short time later, merozoite moves into the erythrocyte through a pinch-point (the tight-junction) and undergoes asexual development in its intra-erythrocytic life-cycle [6]. This life-cycle includes progression through the ring, trophozoite, and finally the mature schizonts stages producing tens of daughter merozoites for re-invading new RBCs - a cyclical process that is responsible for the onset of clinical symptoms. As parasites reside and develop within RBCs, they bring about physiological and biochemical changes within host cells [7]. Moreover, interactions by way of parasite-encoded molecules may affect the mobility and trafficking of RBCs within the host, possibly increasing the infection severity. A sub-population of intra-erythrocytic parasites gives rise to the sexual-stage parasites (gametocytes), which migrate to peripheral blood vessels in the skin. These are then taken up by feeding mosquitoes, which completes the cycle through the generation of sporozoites by sexual reproduction in the midgut of the mosquito and their moving into the salivary gland - ready to infect new hosts via a blood meal [8, 9].

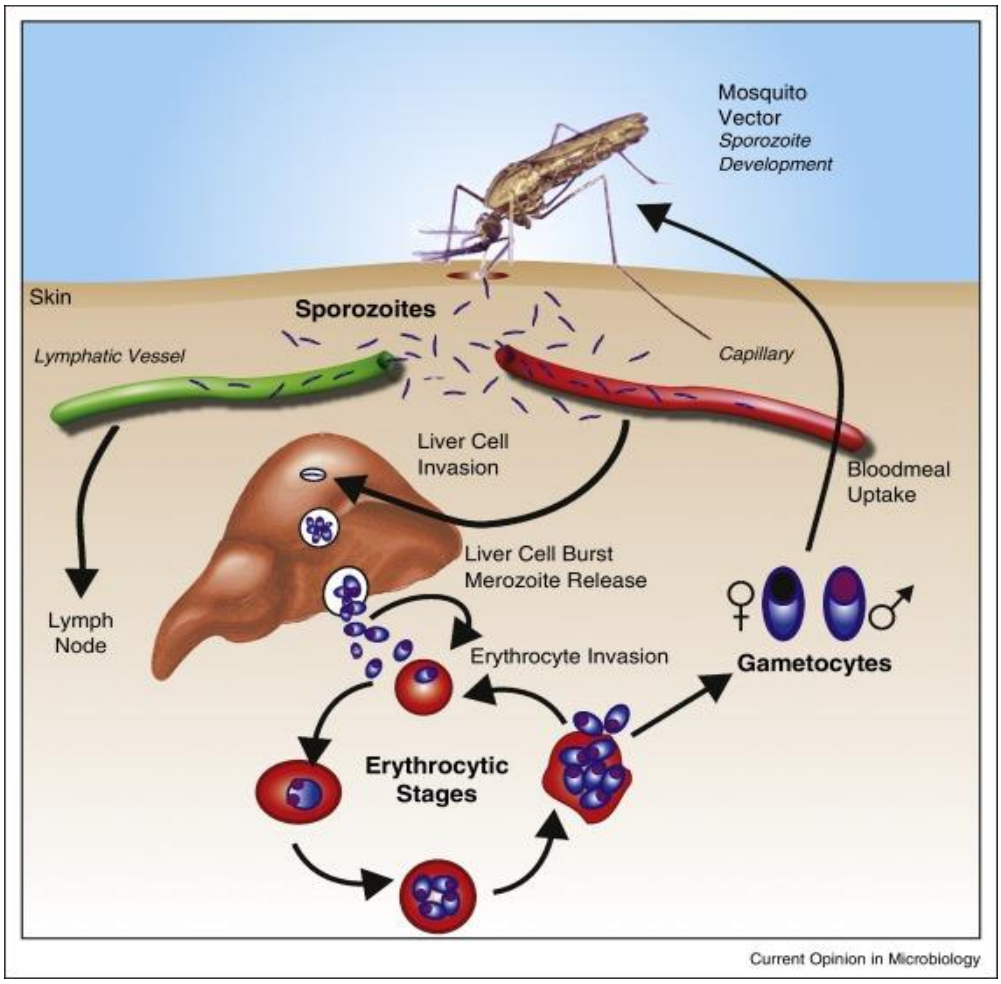

Figure 1.1 Life cycle of Plasmodium spp. *The parasites (sporozoites) are transmitted to a human host via the bite of an infected female Anopheles mosquito. Sporozoites migrate through the skin and are taken up by the hepatocytes. Here, they undergo asexual reproduction to produce merozoites.*

Merozoites enter the blood stream and quickly infects RBCs. Within the RBCs, merozoites hijack host machinery and undergo the ring, trophozoite, and mature schizonts stages followed by rupture of the infected RBCs (schizogony) and release of more merozoites. The merozoites thus released infect new RBCs to either continue multiplying or, alternatively, develop into the sexual-stage of the parasite (gametocytes). The gametocytes migrate to the dermis where they may be taken up by mosquitoes, and undergo sexual reproduction to continue its life cycle[10].

1.2 The rodent model of malaria

In the field of malaria research, the rodent model is very important as the laboratory maintenance of the complete *P. falciparum* life-cycles remains very difficult. Rodents are the best non-primate models. Since their isolation from the wild between 1948 and 1974 in Central West Africa, rodent malaria parasites, *Plasmodium berghei* (used in this project), *P. chabaudi*, *P. vinckei* and *P. yoelii*, have enabled us studying various aspects of host-parasite-vector interactions, due to our easy access to stages of the parasite in mosquitoes and in host livers in order to evaluate potential interventions in malaria control [11]. Although none of the rodent *Plasmodium* species is the perfect model for *P. falciparum*, different species can be used to study different aspects of the infection. For instance, *P. chabaudi* is a model that best to understand the interplay between the parasite and the host immune response, while *P. berghei* is a better model for studying the biology of transmission[11].

In addition to laboratory study of the parasite life cycle, rodent malaria parasites are more amenable to genetic modifications than *P. falciparum* [12]. In fact, it can take as little as two weeks to obtain a clonal population of *P. berghei* transgenic parasites, which will take at least two months for the human parasites. Moreover, the availability of fluorescent rodent parasite lines and transgenic mice permits exploration of specific host parasite interactions that are not yet available for studies of human malaria parasites [13].

1.3 Progress in infection control measures

Between the years 2000 and 2013, the malaria prevalence and mortality have substantively declined by 48% and 47% respectively [14]. A combination of improved vector control and drug treatment, especially the use of insecticide-treated bed-nets (particularly protecting young children), indoor residue spraying, and development and use of newer and more effective anti-malarial drugs have contributed to this decline. Unfortunately, the emergence and spread of drug-resistant parasites has contributed to the re-emergence of malaria, and also has stagnated malaria control [2].

Despite decades of intense research, there is currently no effective vaccine against malaria. The leading malaria vaccine candidates include RTS,S/AS01, a pre-erythrocytic vaccine based on the circumsporozoite protein (CSP) combined with hepatitis B surface antigen; AS01, a combination of mono-phosphoryl lipid A (MPL, a toll-like receptor 4 agonist); and QS21 (a derivative from Quill A) and lipids [15, 16]. The results from phase III clinical trial of RTS,S on 15,460 children in seven countries in the sub-Saharan Africa suggested its relatively low efficacy (26-50%) in reducing the malaria episodes in children with and insignificant effect on deaths [17].

A numbers of combined vaccines are in the process of development, which are intended to target a range of *Plasmodium* antigens that are expressed at different stages of life cycle, such as, GRURP-*Pfs*48/45 - a multistage, chimera vaccine; PfSPZ - a whole attenuated, purified, cyropresevered vaccine; and transmission-blocking vaccine [18] [19, 20] [21]. Despite serious efforts, the progress has been slow due to major gaps in understanding host-parasite interactions and protective immunological mechanisms. It is thus important to understand the biology of the parasite for identifying potential vaccine candidates, as well as understanding how to generate protective immunity via next-generation vaccines.

Antimalarial drugs are effective in the treatment and control of malaria, especially the Artemisinin Combination Therapy (ACT). Artesunate (an artemisinin derivative) is the WHO-recommended treatment for patients with uncomplicated malaria due to its greater ability to reduce parasite numbers than the other antimalarials [22-24]. Artesunate acts faster and also acts over a wider range of parasite developmental stages than the other anti-malarials [25]. However, the emergence of Artemisinin resistance highlights the importance of understanding the mechanisms of drug resistance. Many studies have reported that the use of the short course monotherapy with Artesunate has been responsible for emergence of resistance in Southeast Asia [26, 27]. Artesunate, short-acting drug has been combined with a longer-acting antimalarial drug, to develop ACT (Artemisinin-based Combination Therapy) to prevent/delay the emergence of resistance. Artesunate-mefloquine therapy is one such combination; compared to artesunate mefloquine produces a slower decline in the total number of parasites but it has a longer half-life and additionally it also destroys the asexual blood-form of a malaria parasite. Slower parasite clearance under artesunate treatment has recently been observed in western Cambodia and adjacent border of western Thailand [28, 29], which has been interpreted as evidence for the emergence of Artemisinin-resistant parasites [29].

In endemic populations, the naturally-acquired immunity to malaria might require 10-15 years of exposure to the parasite to develop [30]. Studies have shown that in countries with high transmission rates, such as Kenya and Gambia, the incidence of cerebral malaria and severe malaria were the lowest [31] [32] [33, 34], while severe malaria continues to occur among older children and

adults in areas with low transmission [35, 36]. These observations suggest that there is a strong relationship between parasite exposure and immunity to malaria, and support the argument that implementing control measure to prevent the transmission of infection could contribute to the poorer outcomes for some individuals infected with *Plasmodium [37]*. Therefore, a better understanding of host-parasite interactions may aid the development of new malaria control measures.

1.4 Host-parasite interaction

The life cycle of malaria parasite is complex since it occurs in different tissue sites in two different hosts – the vertebrate human host and the female *Anopheles* mosquito. The outcome of infections depend on the interactions between the host and the infecting species of *Plasmodium*. Parasites reside and develop within host RBCs, where they bring about changes in the physiological and biochemical processes within these host cells [7].

During the blood-stage malaria, the initial attachment of parasites to host erythrocytes occur through the interactions between erythrocyte receptors and parasite ligands of two protein families, the Erythrocyte Binding Ligands (EBL) family of proteins and *P. falciparum* reticulocyte binding protein homolog (PfRh or PfRBL) proteins that are present on merozoite surface [38, 39].

Merozoites can invade mature RBCs using two independent pathways - a sialic acid (SA)-dependent [40] and a SA independent one. Parasite molecules involved in the sialic acid-dependent pathway are the Erythrocyte Binding Ligands (EBL) family of proteins. During the invasion process, micronemes-apical organelles of merozoites contain the EBL proteins EBA-175, EBL-1, EBA-140 that binds to major sialyated proteins on the surface of RBC such as glycophorins A, B and C respectively [41-43] - the major sialyated proteins on the RBC surface. Among Reticulocyte-binding protein Homologue (RH), PfRH1 is the only member that binds SA residues, and PfRH2, PfRH4, PfRH5, and MSPs are components of the SA-independent pathway in which human erythrocyte band 3 function as a receptor [44, 45]. It was thought that targeting of proteins involved in the invasion process is less tractable because of multiple redundant pathways and extensive sequence variations in the parasite proteins. However, it has recently been suggested that PfRH5 is essential for invasion process since it cannot be deleted in any strain of *P. falciparum* [46] and it is a ligand for the host receptor Basigin [47, 48]. The blocking of PfRH5-basigin interaction by soluble basigin, basigin knockout or anti-basigin antibodies were shown to protect against malaria by blocking merozoites invasion of multiple strains of *P. falciparum* [49], and thus has been proposed as a novel drug target in malaria [50].

On the other hand, it has also been observed that delivering of PfRH5-based vaccines to *Aotus* monkeys provided protection against challenge with heterologous-strain of blood-stage *P. falciparum in vivo*, and the protection depended on the concentration of anti-PfRH5 antibody and parasite-neutralizing activity [51]. Moreover, anti-PfRH5 antibody, derived from natural human infections, has erythrocyte invasion inhibitory functions ***in vitro*** [52] as well the ability to reduce risk of malaria in children by increasing the concentrations of IgG3 subclass of antibodies against PfRH5 [53]. Thus, PfRH5 is considered an important candidate in anti-malarial vaccine research development.

Additionally, apical membrane antigen (AMA1) and rhoptry neck protein (RON) have been shown essential for RBC invasion by triggering junction formation [54], with AMA1 perceived as a target vaccine candidate for inducing naturally-acquired protection against malaria [55, 56], since it is immunogenic and is safe for use in human [57]. However, the polymorphic nature and strain-specific protection limits its use [58].

Erythrocyte receptors, on the other hand, play an important role in the merozite invasion process. CD55 is a 70 kDa glycoprotein attached to the erythrocyte membrane by a glycosylphosphatidylinositol (GPI) [59]; CD55 knock-down results in significant reduction in parasite invasion while CD55-null cells were found resistant to invasion [59].

Following invasion, parasites within the human erythrocytes undergo an intra-erythrocytic cycle that includes its progression through the ring, trophozoite and mature schizont stages, during which the parasites extensively remodel the infected red blood cells (pRBCs) by exporting several hundred proteins into the host cytoplasm, some of which can serve as ligands for adhesion to endothelial receptors [60]. Remodelling of iRBCs requires the development of a tubulovesicular network to sort and distribute proteins to target locations beyond its own plasma membrane (PM) and the parasitoporous vacuole membrane (PVM). Key exomembrane-bound structures of various sizes are formed during the construction of this network, including Maurer's clefts (MCs) [61], electron dense vesicles (~80 nm diameter) [62, 63], and J-dots [64]. Early in the intra-erythrocytic cycle (i.e. within 5 hours of invasion), the parasite generates MCs via budding from the PVM, and begins exporting proteins into the erythrocyte cytoplasm. Subsequently, parasites develop into trophozoites (5-10 hours post-invasion) and MCs migrate towards and become tethered to the erythrocytic membrane. These structural changes to the host RBC increase its rigidity [65]. For example, during *P. falciparum* infection, RBC surface "knob" formation is accomplished by the knob associated histidine-rich protein (KAHRP) and adherence of the iRBC to the vascular endothelium [66] via binding of *P. falciparum* erythrocyte membrane protein (PfEMP1) to a host receptor. The PfEMP1 protein family is antigenically highly diverse since they are encoded by 60 *var* (variable) genes per

haploid genome [67-70]. This high sequence diversity in PfEMP1 proteins facilitates evasion of the host immune response, exacerbating the pathology and disease severity [71].

Duffy binding-like domain (DBL) α, the N-terminal region of PfEMP1 play a key role in binding to uninfected erythrocytes via glycosaminoglycan heparin sulphate [72] in a process called rosetting that obstructs flow of blood in micro-capillaries [73]. It has recently been shown that anti-coagulants, heparin and sevuparin can block this resetting and has thus been proposed as possible adjunct therapies for severe malaria [74]. Host platelets may also play a protective role in the early stages of blood-stage infection by binding to the infected erythrocytes and killing the parasites within [75].

PfSEA, a parasite protein involved in RBC egress, is considered a potential immune target since anti-PfSEA antibodies are able to slow down parasite replication by arresting schizont rupture. However, the mechanism by which anti-PfSEA-1 antibodies access intracellular schizonts is not clear [76, 77]. It has recently been observed that the parasiteproteins plasmepsins IX and X are essential for invasion and egress controlling maturation of the enzymes subtilisin-like serine protease SUB1 in exoneme secretory vesicles that are required to disrupt the host cell membranes. Therefore, plasmepsins are selected as a potential drug target, by way of inhibiting its function using an enzyme inhibitor such as aspartic protease- a hydroxyl-ethyl-amine-based scaffold compound [78, 79].

1.5 Host immune response during blood-stage malaria

Humoral immune responses primarily confers immunity to blood-stage malaria; ; cellular and innate immune responses also play important role in controlling parasite growth but they may also contribute to malaria pathology [80]. Humoral or antibody and T cells responses are important of merozoites and intra-erythrocytic parasites respectively. Antibodies may opsonise merozoites to uptake or inhibit their invasion of RBCs. A number of *in vivo* mechanisms proposed to be involved in the control of pRBCs by antibody include cellular killing via phagocytosis, blocking of rosetting of RBCs, and neutralization of parasite toxins to prevent excessive inflammation [81]. Studies in humans infected with *Plasmodium falciparum* and in experimental mouse models suggest that both CD4+ T helper 1 (Th1) cells and interferon-γ (IFN- γ) are critically required to control the primary peak of parasitemia [82, 83]. A balance between pro-inflammatory and anti-inflammatory responses is also important in limiting the development of immune-mediated pathologies such as cerebral malaria and anemia [84]. Monocytes, macrophages, ploymorphonuclear granulocytes (PMNs) and dendritic cells (DCs) play important role in parasite clearance [85-88]. Macrophages in spleen and liver mainly involved in the phagocytic removal of malaria parasites [89, 90]. Phagocytic response

occurs through interaction between pathogen-associated molecular patterns (PAMPs) of parasitic origin and pattern recognition receptors (PRRs) on the host cell surface [91, 92]. These interactions activate a cascade of distinct transcriptional programmes and multiple downstream signalling pathways that support parasite clearance [93-95]. Additionally, complement factors opsonize and enhance phagocytic removal of parasites [85, 96]. The immune response during malaria is very complex and dynamic, which influences the severity of infection [97]. The level of expression of several cytokines such as IL10, TGF-ß, IL-17, IFN-γ, TNF-α, IL-6, IP-10, TNF-R2, TLR2, IL-8, IL-15, MCP-1, EOTAXIN, and IL-5 have been found to alter with the disease conditions. Therefore, targeting the pathways involved in these processes could lead to novel therapeutic interventions. Interleukin IL-18 plays a protective role in malaria by mediating the IFN-γ production [98], and natural killer (NK) cells are involved in the early control through production of IFN-γ [99]. Tumour Necrosis Factor-alpha (TNF-α) has been observed to reduce intracellular parasitemia by reducing erythrocyte invasion process [100].

1.6 Mechanisms of antibody-mediated parasite control in malaria

Antibodies are important component of acquired-immunity to malaria, which has been demonstrated in the fundamental studies in which passive transfer of immune serum, firstly in rhesus monkeys [101] and later in malaria-infected children resulted in the reduction of parasite load along with improvement in the clinical status [102-104]. These findings demonstrated that parasite-specific antibodies are able to effectively control the number of parasites in human infections as well in *in vivo* animal models.

In endemic populations, development of naturally-acquired immunity to malaria takes as long as 10-15 years of exposure to the parasites [30]. Efforts had been made to identify potential antigenic targets of protective antibodies [105, 106]. Mechanisms by which they control parasite numbers *in vivo* have also been reviewed [105, 107-109]. Protection against malaria is thought to depend on the functionality of antibody produced against either parasite proteins exported on the surface of pRBC or to those expressed on the surface of the merozoites [105]. The mechanism by which antibodies protect against malaria remains unclear, although this information is a key to development of effective anti-malarial vaccines.

A number of possible antibody-mediated mechanisms have been proposed and disclosed in elegant *in vitro* assays. These include Growth Inhibition Assays (GIAs) [110, 111] to assess if antibodies can reduce parasite growth in the RBC over a few replication cycles; opsonic phagocytosis assays and antibody-dependent cellular inhibition (ADCI) assays [112-114] to assess whether

antibodies facilitate uptake and/or inhibition by phagocytes; and complement-fixing and killing assays [115, 116] to assess how well the antibodies facilitate C1q deposition and complement-dependent direct killing. There is a lack of clear understanding of the correlation between functional efficacy in GIAs and immunity to malaria [117-120]; however, in recent years development of capacities to mediate opsonic phagocytosis or C1q-fixation *in vitro*, mostly of merozoites, have demonstrated its correlation with protection against *P. falciparum* malaria symptoms and high density parasitemia [114-116]. More recently, it has been suggested that antibodies against the pRBC surface protein, PfEMP1, which drive opsonic phagocytosis *in vitro*, afforded partial protection against malaria and that these antibodies develop slightly earlier than the merozoite-targeting antibodies [121]. The epidemiological data in humans supports the notion that multiple mechanisms act together against merozoites and pRBC in the antibody-mediated pRBC control during the blood-stage infection. However, few, if any of these mechanisms, have been convincingly observed *in vivo*.

1.7 Measuring parasite clearance and growth *in vivo*

During blood-stage *Plasmodium* infection, the total number of parasites may increase until the host-mediated control or drug intervention slows down or halts parasite growth (Figure1.2) [122-125]. It is also believed that parasite clearance is accelerated by host clearance mechanisms, e.g. splenic pitting [122, 126, 127], or phagocytosis [82, 128]. Measuring parasite clearance *in vivo* is difficult, especially during the period of parasite replication. During active infection the total parasite load in the body depends on two competing processes: 1) host control of parasite numbers, and 2) parasites maintaining their numbers. The rate of parasite population growth likely depends on the replication efficiency of the parasites that is influenced by the number of merozoites produced from each parasite, and their survival capacity and ability to invade newer RBCs minus the rate of parasite clearance or control by the host. Therefore, to identify treatments and interventions that act by impairing parasite proliferation and those that act by enhancing host removal of parasites, we need to quantify parasite replication and control *in vivo*.

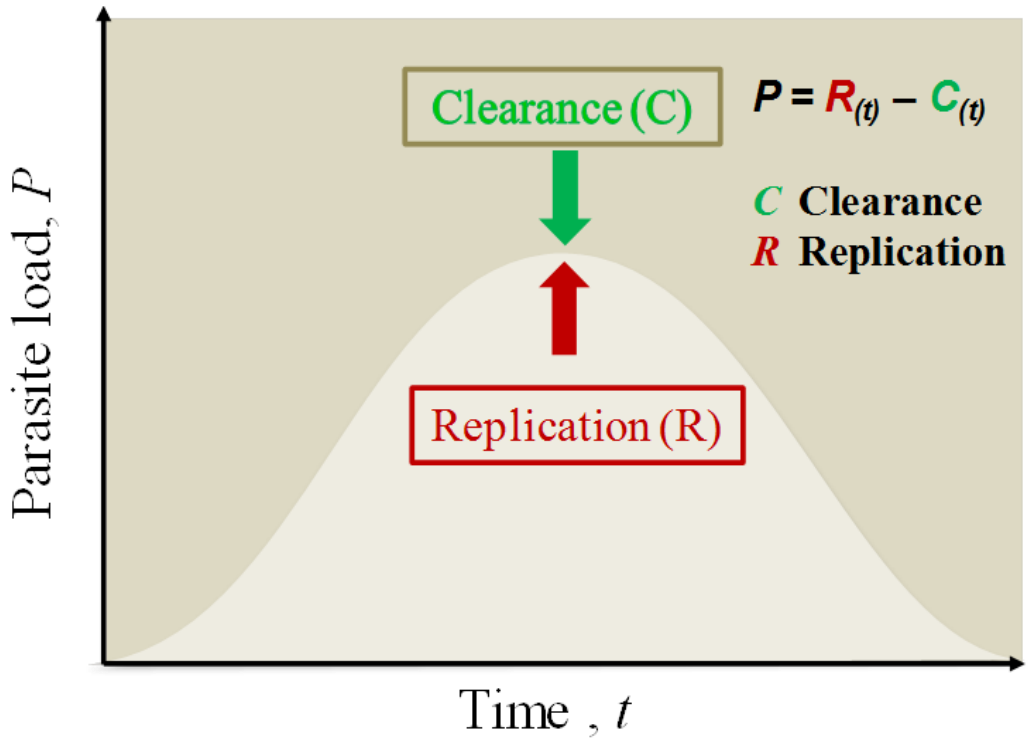

Figure 1.2 A hypothetical parasitaemia curve *during blood-stage malaria showing that the resulting parasitaemia is the net effect of the parasite replication rate minus drug or host-mediated parasite clearance over the course of infection.*

1.8 Thesis hypothesis, and aims and overall objective

Hypotheses:

1. Increased host clearance or reduced parasite replication is responsible for host- or drug-mediated parasite control *in vivo*.

2. In mouse model, *Plasmodium*-specific antibodies control infection by inhibiting the invasion of RBC, via binding to merozoites.

3. During blood-stage infection, parasites export some proteins to subvert host immune control.

Aims:

1. To explore the mechanisms of parasite control during blood-stage malaria using an *in vivo* mouse model, *Plasmodium berghei* ANKA;

2. To determine mechanisms by which antibodies control parasite numbers during non-lethal blood-stage malaria

3. To identify novel *Plasmodium* exported proteins that are involved in host interaction.

Overall Objective:

The overall objective of my doctoral study (Ph.D.) was exploration of host mechanisms of parasite control during blood-stage malaria *in vivo* in rodent malaria model.

Chapter Two

Study material and methods

2.1 Materials

2.2.1 Mice and their ethical use in the experiements

Mice/rats	Description
C57BL/6	Immune competent, 6-12 weeks old female mice
Balb/c	Immune competent , 6-12 weeks old female mice
rag1$^{-/-}$	Immune deficient (T and B cell deficient), 6-12 weeks old female C57BL/ 6 background mice
SCID	Immune deficient, 6-12 weeks old female Balb/c background mice
Wistar rats	Used to propagate parasites to be transfected in the screening of 117 KO vectors. Outbred, 200 g – 250 g (~ 8weeks), female

Mice used for screening of 117 KO vectors, described in chapter five, were maintained under specific pathogen-free conditions at the Welcome Trust Genome Campus Research Support Facility (Cambridge, UK). These animal facilities are approved by and registered with the UK Home Office. All procedures were in accordance with the Animals (Scientific Procedures) Act 1986. The protocols were approved by the Animal Welfare and Ethical Review Body of the Wellcome Trust Genome Campus.

Mice used for the exploration of host immune mechanisms and *in vivo* function of antibody in parasite control at QIMR were purchased from Australian Resource Centre (Canning Vale, Western Australia). Mice were housed in specific-pathogen free conditions in accordance with QIMR Berghofer animal ethics standards and the "Australian Code of Practice for the Care and Use of Animals for Scientific Purposes" (Australian National Health and Medical Research Council), and the experimentations were approved by the QIMR Berghofer Animal Ethics Committee (Herston, QLD, Australia; approval number:A1503-601M.

2.1.2 Parasites

Parasite	Description	Reference
P. berghei ANKA (*Pb*A)	A transgenic *Pb*A line (231c1l) expressing luciferase and GFP under the control of the ef1-α promoter. Lethal experimental model. C57BL/6 mice succumb to cerebral malaria after approximately 1 week of infection.	[129]
P. chabaudi chabaudi AS (*Pc*AS)	A model of resolving infection. C57Bl/6J mice resolve infection with a standard dose within 15 days.	[130]
P. yoelii 17X non-lethal (*Py*17XNL)	Model of resolving infection. C57Bl/6J mice resolve infection with a standard dose by day 30.	[131]

Aliquots of *Plasmodium* parasite-infected red blood cells (Stabilates) stored at -80◦C.

2.2 Reagents

2.2.1 Infections

Items	Source
5.0 mL tubes	Greiner Labortechnik (Frickenhausen, Germany)
30.0 mL tubes	Sarstedt (Pookara, Australia)
Haemocytometer	Pacific Laboratory Product (Blackburn, VIC, Aus)
Immersion oil	Merck (Darmatadt, Germany)
CliniPure Haem Kwik Fixative	Grale Scientific (Ringwood, VIC, Aus)
CliniPure Haem Kwik Stain No 1	Grale Scientific (Ringwood, VIC, Aus)
CliniPure Haem Kwik Stain No 2	Grale Scientific (Ringwood, VIC, Aus)
Heparin 5000 IU in 5mL	Pfizer (New York, NY, USA)
Trypan Blue 0.4%	Thermo Fischer Scientific
Sodium chloride 0.9%	Baxter (Toongabbie, NSW, Aus)
1mL Syringe	Terumo (Tokyo, Japan)
26 G needle	Terumo (Tokyo, Japan)

2.2.2 CTFR-labelling of pRBCs

Items	Source
CellTrace™ Far Red (CTFR)	Life Technologies
DMSO	Life Technologies
DPBS	Pacific Laboratory Product (Blackburn, VIC, Aus)
5mL tubes	Greiner Labortechnik (Frickenhausen, Germany)
50mL Falcon	Greiner Labortechnik (Frickenhausen, Germany)

2.2.3 *Plasmodium*-specific ELISA

Reagent	Source
Corning Costar Flat bottom 96-well plates	Greiner Labortechnik (Frickenhausen, Germany)
OPD	Sigma Aldrich Pty Ltd (St Louis Missouri, USA)
Tween 20	Sigma Aldrich Pty Ltd (St Louis Missouri, USA)
Streptavidin-HRP	BD Biosciences (Franklin Lakes, NJ, USA)
Anti- IgG	Jackson ImmunoResearch (West Grove, PA, USA)

2.2.4 Complement component 3 ELISA

Reagent	Source
Corning Costar Flat bottom 96-well plates	Greiner Labortechnik (Frickenhausen, Germany)
OPD	Sigma Aldrich Pty Ltd (St Louis Missouri, USA)
Tween 20	Sigma Aldrich Pty Ltd (St Louis Missouri, USA)

Streptavidin-HRP	BD Biosciences (Franklin Lakes, NJ, USA)
Goat IgG Fraction to Mouse Complement C3	MP Biomedicals, USA
Peroxidase-Conjugated Goat IgG Fraction to Mouse Complement C3,	MP Biomedicals, USA

2.2.5 Surface and intracellular immune staining of pRBCs

Reagent	Source
Falcon U-bottom 96-well plates	Corning Incorporated- Life sciences, USA
BD Cytofix/Cytoperm™ Fixation/Permeabilization Solution	Fisher Scientific
Anti-RBC antibody 34-3C (1.5µg/mL)	Abcam, Cambridge, MA, USA).
PE-Goat anti-IgG	BioLegend, San Diego, CA 92121

2.2.6 Oligonucleotides used for barcode amplification and illumina sequencing

Barcodes - a short nucleotide sequence that were inserted in the backbone of each knock-out vector construct to represent a particular knock-out gene. The presence of barcodes in the blood and tissues DNA were quantified by polymerase chain reaction (PCR) amplification, with an index primer used to tag each sample for individual identification and then samples were sequenced by next-generation sequencing for barcode counting analysis.

1st PCR primers	Primer arg 91_Illumina	TCGGCATTCCTGCTGAACCGCTCTTCCGATCTGTAATTCGTGCGCGTCAG
	Primer arg97_Illumina	ACACTCTTTCCCTACACGACGCTCTTCCGATCTCCTTCAATTTCGATGGGTAC
Illumina adapter	PE 1.0 Primer_Illumina PCR	AATGATACGGCGACCACCGAGATCTACACTCTTTCCCTACACGACGCTCTTCCG ATC*T
Index tags	iPCRindex1	CAAGCAGAAGACGGCATACGAGATTGCTAATCACTGAGATCGGTCTCGGCATT CCTGCTGAACCGCTCTTCCGATC*T
	iPCRindex2	CAAGCAGAAGACGGCATACGAGATTAGGGGGATTCGAGATCGGTCTCGGCATT CCTGCTGAACCGCTCTTCCGATC*T
	iPCRindex3	CAAGCAGAAGACGGCATACGAGATAGTTTCCCAGGGAGATCGGTCTCGGCATT CCTGCTGAACCGCTCTTCCGATC*T
	iPCRindex4	CAAGCAGAAGACGGCATACGAGATCCTGGGAGGTAGAGATCGGTCTCGGCATT CCTGCTGAACCGCTCTTCCGATC*T
	iPCRindex5	CAAGCAGAAGACGGCATACGAGATATACCACAAATGAGATCGGTCTCGGCATT CCTGCTGAACCGCTCTTCCGATC*T
	iPCRindex6	CAAGCAGAAGACGGCATACGAGATGATCTCTCGGGGAGATCGGTCTCGGCATT CCTGCTGAACCGCTCTTCCGATC*T

iPCRindex7	CAAGCAGAAGACGGCATACGAGATACCCTATACTCGAGATCGGTCTCGGCATT CCTGCTGAACCGCTCTTCCGATC*T
iPCRindex8	CAAGCAGAAGACGGCATACGAGATCTCAATTAAGAGAGATCGGTCTCGGCATT CCTGCTGAACCGCTCTTCCGATC*T
iPCRindex9	CAAGCAGAAGACGGCATACGAGATCGACAGAACGTGAGATCGGTCTCGGCATT CCTGCTGAACCGCTCTTCCGATC*T
iPCRindex10	CAAGCAGAAGACGGCATACGAGATTCGCCATTATGGAGATCGGTCTCGGCATT CCTGCTGAACCGCTCTTCCGATC*T
iPCRindex11	CAAGCAGAAGACGGCATACGAGATATGTTCCGGCCGAGATCGGTCTCGGCATT CCTGCTGAACCGCTCTTCCGATC*T
iPCRindex12	CAAGCAGAAGACGGCATACGAGATTCTTGAAGTGAGAGATCGGTCTCGGCATT CCTGCTGAACCGCTCTTCCGATC*T
iPCRindex13	CAAGCAGAAGACGGCATACGAGATGAAGGCCAGCTGAGATCGGTCTCGGCATT CCTGCTGAACCGCTCTTCCGATC*T
iPCRindex14	CAAGCAGAAGACGGCATACGAGATCCAATGTGCAGGAGATCGGTCTCGGCATT CCTGCTGAACCGCTCTTCCGATC*T
iPCRindex15	CAAGCAGAAGACGGCATACGAGATATCGAAGGACCGAGATCGGTCTCGGCATT CCTGCTGAACCGCTCTTCCGATC*T
iPCRindex16	CAAGCAGAAGACGGCATACGAGATTCGGGTGCGAAGAGATCGGTCTCGGCATT CCTGCTGAACCGCTCTTCCGATC*T
iPCRindex17	CAAGCAGAAGACGGCATACGAGATGTAATTTACGGGAGATCGGTCTCGGCATT CCTGCTGAACCGCTCTTCCGATC*T
iPCRindex18	CAAGCAGAAGACGGCATACGAGATATATCGACTACGAGATCGGTCTCGGCATT CCTGCTGAACCGCTCTTCCGATC*T
iPCRindex19	CAAGCAGAAGACGGCATACGAGATTGATTCTTACAGAGATCGGTCTCGGCATT CCTGCTGAACCGCTCTTCCGATC*T
iPCRindex20	CAAGCAGAAGACGGCATACGAGATACGGCGGGCCTGAGATCGGTCTCGGCATT CCTGCTGAACCGCTCTTCCGATC*T
iPCRindex21	CAAGCAGAAGACGGCATACGAGATCTTGCGTGGAGGAGATCGGTCTCGGCATT CCTGCTGAACCGCTCTTCCGATC*T
iPCRindex22	CAAGCAGAAGACGGCATACGAGATTAATCAAAGACGAGATCGGTCTCGGCATT CCTGCTGAACCGCTCTTCCGATC*T
iPCRindex23	CAAGCAGAAGACGGCATACGAGATGGCGGGCTCTAGAGATCGGTCTCGGCATT CCTGCTGAACCGCTCTTCCGATC*T
iPCRindex24	CAAGCAGAAGACGGCATACGAGATCCTCCATTTCTGAGATCGGTCTCGGCATT CCTGCTGAACCGCTCTTCCGATC*T
iPCRindex25	CAAGCAGAAGACGGCATACGAGATAACCAGCGCTGGAGATCGGTCTCGGCATT CCTGCTGAACCGCTCTTCCGATC*T
iPCRindex26	CAAGCAGAAGACGGCATACGAGATTATTCGTCAACGAGATCGGTCTCGGCATT CCTGCTGAACCGCTCTTCCGATC*T
iPCRindex27	CAAGCAGAAGACGGCATACGAGATGCGCTGATGCAGAGATCGGTCTCGGCATT CCTGCTGAACCGCTCTTCCGATC*T
iPCRindex28	CAAGCAGAAGACGGCATACGAGATCTCATATGGCTGAGATCGGTCTCGGCATT CCTGCTGAACCGCTCTTCCGATC*T
iPCRindex29	CAAGCAGAAGACGGCATACGAGATACAGGGGCAGGGAGATCGGTCTCGGCAT TCCTGCTGAACCGCTCTTCCGATC*T
iPCRindex30	CAAGCAGAAGACGGCATACGAGATGGTTTTATACCGAGATCGGTCTCGGCATT CCTGCTGAACCGCTCTTCCGATC*T
iPCRindex31	CAAGCAGAAGACGGCATACGAGATGCATGACTTTAGAGATCGGTCTCGGCATT CCTGCTGAACCGCTCTTCCGATC*T

iPCRindex32	CAAGCAGAAGACGGCATACGAGATTTCTGAGTTCTGAGATCGGTCTCGGCATT CCTGCTGAACCGCTCTTCCGATC*T
iPCRindex33	CAAGCAGAAGACGGCATACGAGATCGATTAAGCTGGAGATCGGTCTCGGCATT CCTGCTGAACCGCTCTTCCGATC*T
iPCRindex34	CAAGCAGAAGACGGCATACGAGATTCTCTTAAGCCGAGATCGGTCTCGGCATT CCTGCTGAACCGCTCTTCCGATC*T
iPCRindex35	CAAGCAGAAGACGGCATACGAGATCCGACAGGTGAGAGATCGGTCTCGGCATT CCTGCTGAACCGCTCTTCCGATC*T
iPCRindex36	CAAGCAGAAGACGGCATACGAGATAGTATCACTATGAGATCGGTCTCGGCATT CCTGCTGAACCGCTCTTCCGATC*T
iPCRindex37	CAAGCAGAAGACGGCATACGAGATGTTCGCTGATGGAGATCGGTCTCGGCATT CCTGCTGAACCGCTCTTCCGATC*T
iPCRindex38	CAAGCAGAAGACGGCATACGAGATTCCCATGGCGCGAGATCGGTCTCGGCATT CCTGCTGAACCGCTCTTCCGATC*T
iPCRindex39	CAAGCAGAAGACGGCATACGAGATGGAGTTCAACAGAGATCGGTCTCGGCATT CCTGCTGAACCGCTCTTCCGATC*T
iPCRindex40	CAAGCAGAAGACGGCATACGAGATACTGCGTATATGAGATCGGTCTCGGCATT CCTGCTGAACCGCTCTTCCGATC*T
iPCRindex41	CAAGCAGAAGACGGCATACGAGATTACGTCGTGCGGAGATCGGTCTCGGCATT CCTGCTGAACCGCTCTTCCGATC*T
iPCRindex42	CAAGCAGAAGACGGCATACGAGATCCTTCTGTCCCGAGATCGGTCTCGGCATT CCTGCTGAACCGCTCTTCCGATC*T
iPCRindex43	CAAGCAGAAGACGGCATACGAGATATACTTGTTAAGAGATCGGTCTCGGCATT CCTGCTGAACCGCTCTTCCGATC*T
iPCRindex44	CAAGCAGAAGACGGCATACGAGATTACCCAGGAGTGAGATCGGTCTCGGCATT CCTGCTGAACCGCTCTTCCGATC*T
iPCRindex45	CAAGCAGAAGACGGCATACGAGATGGGGTTTTCTGGAGATCGGTCTCGGCATT CCTGCTGAACCGCTCTTCCGATC*T
iPCRindex46	CAAGCAGAAGACGGCATACGAGATACTGCTCGTGCGAGATCGGTCTCGGCATT CCTGCTGAACCGCTCTTCCGATC*T
iPCRindex47	CAAGCAGAAGACGGCATACGAGATGAAGCATAATAGAGATCGGTCTCGGCATT CCTGCTGAACCGCTCTTCCGATC*T
iPCRindex48	CAAGCAGAAGACGGCATACGAGATATACAGTCGCTGAGATCGGTCTCGGCATT CCTGCTGAACCGCTCTTCCGATC*T
iPCRindex49	CAAGCAGAAGACGGCATACGAGATCTGTCGCAAGGGAGATCGGTCTCGGCATT CCTGCTGAACCGCTCTTCCGATC*T
iPCRindex50	CAAGCAGAAGACGGCATACGAGATTGCAATCTAACGAGATCGGTCTCGGCATT CCTGCTGAACCGCTCTTCCGATC*T

2.3 Media and stock solutions

RPMI/PS: 10.0 mL penicillin; 1.0 L RPMI prepared in-house by QIMRB core services

PBS: Prepared in-house by QIMRB core services

5% sucrose water: 5.0 gm sucrose; 100.0 mL sterile milli-Q water

0.2mg/mL Anhydrotetracycline hydrochloride (ATc): Anhydrotetracycline hydrochloride (ATc) Sigma-Aldrich 20.0 mg; 2.6 mL of absolute ethanol; 100.0 mL of 5% sucrose water of ATc and dissolve in 2.6 mL ethanol to prepare ATc stock concentration 7.5 mg/mL.

FACS Buffer: Bovine serum albumin (BSA) (Life Technology) 100g/L; 10%w/v Sodium Azide 1mL/L; 0.5M EDTA in PBS pH8 (Sigma) 10mL/L; 1L PBS; filtered and de-gassed through 0.2 μm bottle-top filter at 4ºC for 20 minutes.

FACS Block: Generated in-house by harvesting supernatant of 120/G8 hybridoma to block Fc receptor.

4% PFA: Paraformaldehyde powder (MP Biomedicals, USA) 4.0 g/100mL; PBS 100 mL; added ~20μL NaOH while gently heating and stirring until powder dissolves. Add HCL until pH is 7. Aliquots of this were stored at -20ºC until use. 1-2% PFA was made with the addition of PBS just prior to use.

1.6% saline (w/v): 1.6g of NaCl in 100.0 mL sterile milli-Q water

12% saline (w/v): 12g of NaCl in 100.0 mL sterile milli-Q water

33% percoll: 1:3 v:v of Percoll in PBS

ELISA bicarbonate coating buffer: 1.0 L PBS; 1.59 g Na_2CO_3; 2.93 g $NaHCO_3$; pH adjusted to 9.6; filtered

ELISA blocking buffer: 1.0 L PBS; 1% BSA; 0.05% Tween 20; filtered.

ELISA wash buffer: 0.5 mL Tween20; 1.0L PBS.

***Pc*AS and *Py*17XNL antigens:** prepared in house.

2.4 Methods

2.4.1 Setting up passage mice with parasitized RBCs

Non-lethal *Py*17XNL *and Pc*AS parasites were used after a single *in vivo* passage in wild type C57BL/6 mice. In order to conduct this procedure, 350 µl of the frozen stabilates were firstly thawed at room temperature – one fifth the blood volume of sterile 12% NaCl (w/v) (BDH Chemicals, Kilsyth, Victoria, Australia) was then added in drops into each thawed stabilate and incubated on ice for five minutes. RBCs were transferred into a 10 mL falcon tube and washed in ten times the blood volume of 1.6% NaCl (w/v) at 1200 rpm for 10 minutes at room temperature (RT). Supernatants were discarded and RBCs were then resuspended in 1.0 mL of sterile PBS. 200 ul of this preparation was then injected intravenously (i.v) into naive mice. Parasitemia was assessed on day 4 post-infection - mice were culled and used in subsequent procedures if the parasitemias were between 1-5%. In some experiments, lethal *Pb*ANKA parasites were used following a single *in-vivo* passage in C57BL/6 mice. For these passages, one vial containing approximately 350 µl of frozen *Pb*ANKA parasites was thawed, and 200 µl of this was injected via intraperitoneal (i.p.) route into C57BL/6 mice. Similarly, mice were culled and used in subsequent procedures at 1-5% parasitemia.

2.4.2 Infection of mice with parasitized RBCs

Passage mice were culled by CO_2 inhalation. Blood was then collected by cardiac puncture using an insulin syringe and washed in 10.0 mL of RPMI culture media containing heparin, penicillin and streptomycin, spinned at room temperature for seven minutes at 1200 rpm.Supernatants were discarded and pRBCs resuspended in 1.0 mL of RPMI/PS. Next, the total numbers of RBCs and parasitised RBCs were determined. Naive mice were infected i.v. with either 10^4 pRBCs (*Py*17XNL) or 10^5 pRBCs (*Pc*AS) or 10^5 pRBCs (*Pb*ANKA).

2.4.3 Cell counts

Red and white blood cells were stained with 0.1% w/v trypan blue (Sigma, St. Louis, Mo, USA) in PBS and counted using a haemocytometer under x10 objective on a light microscope. Dead cells were excluded based on the uptake of trypan blue. Viable cells in all 25 small squares on the hemocytometer were counted. The total number of cells in 1.0 mL of blood was calculated as cell count on haemocytometer x dilution factor x 1000 (volume of blood) x volume of the chamber (10^4).

2.4.4 Preparation of crude parasite antigen

Crude antigenic extract from *Py*17XNL or *Pc*AS-infected RBCs was prepared using an adapted version of a previously described protocol [132, 133]. Briefly, mice were infected with *Py*17XNL or *Pc*AS as described above. When parasitaemia reached 20-30%, blood was collected by cardiac puncture into heparinized tubes. RBCs were washed once in RPMI at 1200xg for 7 minutes at room temperature, and then lysed using ultrapure water followed by four washes in ice-cold PBS at 16,000xg for 25 minutes at 4^{o}C, and three cycles of freezing (2 hours at -80^{o}C) and thawing (30 minutes at room temperature). Extracts were also processed from RBCs of uninfected C57BL/6 mice for use as negative controls in ELISA. All extracts were stored at -80^{o}C until their use. These are the whole parasite crude antigens.

2.4.5 Quantification of protein concentration

The concentration of proteins in the purified extracts was determined by Bradford assay (Thermo scientific) according to the manufacturer's instructions. Briefly, two microliters of a serially diluted test sample or bovine serum albumin (BSA) (Sigma) proteins were added into a 96 well flat-bottomed tissue culture plate (Becton Dickinson Labware) that contained 200 µl per well of the protein assay reagent. Absorbance at 595 nm was read on a Biotek synergy H4 ELISA plate reader (Biotek, USA) and the concentration of the test sample calculated from the BSA protein standard curve.

2.4.6 Generation of immune serum

C57BL/6 mice were immunized against *Plasmodium yoelli* 17XNL, *Plasmodium chabaudi chabaudi* AS infection to generate immune serum, while age-matched control mice were maintained for non-immune serum. Passage mice were sets from a frozen stabilates (infected red blood cells) prior to infection. Mice were infected intravenously via a lateral vein with 1 x 10^4 (*Py*17XNL) or 1 x 10^5 (*Pc*AS and *Pb*A) freshly prepared parasitized RBCs (pRBCs). Parasitemia was monitored at different days post infection until resolution of infection. Parasite-specific antibody titer was measured before collecting cardiac blood to generate serum. Once parasite-specific antibody titer was reached a steadily state achieved then the mice were euthanized by CO_2 inhalation. Whole blood was collected via cardiac bleed using a 26 gauge insulin syringe with a needle into an eppendorf tube for serum collection. Prior to serum separation blood tubes were incubated at room temperature for 1

hour and then overnight at 4ºC. The blood samples were then centrifuged at 13000xg for 10 minutes at room temperature (RT) and serum was collected and sorted at -80ºC prior to use.

2.4.7 CellTrace™ Far Red (CTFR) labelling and adoptive transfer of donor pRBCs

Rodent malaria parasite-specific infected red blood cells were passaged through C57BL/6J mice prior to being used. Passage mice were selected for cardiac bleed when parasitemia of passage mice reached around 5% with mostly ring stage parasite life-cycle stages present. Whole blood was collected by cardiac bleed using a 26-gauge insulin syringe with a needle into 5mL RPMI/PS containing 5U/mL heparin sulphate. Heparinised donor blood containing pRBCs was washed twice in Ca^{2+}/Mg^{2+}-free phosphate buffered saline (PBS-A) at 1200xg for 10 mins at room temperature, then blood was resuspended in 5 mL PBS-A. A 50µg vial CellTrace™ Far Red (CTFR) was dissolved in 25µl of dimethyl sulphoxide (DMSO) for 10 mins prior to mixing with 5mL of resuspended RBC and then incubated for 20 minutes at room temperature on the roller. Cells were washed twice in 10x volume of PBS-A. Successful CTRF labeling of RBCs was confirmed by flow cytometry using a LSRII Fortessa analyzer (BD Biosciences) and Flowjo software (Treestar, CA, USA). CTFR-labelled RBC was resuspended in 2mL volumes per donor mouse, and injected in 200µl volumes via intravenous injection (i.v) using 26G needles.

2.4.8 *in vivo* Clearance/Growth Assay

In this thesis, I have used established mouse models of blood-stage *Plasmodium* infection to explore how parasites circulating in the bloodstream may be controlled by the host. Most importantly, I employed and further modified an RBC adoptive transfer approach developed in our laboratory to examine parasite clearance and replication *in vivo*. Hereafter I refer to this assay as the "Clearance/Growth" assay. This assay entails the study of a fluorescently-labeled single generation of infected parasitised RBC by flow cytometry [134]. In this assay, donor RBCs (including infected and uninfected RBCs) are labeled with fluorescent dye CellTrace™ Far-Red (CTFR), referred to as Generation 0 (Gen_0), and intravenously injected into recipient mice. Gen_0 pRBC were then tracked over time to observe the development of the parasites within the donor RBCs and their subsequent rupture and re-appearance as parasite progeny in recipient (ie. unlabelled) RBCs, referred to as Generation 1 (Gen_1 pRBC).

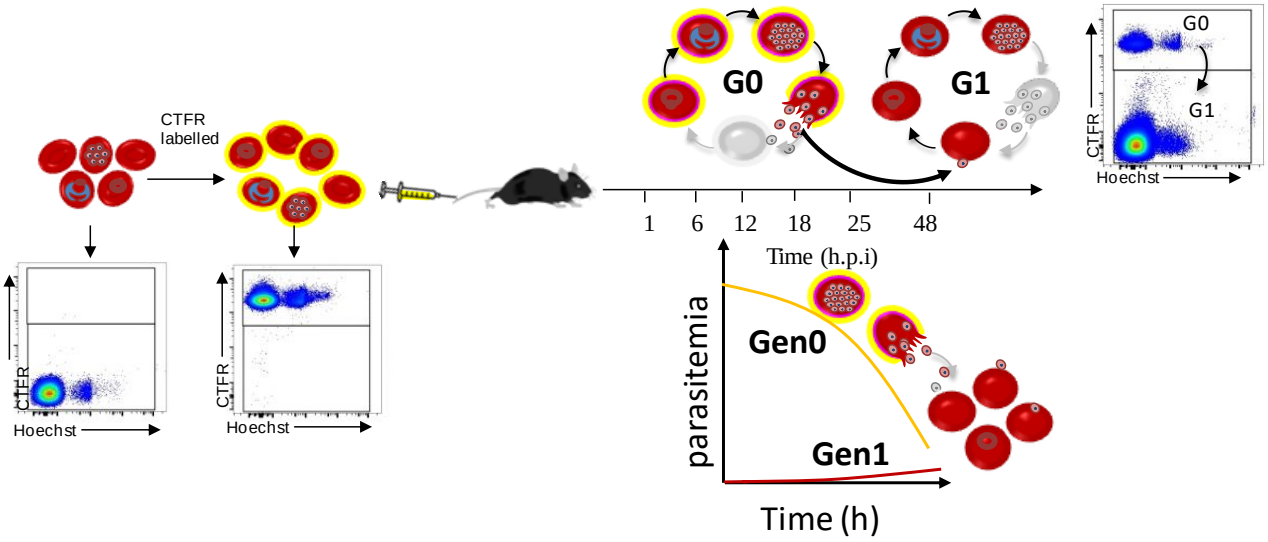

Figure 2.1 Clearance/Growth assay. *PbGFP-infected cardiac blood was labelled with CellTrace™ Far-Red (CTFR) washed and injected into recipient mice. Tail bleeds of recipient mice were done at 1-97 h.p.i and parasitemia measured by flow cytometry.*

2.4.9 Flow cytometric based quantification of parasitized RBCs

A modified protocol of a previously established flow cytometric method was employed to measure parasitemia more rapidly [135]. Briefly, a single drop of blood, from a tail bleed or cardiac puncture, was diluted and mixed in 250µl RPMI containing 5U/mL heparin sulphate. Diluted blood was simultaneously stained with Syto 84 (5µM; Life Technologies) to detect RNA/DNA, and Hoechst 33342 (10µg/mL; Sigma) to detect DNA, for 30 minutes, in the dark at room temperature. Staining was quenched with 10x volume of ice-cold RPMI, and samples were immediately analysed by flow cytometry, using a BD FACS CantoII analyser (BD Biosciences) and FlowJo software (Treestar, CA, USA). pRBC were readily detected as being Hoechst33342+ Syto84+, with white blood cells excluded on the basis of size, granularity, and much higher Hoechst33342/Syto84 staining compared to pRBC. Parasitemias were routinely measured daily for up to 50 days post infection.

2.4.10 Depletion of phagocytes

Mouse phagocytes including macrophages, monocytes, and dendritic cells were depleted with a single intravenous injection of a 200 µl volume of clodronate-containing liposomes (www.clodronateliposomes.com) via a lateral tail vein using 26G needles 3 days prior to infection [136, 137].

2.4.11 Depletion of complement factors C3/C5

To deplete mice of the complement components C3/C5, 10µg of Cobra Venom Factor (CVF) (Quidel) was injected intraperitoneally 16 hr prior to infection (day -1), and then daily on days +1, +2 and +3; control mice were injected with saline. To evaluate the efficacy of CVF treatment, C3 depletion efficacy was measured in serum by sandwich enzyme-linked immunosorbent assay (ELISA). Costar EIA/RIA 96-well flat bottom plates were coated overnight at 4ºC with 2.0µg/mL primary antibody (Goat IgG Fraction to Mouse Complement C3, MP Biomedicals) in PBS. Wells were washed three times (all washes in 0.005% Tween in PBS) and then blocked for 1 hr at room temperature (RT) with 1% BSA in PBS. Wells were washed three times, and 100µl of sera in duplicate at 1/9000 and 1/27000 was added and incubated for 1 hr at RT. Following six washes, wells were incubated in the dark with a secondary antibody (Peroxidase-Conjugated Goat IgG Fraction to Mouse Complement C3, MP Biomedicals) for 1hr at RT. Unbound antibodies were washed off six times prior to incubating wells in the dark with streptavidin HRP (BD Biosciences) for 30 mins at RT. Wells were washed six times prior to development with the substrate (OPD; Sigma-Aldrich) for five minutes in the dark before termination with 1M HCl. Absorbance was determined at 492nm using Biotek synergy H4 ELISA plate reader (Biotek, USA).

2.4.12 *In vivo* and *in vitro* staining of pRBCs with antibodies in immune serum with/without permeabilisation

In vivo and *in vitro* staining of pRBCS was done in diluted blood collected from infected mice receiving immune serum, non-immune serum or no serum. Briefly, diluted blood was incubated with/without anti-RBC antibody 34-3C as primary antibody (1.5µg/mL; ab109101). Cells were washed three times in FACS buffer (1% w/v BSA (Life technologies), 5mM EDTA in PBS) prior to incubation with secondary antibody FITC Goat anti-mouse IgG (3µg/mL; Biolegend, San Diego, CA). In order to fix and permeabilise the pRBCs, diluted blood was mixed with cytofix buffer (BD Cytofix/Cyto perm^{TM} solution kit from BD Life Sciences) at 1:1 volume and then incubated with anti-RBC antibody 34-3C (1.5µg/mL) and immune and non-immune serum in 1X cytoperm buffer. Cells were washed in 1X cytoperm buffer (BD Life Sciences) prior to incubation with secondary antibody FITC-goat anti-mouse IgG (3µg/mL). Then cells were stained with cell-permeant RNA/DNA stain, Syto™ 84 (5 µM; Life Technologies) and with DNA stain, Hoechst 33342 (10 µg/mL; Sigma). Staining was quenched with 10 volumes of ice-cold RPMI medium, and samples were analysed immediately by flow cytometry using a LSRII Fortessa analyser (BD Biosciences) and FlowJo software (Treestar, CA, USA).

2.4.13 Estimation of *Plasmodium*-specific immunoglobulins in serum by ELISA

Costar EIA/RIA 96-well flat bottom plates were coated overnight at 4^{o}C with 100µL/well of 2.5µg of soluble antigen/mL in bicarbonate coating buffer. Wells were washed three times (all washes in 0.005% Tween in PBS) and then blocked for 1hr at 37^{o}C with 1% BSA in PBS (Blocking buffer). Wells were washed three times and 100µL of sera diluted to 1/400, 1/800, 1/1600 or 1/3200 was added before being incubated for one hour at 37^{o}C. Following six washes, wells were incubated in the dark with biotinylated anti-total IgG for one hour at room temperature. Unbound antibodies were washed off (six times) prior to incubation with streptavidin HRP in the dark for 30 minutes at room temperature. Wells were washed six times and developed with 100µL of OPD for 3-5 minutes in the dark before termination with an equal volume of 1M HCl. Absorbance was determined at 492nm using a Biotek synergy H4 ELISA plate reader (Biotek, USA). Data were analysed using Gen5 software (version 2) and GraphPad Prism (version 6).

2.4.14Preparation of vector DNA for transfection

To minimise expenses and labour in DNA production, a pooled midiprep procedure was adopted to produce the DNA for transfection in *P. berghei* experiments. Vectors were generated using

a 96-well method (detailed protocol described in [138]). Vectors were inoculated from a master plate of glycerol stocks (-80ºC) in 1 mL of TB-kan (30 µg/mL kanamycin) in a 96-deep well plate and incubated overnight at 37ºC with shaking. For each transfection, two wells were inoculated with each vector to be used in an experiment. Following the overnight incubation, all wells from a single experiment were pooled together and then processed with a QIAFilter Midi kit (according to manufacturer's instructions, however using 2x volumes of P1, P2 and P3 due to the use of a low copy vector). The resulting DNA was spiked with additional DNA for 7 reference vectors (prepared by Ana Rita Gomes) – 4 redundant in the blood stages: *p25*, *p28*, *soap*, *p230p*; and three known to result in attenuated growth: *plasmepsin IV*, *methyltransferase-like protein, putative* and *oxoisovalerate dehydrogenase subunit beta, mitochondrial, putative (BCKDHB)*. The use of these universal reference vectors allowed the calibrated comparison of all *Plasmo*GEM barseq experiments. The pooled DNA was digested then with NotI, precipitated with isopropanol and resuspended in 6 µl TE buffer in preparation for transfection.

2.4.15 Schizont preparation and transfection

Plasmodium berghei was isolated from thicket rats of central Africa as these animals are one of the natural hosts for this rodent malaria parasite. For *in vitro* schizont cultures, parasites were first passaged into female Wistar rats to achieve maximal transfection efficiency. A female Wistar rat was infected by intraperitoneal (i.p) injection and monitored until blood parasitemia reached 1-3%. Infected blood was then harvested by cardiac puncture and prepared as a schizont culture: 25x blood volume schizont medium (RPMI 1640 supplemented with 25mM L-glutamine, 25mM HEPES, 10mM NaHCO3, 100 U/mL penicillin/streptomycin and 25% fetal bovine serum) was added and the flask gassed for 90 seconds with malaria gas mixer (1% O_2, 3% CO_2, 96% N_2) before incubating overnight with shaking. The next day, smeared thin blood film was prepared from the culture to check for the presence of mature schizonts and these were purified on a 55% Nycodenz/PBS (v/v) cushion with low brake. The schizont-containing interface was collected with a Pasteur pipette and washed with schizont medium. Schizonts were pelleted by centrifugation (at 500 x g for 2 mins), and the pellet resuspended in 16 µl P3 solution (Lonza). The 6 µl vector pool was then added to this mixture and transfection was carried out in 16-well Lonza cuvette strips with the programme, FI-115. The transfection mixture was immediately injected intravenously into the tail veins of 6-8 week old, C57BL/6 (B6), *rag1*$^{-/-}$, Balb/c and SCID mice. The next day, drinking water was supplemented with pyrimethamine to begin selection (0.7 mg/mL).

2.4.16 Blood DNA extraction by phenol-chloroform methods

DNA was purified by phenol-chloroform extraction for a maximal yield of DNA from low parasitemia samples. Red blood cells were lysed by adding 10 pellet volumes of ammonium chloride lysis buffer 0.15M NH_4Cl, 0.01M $KHCO_3$, 1mM Na_2EDTA; pH 7.4) and incubating on ice for 5 minutes. The lysate was centrifuged (at 5000xg for 5 mins) and the parasite pellet resuspended in 500 µl TNE buffer (50mM Tris-HCl, 100mM NaCl, 5mM EDTA; pH 8.0). Two µl of RNase A (20 mg/mL) and 55 µl of 10 % SDS was added to the resuspended pellet and incubated for 10 minutes at 37°C. Subsequently, 10 µl of proteinase K (20 mg/mL) was added and the mixture was vortexed and incubated at 37 °C for 30 minutes. The lysate was combined with 500 µl of 25:24:1 phenol:chloroform:isoamyl alcohol, mixed by thorough shaking and then centrifuged for (at 10000g for 5 mins). The aqueous supernatant was transferred to a new tube and 500 µl of chloroform-isoamyl alcohol was added. The tube was mixed thoroughly and then centrifuged (at 10000g for 5 mins). The aqueous phase was transferred to a new tube, 3µl of pellet paint (co-precipitant) was added and the DNA was precipitated overnight at -20^{o}C after the addition of 500 µl isopropanol. The isopropanol was then removed and the pellet dried and then resuspended in 50 µl or 100 µl of TE buffer.

2.4.17 Perfusion, organ harvest and genomic DNA extraction

On day 7 post-infection, mice were terminally anesthetised, perfused and organs (including spleen, lung, heart, brain, liver, kidney and adipose tissue) were collected. Each tissue sample was weighed and preserved at -80^{o}C prior to DNA extraction. Samples were mashed using a tissue homogenizer in 500µl PBS and 100µl of mashed tissue (for spleen 50µl) used for DNA extraction using Qiagen DNeasy Blood and Tissue kit (according to the manufacturer's instructions).

2.4.18 Barcode amplification

PCR was used to amplify barcodes from the extracted genomic DNA. A 50µl Advantage 2 Polymerase reaction was prepared, according to the manufacturer's instructions, with the primers, arg91 and arg97 [139]. One µl (5-7ng) of phenol-chloroform extracted gDNA was used as the template for the reaction. The protocol for the PCR was as follows: 95^{o}C 5' //95^o C 30" / 55^o C 20" / 68^o C 8" (x35) // 68^o C 10' //. Barcodes were amplified in parallel from a final sample to yield the 'input pool' i.e. the DNA used for transfection. This parallel amplification was important to ensure that absence of a barcode in the population was not due simply to a failure of the bacteria carrying

that vector to grow. 5 µl of the product from the first PCR reaction was used as the template for a subsequent PCR reaction, in which Illumina adapters were added (to adhere the product to the Illumina flow cell), and index tags were inserted (to allow the sample corresponding to each read to be determined after sequencing). The PCR parameters were as follows:

95º C 5' // 95º C 30" / 68º C 15"(x10) // 68º C 5' //

Following the second PCR, DNA was purified using a QIAGEN MinElute PCR purification kit. Eluted DNA was quantified using the Qubit system and 100 ng of each sample was taken and pooled together. Up to 48 samples were sequenced per run of the Illumina sequencer. A water control was used throughout the entire experiment to ensure that reagents were not contaminated with trace amounts of barcodes.

2.4.19 Barcode sequencing

Due to their low complexity, PCR amplicon libraries were further diluted to 1nM and then spiked with 40-50% of PhiX before being loaded at a low cluster density (4 x10^5 clusters/mm2). All samples were loaded and run on a MiSeq instrument by the low-throughput Illumina. Reads were paired-end and 150 nucleotides in length collected. These steps were conducted by the Sanger Institute Illumina C team.

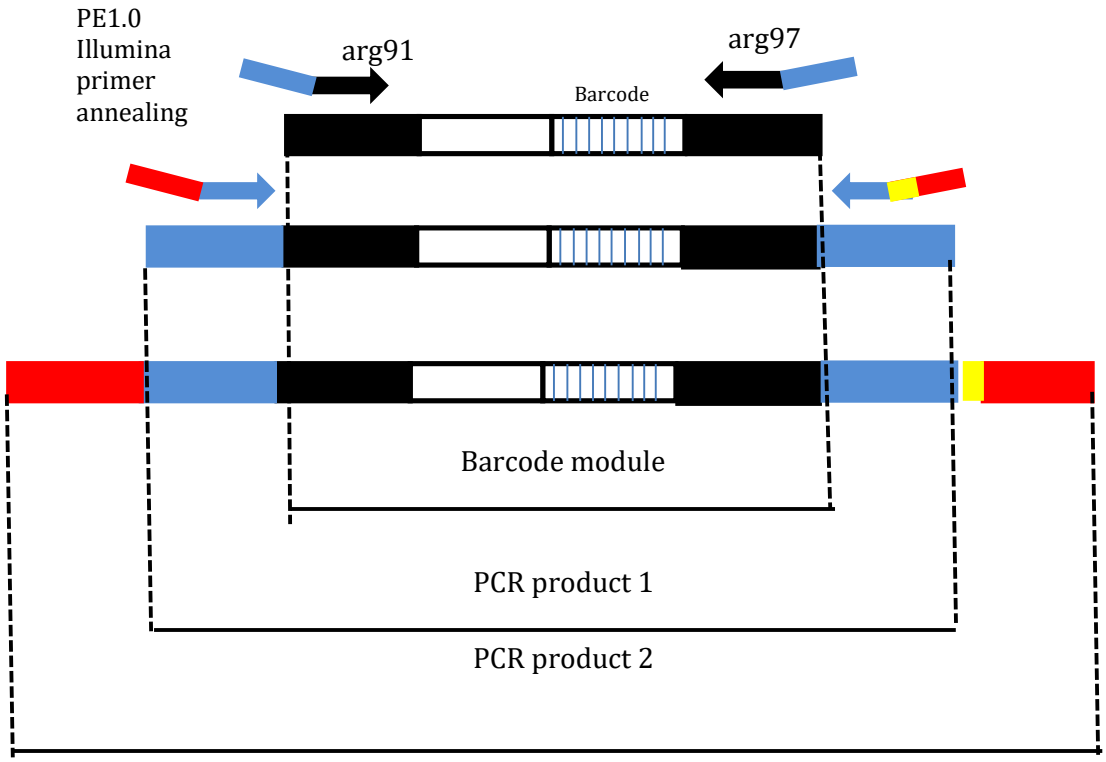

Figure 2.2 Schematic of the barcode module *illustrating primer annealing sites and amplification steps.*

2.4.20 Analysis of barcode-based sequencing data

Using a Perl script written by Frank Schwach, barcode sequences were extracted from the sequencer output files (*fastq*) and total numbers of barcodes (***b***) for each gene ***(g)***, for every time point (***d***, 4-7), for each mouse (***m***, 1-3) was calculated, (i.e., $\boldsymbol{bd, m, g}$). This was also calculated for the input samples.

The relative abundance (***p,*** proportion) of each barcode ($\boldsymbol{p\ d, m, g}$) within the pool was then determined by dividing the number of barcodes of each gene by the sum of barcodes for all genes of each sample (represented by the index tag), i.e.

$$\boldsymbol{p\ d, m, g = \frac{bd, m, g}{\sum_{G0}^{Gn} b, d, m, g}}$$

Note: The quantification was considered reliable for barcodes accounting for at least 0.1% of all counts.

The daily fold-change (***c***) of the relative abundance of each mutant ($\boldsymbol{cd, m, g}$) was determined by dividing the relative abundance of each mutant on a particular day by the relative abundance of that mutant on the previous day, i.e.:

$$\boldsymbol{cd, m, g = \frac{pd + 1m, g}{pd, m, g}}$$

The relative fitness (***f***) of a mutant ($\boldsymbol{fd, m, g}$) was calculated by normalizing the fold-change of a mutant using the mean fold-change of the reference mutants ($\boldsymbol{\frac{1}{n}\ \sum_{R0}^{Rn} Cd, m, Rn}$) .

$$\boldsymbol{fd, m, g = \frac{Cd, m, g}{\frac{1}{n}\ \sum_{R0}^{Rn} Cd, m, Rn}}$$

Note: Barcode sequencing analysis of the blood samples was based on the **fitness value** at Day 7, whereas for the tissue sample was based on **relative abundance** at Day 7.

2.4.21Statistical analysis

Comparisons between two groups were performed using non-parametric Mann-Whitney (unpaired datasets or Wilcoxon (paired datasets) tests. Where depicted, one-way or two-way ANOVA and Tukey's post-test were employed for multiple comparisons among three or more groups. $p<0.05$ was considered significant ($p<0.05$=*; $p<0.01$=**; $p<0.001$=***; $P<0.0001$=****). Graphs depict mean values (SEM), except where individual mouse data points are depicted, in which case median values are shown. All statistical analyses were performed using GraphPad Prism 6 software.

Chapter Three:

Exploring mechanisms of parasite control during blood-stage *Plasmodium* infection

3.1 Abstract

Symptoms of malaria occur during the blood-stage of infection and can vary from asymptomatic infections to life-threatening syndromes such as cerebral malaria. Disease severity often correlates with the number of blood-stage parasites in the body. It is likely that both host and parasite factors are involved in determining parasite growth kinetics *in vivo*. However, our understanding of these factors is incomplete. Given that an effective malaria vaccine currently remains elusive, and that resistance has emerged against the currently available anti-malarial drugs, it is important to identify new approaches for controlling the number of parasites *in vivo*.

Here, I have used experimental mouse models of blood-stage *Plasmodium* infection to directly measure parasite maturation, clearance and replication rates *in vivo*. I observed that parasite control can be achieved in a number of ways including (i) anti-malarial drugs that inhibit or arrest parasite development within a red blood cell, (ii) drugs that prevent parasites from progressing from one generation of red blood cells to another, (iii) by host phagocytes actively removing parasitised red blood cells, and (iv) by host-mediated impairment of parasite maturation within red blood cells.

3.2 Introduction

Blood-stage malaria initiates once the merozoite form of the *Plasmodium* parasite invades host RBCs and enters the intra-erythrocytic stage of its life-cycle. This includes progression through ring, trophozoite and schizont stages before each parasitised RBC ruptures to release tens of daughter merozoites that go on to invade new RBCs. The severity of the disease, particularly elicited in humans by *P. falciparum*, strongly correlates with the total number of parasites in the body. Thus parasite load, disease severity and infection outcome can be considered to be determined by two opposing biological processes: 1) how effectively the host can control parasite numbers, and 2) how efficiently parasites can replicate within the host. The rate of parasite replication is dependent on multiple factors, such as the replication efficiency of the parasite (including the number of merozoites produced from each parasite, their survival capacity, and ability to invade RBC's). The host mononuclear phagocytic system (MPS) is thought to play a major role in controlling infection, for example via removal of parasitized RBC by macrophages in the spleen and liver [86]. Similarly, splenic function increases during acute malaria [140, 141], and parasite clearance can be delayed in splenectomized patients after artesunate treatment [142]. It has been shown in animal models that the spleen could remove intraerythrocytic parasites leaving the RBC intact, a process called "pitting" [143]. Thus splenic "pitting" is thought to be a host mechanism of parasite removal. However, despite these reports, *in vivo* mechanisms of parasite clearance in blood-stage malaria remain unclear. Moreover, we have defined "delayed maturation" as a theoretical mechanisms by which parasites growth could be controlled. Parasites with delayed maturation perhaps represented drug-mediated or immune-damaged parasites with impaired development which occurs as a parasite survival mechanisms in response to environmental stress [122, 144].

In this chapter, I sought to investigate host mechanisms of parasite control during blood-stage malaria in an established mouse model, *Plasmodium berghei* ANKA (*Pb*ANKA) infection of C57BL/6J mice, both in the presence and absence of anti-malarial drugs. I have also used our laboratory's unique *in vivo* Clearance/Growth assay to examine in detail the biology of a single cohort of pRBC. *Pb*ANKA infection of C57BL/6J mice is a lethal model, since it induces symptoms similar to those in the human severe malaria, and has been used predominantly to study pathology associated with cerebral malaria. [145]. However, recent reports show that in addition to cerebral symptoms, *Pb*ANKA infection causes widespread pathology such as liver damage, respiratory distress and metabolic acidosis [146-150]. Even though the pathogenesis of human severe malaria is not fully understood, disease severity strongly correlates with total numbers of parasites in the body, i.e., the sum of those circulating freely in the bloodstream and those sequestered in tissues [151]. The infection is typically fatal within a relatively short timeframe (approximately one week) [146].

Artesunate (an artemisinin derivative) is a WHO-recommended treatment for patients with uncomplicated malaria, due to its faster reduction in parasitemia compared to previous anti-malarials [22-24]. A unique feature of artesunate is that it appears to target a wide range of parasite developmental stages [25]. The clearance of artesunate-treated, killed or damaged parasites are thought to be accelerated by host immune mechanisms [122, 124]. Currently, the rate of parasite disappearance from circulation following drug treatment is used to detect parasite resistance to artemisinins [152-154]. Furthermore, it is hypothesised by some [155, 156], that the total reduction of parasites after drug treatment is dependent on 1) drug-mediated killing or impairment of parasite development [157], and 2) host-mediated clearance [126].

Many studies have reported that the emergence of resistance in Southeast Asia is due to the short course of Artesunate monotherapy [26, 158]. Since artesunate is a short-acting drug, it has been combined with longer-acting antimalarial drugs to increase efficacy and prevent/delay the development of resistance. These regimens, of which there are several, are collectively termed Artmisinin-based Combination Therapies (ACT)[159, 160]. Artesunate-mefloquine is one of the five ACTs recommended by the WHO for the treatment of uncomplicated malaria (WHO 2015). Many studies have reported that the combination of short-acting artemisinin derivative (artesunate) with longer acting mefloquine is effective in the treatment of uncomplicated, multi-drug resistant malaria [161-163], and that mefloquine has an effect on the asexual form of the parasite (schizontocidal effect). Despite intensive research into anti-malarial drugs, there remains some debate regarding the mode of action of artemisinins. It may be beneficial to better understand mechanisms of anti-malarial drug action *in vivo*, particularly to aid the design of next-generation anti-malarial drug therapies.

3.3 Results

3.3.1 Artesunate effectively controls ongoing *Plasmoduim berghei* ANKA (*Pb*A) infection *in vivo*

Before exploring *in vivo* mechanisms of action for artesunate, it was important to first confirm that artesunate was indeed effective in mice infected with *Pb*ANKA (*Pb*A). To do this, mice were infected with *Pb*A, and artesunate treatment was initiated 5 days post-infection when mice are known to exhibit signs of severe malaria such as liver damage [164] [165]. Parasitemia was measured daily using flow cytometry from day 0 – day 5 p.i. and every 12 h following initiation of treatment with 200 µg doses of sodium Artesunate (i.e. 10 mg/kg, every 12h for 2.5 days) or control saline. All mice in the control group (6/6) exhibited high clinical scores, requiring euthanasia between days 6-9 (6/6). In contrast, none of the treated mice (0/6) exhibited serious illness by day 13 (0/6), although parasitemia increased, as expected, once artesunate cover was removed (Figure 3.1). Thus, the data confirmed that artesunate was effective as a short-acting drug against *Pb*A infection in mice, which permitted further studies into *in vivo* mechanisms of action of this anti-malarial drug.

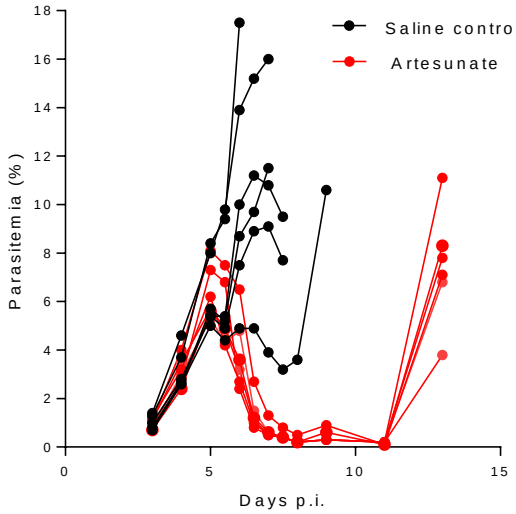

Figure 3.1 Effectiveness of Artesunate in vivo. *The time course parasitaemia due to Plasmodium berghei ANKA in the saline control (black) and Artesunate-treated (red) mice analysed. C57BL/6J (n = 5/group) mice were infected intravenously with 1x10^5 pRBCs of Plasmodium berghei ANKA (PbA) and parasitemia was measured was measured daily beginning at the day 3 p.i., 200µg of Artesunate (red) or saline controls (black) was administrated for every 12h (beginning at the day 5 p.i) for 2.5 days. Data representative of two independent experiments showing similar results.*

3.3.2 *In vivo* anti-malarial drug treatment prolongs the presence of Gen_0 parasites in the circulation

To investigate mechanisms of action of different anti-malarial drugs, I used the *in vivo* Clearance/Growth assay, as described in detail in the Material and Methods, in which a single generation of fluorescently-labeled infected parasite "donor pRBCs" are infused and tracked *in vivo* [134]. This approach differentiates a single generation of parasites from their progeny, i.e. the donor pRBCs that we transfused into the recipient mice, which we define as Gen_0, from the progeny of these transfused parasites in unlabelled (i.e. recipient) RBCs, defined as Gen_1. We transfused mice with labelled Gen_0 pRBCs, immediately treated with different doses of artesunate, mefloquine or control saline and examined Gen_0 and Gen_1 pRBC over time (Fig 3.2A & B). Mefloquine is thought to cause slower declines in parasite numbers compared to artesunate, but has a longer half-life and works by destroying the asexual blood form of the parasite [163]. Therefore, I examined the effects of mefloquine on parasite clearance (Gen_0) and growth (Gen_1).

Anti-malarial drugs (artesunate and mefloquine) were effective in controlling total parasitemia in a dose-dependent manner (Figure 3.2C). Next, I analysed the removal of Gen_0 pRBCs after treatment with anti-malarial drugs to measure increases in the parasite clearance due to treatment. In control-treated mice, Gen_0 pRBCs were largely absent from the circulation by ~24 h, as expected, whereas artesunate or mefloquine-treated mice showed a dose-dependent increase in the numbers of Gen_0 pRBCs remaining in the circulation (Figure 3.2D). The data indicated that artesunate had not accelerated the rate of removal of Gen_0 pRBC, and instead had caused them to remain in circulation for longer (Figure 3.2E). As a result, transitioning of the parasite from Gen_0 to Gen_1 was restricted (Figure 3.2 F & G). Together, these data suggested that anti-malarial treatment caused Gen_0 parasite to remain in circulation longer than without treatment by preventing parasite transition from one generation to the next.

A.

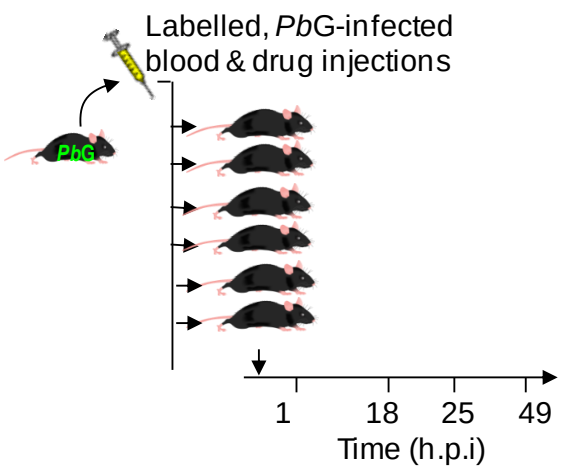
Labelled, PbG-infected
blood & drug injections
PbG
1
18
25
49
Time (h.p.i)

B.

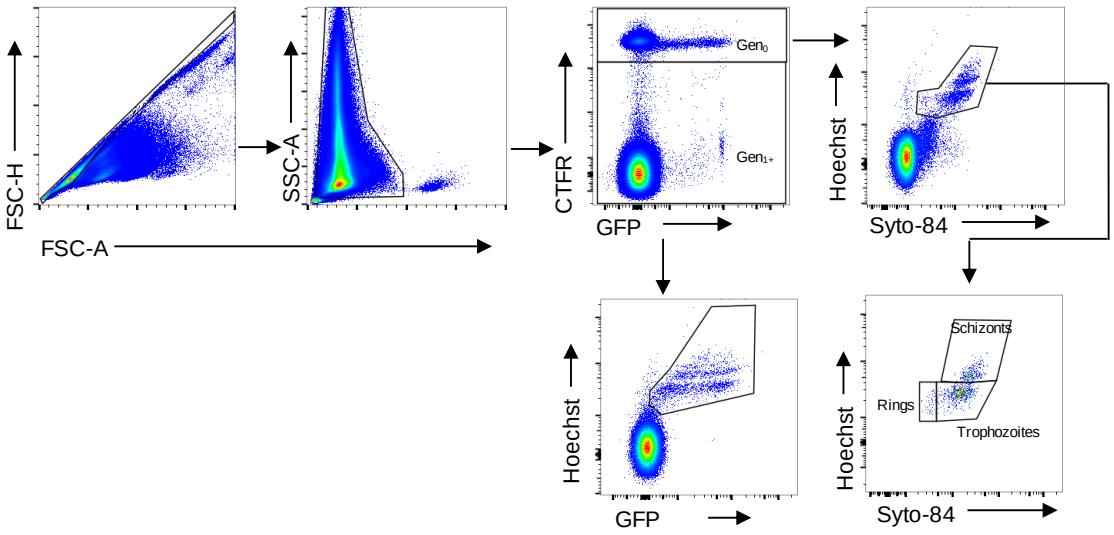
FSC-H
FSC-A
SSC-A
CTFR
Gen0
Gen1+
GFP
Hoechst
Syto-84
Schizonts
Rings
Trophozoites

C.

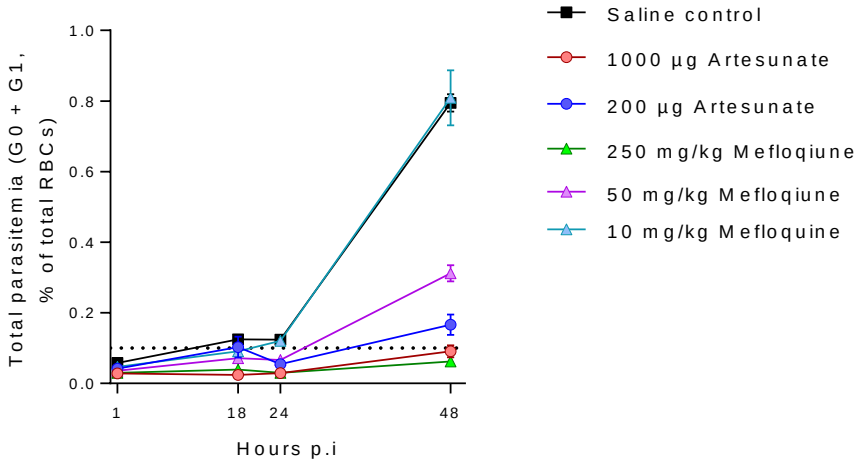
Total parasitemia (G0 + G1, % of total RBCs)
1.0
0.8
0.6
0.4
0.2
0.0
1
18
24
48
Hours p.i
Saline control
1000 µg Artesunate
200 µg Artesunate
250 mg/kg Mefloqiune
50 mg/kg Mefloqiune
10 mg/kg Mefloquine

D. Gen_0 (CTFR$^+$)

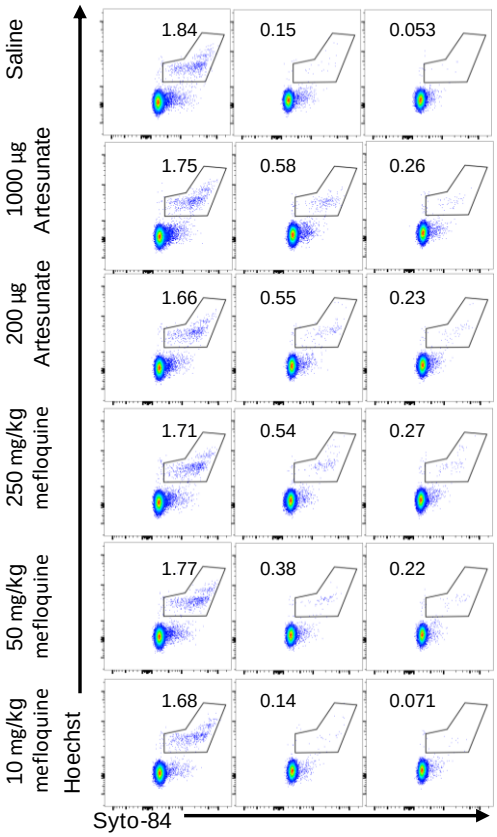

E.

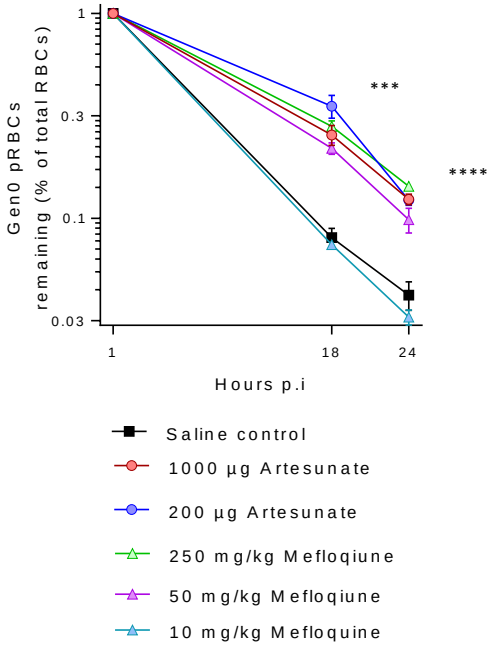

F Gen_{1+} (CTFR$^-$)

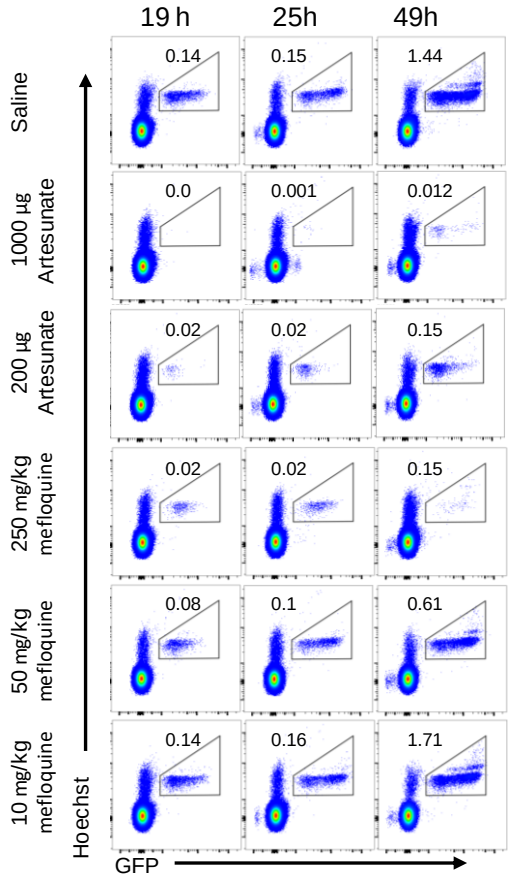

G

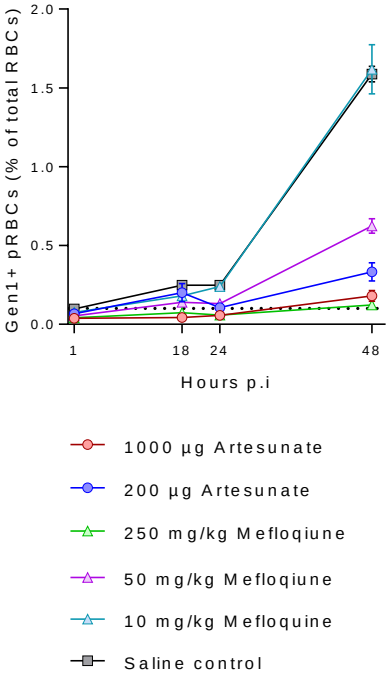

Figure 3.2 In vivo antimalarial treatment causes parasites to linger in the circulation. *(**A**) Naïve mice were intravenously injected with fluorescently labelled P. berghei ANKA-GFP (PbG) infected blood were immediately treated with saline (black/grey) or 1000 µg artesunate (red), or 200 µg artesunate (blue), or 250mg/kg mefloquine (green), or 50 mg/kg mefloquine (pink) or 10 mg/kg mefloquine (purple). (**B**) The gating strategy identified single cells and RBCs, differentiated unlabelled endogenous RBC and adoptively transferred donor RBCs by fluorescent CTFR labelling, identified all parasitised RBC and endogenous RBC (Gen_1 pRBC) by Hoechst DNA labelling and GFP expression, and infected donor cells (Gen_0 pRBC) and the stage of parasite maturation by Hoechst DNA and Syto 84 DNA/RNA labelling. (**C**) Total parasitaemia, (**D**) Representative FACS plots for donor Gen0 pRBC, and (**E**) Proportion of G0 pRBC remaining for 1-25 h.p.i (**F**) endogenous Gen1 RBC with pRBC gates are shown for 19-49 h.p.i and (**G**) parasitaemia of endogenous Gen1 pRBC were calculated. Dotted lines = detection thresholds. (n = 5 per group, error bars are SEM, p<0.001 = ***, p<0.0001 = ****). Data representative of two independent experiments showing similar results.*

3.3.3 Examination of the modes of action for aresunate-mefloquine combined therapy

Here, fluorescently labeled *Pb*G infected blood was transferred into recipient mice and immediately treated with a combination of 200 µg artesunate and 50 mg/kg mefloquine, with either drug alone, or with vehicle alone (Figure 3.3A). All drug therapies caused Gen_0 pRBC to remain in the circulation (Figure 3.3B & C), with artesunate-mefloquine combined treatment exhibiting the strongest effect. Next, I observed that mefloquine alone modestly slowed growth in Gen_1 pRBC (Figure 3.3D). As expected, artesunate alone was effective at preventing detection of Gen_1 pRBC; however, the combination therapy was the most efficient, demonstrating that the combined treatment maintained parasitemia below the level of detection, over time (Fig 3.3E). Together, these data demonstrated that an established ACT regimen did not accelerate the removal of pRBC, and instead, served to prevent parasites transitioning from one generation of RBC to the next.

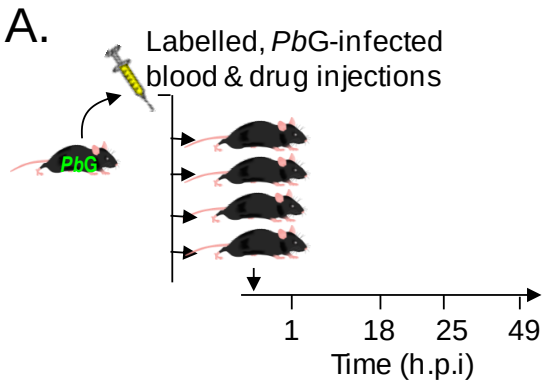

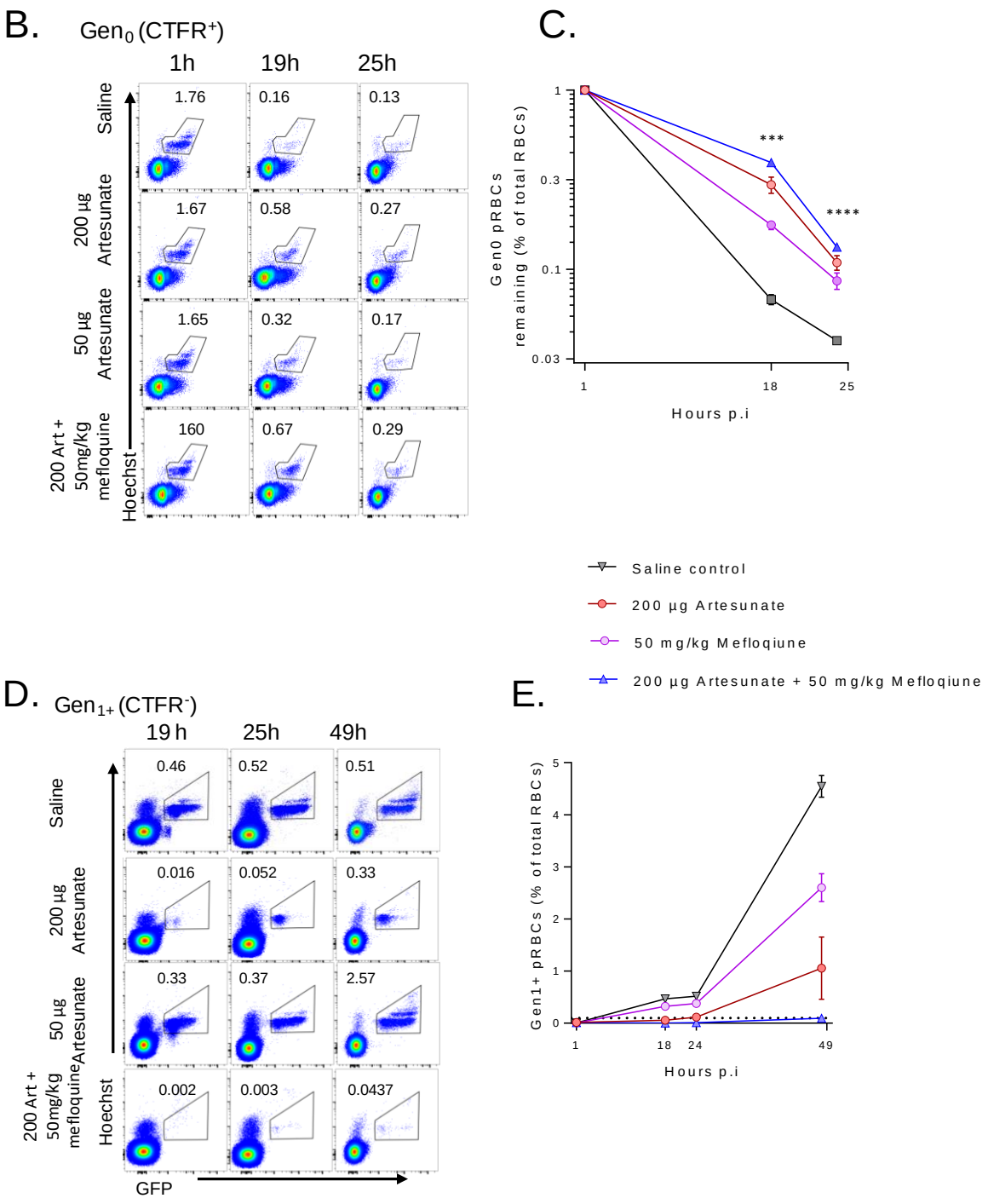

Figure 3.3 Combination therapy with artesunate and mefloquine had strongest effects on parasite persistance and growth. ***(A)*** *Recipient mice were injected with fluorescent-labelled PbG infected blood and immediately treated with control vehicle (black/grey), 200 µg Artesunate (dark red), 50 mg/kg Mefloquine (purple) or both the Artesunate and Mefloquine doses (royal blue). Tail bleeding of the recipient mice was done 1-97 h.p.i at different intervals and parasitaemia measured by flow cytometry.* ***(B)*** *Representative FACS plots showing G0 pRBC gates in vivo over time and* ***(C)*** *Proportion of G0 pRBC remaining for 1-25 h.p.i.* ***(D)*** *endogenous Gen1 RBC with pRBC gates are shown for 19-49 h.p.i and* ***(E)*** *parasitaemia of endogenous Gen1 pRBC were calculated. Dotted lines = detection threshold. (n = 5 per group, error bars are SEM, p<0.001 = ***, p<0.0001 = ****). Data representative of two independent experiments showing similar results.*

3.3.4 Splenectomy does not alter the clearance of Gen_0 pRBC from the circulation

The spleen is thought to play many important roles during malaria, in clearance of damaged pRBCs from circulation [126], pitting of pRBC [166], and the generation of pathogen-specific immune responses [reviewed in [127, 167]. The importance of the spleen in malaria was revealed by studying splenectomized humans and rodents. It was suggested that splenectomized malaria patients had elevated parasitemias and prolonged parasite clearance times after anti-malaria treatment [126, 168]. Further study in animal model suggests that host defense in primary malaria infection requires intact spleen [169-171]. However, the precise role of the spleen in clearing pRBC during malaria, either in the presence or absence of anti-malarial drug treatment, remains unclear. It has evidenced in animal models studies that spleen could remove intraerythrocytic parasites leaving host erythrocytic intact, a process called pitting [143] and splenic pitting is thought to be a host mechanism of parasite removal.

To examine the role of the spleen in clearing pRBC from circulation, splenectomized and sham-operated control mice were infected with fluorescently-labelled, *Pb*G-infected blood, either in the presence or absence of artesunate treatment (Figure 3.4A). Surprisingly, in the absence of any drug treatment, surgical removal of the spleen did not alter the clearance of G_0 pRBC from circulation (Figure 3.4B & C). In contrast, in the presence of artesunate treatment, splenectomised mice removed G_0 pRBC at a slower rate than sham-operated controls (Figure 3.4C). This suggested firstly that the spleen is not absolutely essential for pRBC, and raised the possibility that other organs might be able to compensate the absence of a spleen. In contrast, however, removal of drug affected parasites was impaired by splenectomy. This suggests that the spleen is required for removing drug-affected, and possibly dead parasites. Moreover, given the lack of effect on ring-stage parasites (Figure 3.4F), it appears that the spleen is likely capable of removing later-stage parasites more effectively that early rings. However, splenic removal of drug affected parasites did not alter control of Gen_1 parasite growth (Figure 3.4 D & E), which suggested that artesunate-affected parasites removed by the spleen were likely dead or incapable of replication.

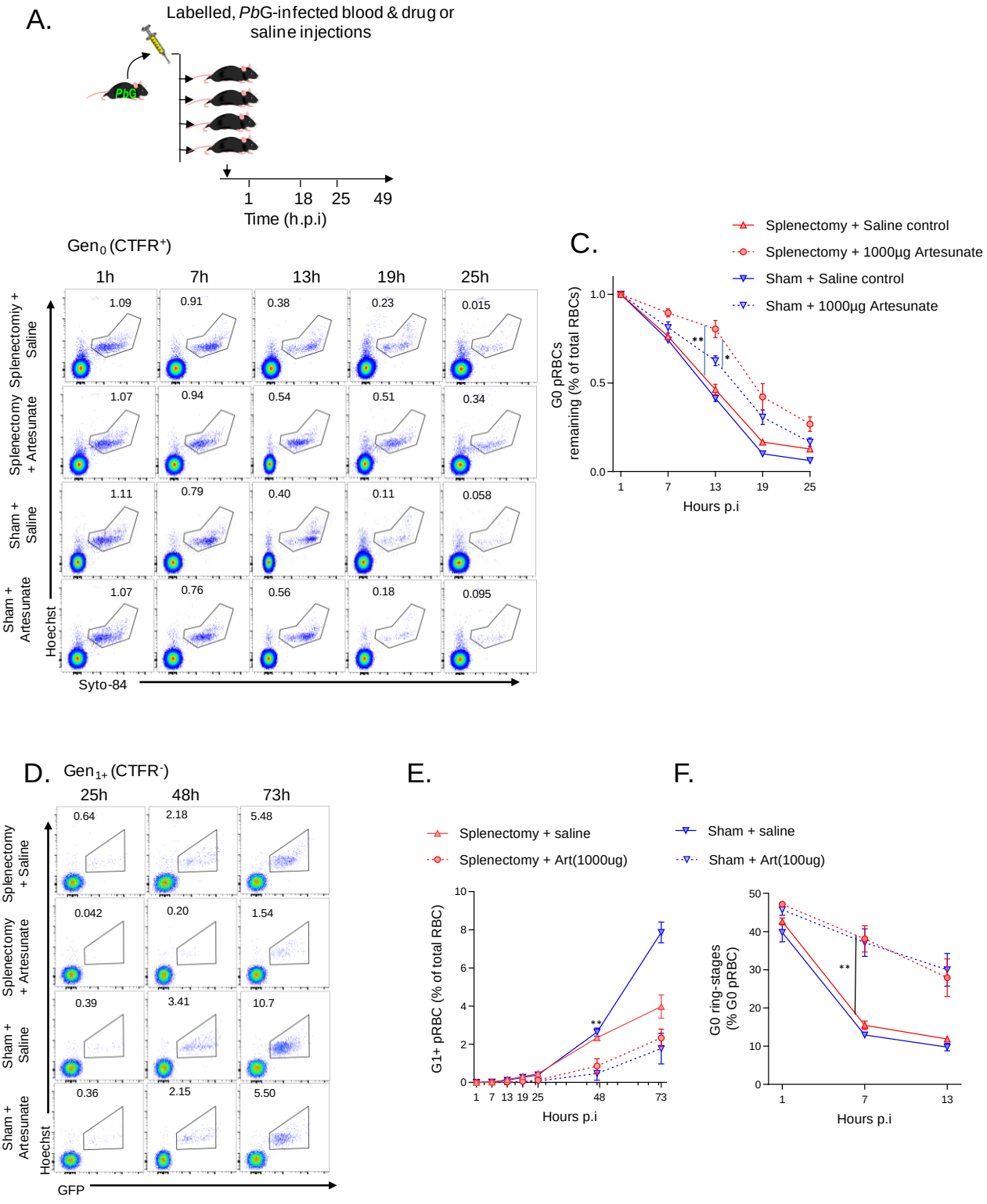

Figure 3.4 In the absence of artesunate treatment G0 pRBC clearance remains unaffected by splenectomy. *(**A**) Splenectomized (Red) and sham control (blue) mice were infected with fluorescent-labelled PbG infected blood and immediately treated with 1000 µg artesunate (dashed lines) or saline (solid lines). Tail bleed of recipient mice were done 1-97 h.p.i at different intervals and parasitaemia measured by flow cytometry. (**B**) Representative FACS plots showing G_0 pRBC gates in vivo over time, (**C**) proportion of G_0 pRBC remaining, and (**D**) FACS plots of Gen_1+ pRBCs are shown for 25-75 h.p.i. and (**E**), Gen_1+ pRBCs were graphed (**F**) The proportion of G_0 pRBCs that*

*were remained in the circulation at ring-stage in vivo (n = 5 per group, error bars are SEM, p<0.01 = **, p<0.001 = ***). Data representative of two independent experiments showing similar results.*

3.3.5 Phagocytes remove Gen_0 pRBC but do not affect parasites progressing to Gen_1.

Phagocytes are important components of the host immune system. In malaria, phagocytes are thought to be essential for removing malaria parasites not only via receptor-mediated phagocytosis but also through the release of parasiticidal mediators [82, 172]. Clearance of pRBC or any parasitic material may also be achieved by circulating phagocytes (monocytes and polymorphonuclear leukocytes) [173]. Phagocytic clearance of parasites may also be enhanced following anti-malarial drug treatment, for example when splenic pitting of drug-damaged parasites from pRBC occurs [124]. Contrary to these views, we observed that in general, artesunate and mefloquine did not accelerate clearance of the Gen_0 parasites and there is a little effect of splenectomy in non-drug treated mice in the clearance of Gen_0 pRBCs. While *in vivo* pitting rates have been estimated, and macrophages have been observed to phagocytose parasites, *in vivo* phagocytic clearance of pRBC has not been directly measured. This raises fundamental questions as to whether phagocytes such as Kuppfer cells (liver macrophages) contribute to clearance, either in the presence or in the absence of anti-malarial drugs.

To examine a role of phagocytes in clearing pRBC *in vivo*, I conducted an experiment in which mouse phagocytic cells were depleted using clodronate-liposomes (Clod-Lip, Netherland) and Gen_0 pRBC kinetics were assessed with/without artesunate treatment. Mice were intravenously injected with clodronate liposomes or control saline 3 days prior to transfusion with fluorescently-labelled, PbGFP (PbG)-infected blood and immediately treated with artesunate or control saline (Figure 3.5A). With the exception of the artesunate treated group, phagocytes depletion did not affect the total parasitemia in the first 25 hours (Figure 3.5B). However, depletion phagocytes resulted in Gen_0 pRBC to remain in the circulation (Figure 3.5C & D) with little effect on the development of Gen_1 pRBC (Figure 3.5 E & F). This was unexpected in view of the common belief that phagocytes actively ingest free merozoites - a phenomenon necessary for transition of Gen_0 to Gen_1. Our data suggests that although phagocytes contributed to the removal of pRBC from the circulation, it also prevented merozoites invasion that is necessary for substantive reduction in net population growth.

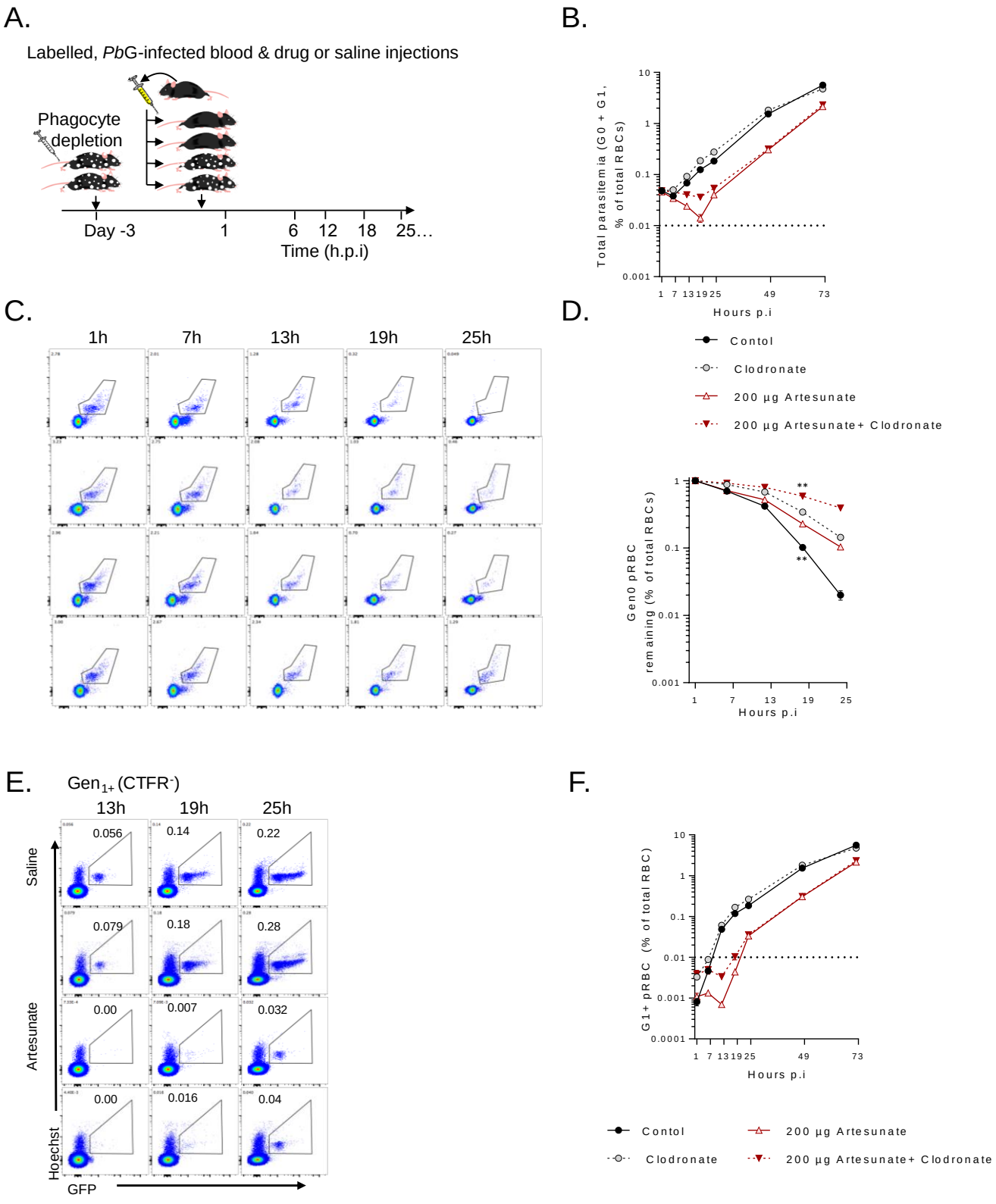

Figure 3.5 Phagocytes remove pRBC from circulation with and without artesunate treatment. *(A) Mice pretreated with clodronate liposomes (dashed lines, hollow circles, and hashed bars) or saline (solid lines, dots and bars), were injected with fluorescently labelled PbG infected blood and immediately treated with saline (black/grey) or 1000 µg artesunate (dark red). Tail bleed of recipient mice were done 1-73 h.p.i at different interval and parasitemia measured by flow cytometry. (B) Total parasitemia, (C) Representative FACS plots for Gen0 labelled pRBCs, (D) proportion of Gen0 pRBC remaining, (E) FACS plots of Gen1+ pRBCs are shown for 13-25 h.p.i., and (F) Gen1+ pRBCs were*

*graphed. Dotted lines = detection threshold, (n = 5 per group). Data representative of three independent experiments showing similar results. Statistics: Mann-Whitney t-test, **P < 0.01.*

3.3.6 Acute host response impairs parasite maturation in Gen_0 pRBC

During blood-stage malaria, the number of parasites can increase exponentially by asexual replication, which occurs after the RBC invasion by merozoites. This includes a progression through ring, trophozoite and mature schizont stages before each pRBC produces tens of daughter merozoites for subsequent re-invasion of RBC. Each cycle is ~24, 48 or 72 hours in duration depending on the *Plasmodium* species. The total numbers of pRBCs increases by around 10-fold each cycle in a naïve individual infected with *Plasmodium falciparum* [174]. However, this rate of increase of pRBC can be reduced by a number of host humoral and cellular immune responses [175-177]. Whether and how other aspects of the host response to infection, such as host innate immune responses, may influence malaria parasite control remain unclear [178].

Animal models of malaria have revealed that during acute infection, specifically before the generation of an effective parasite-specific antibody response, the host is able to partially control parasite growth [135, 179, 180]. However, the precise mechanism(s) by which parasite numbers are reduced *in vivo* remains unknown. A number of potential hosts innate control mechanisms have been suggested, such as phagocytic removal of pRBC, either by the spleen or liver, which is considered as the primary mechanism for host control of parasite numbers [179]. However, only a few studies have attempted to directly measure host removal of pRBCs *in vivo* [180, 181].

Here, we compared the rate of removal of Gen_0 pRBC from the circulation in acutely infected (with *Pb*A-GFP^{neg} pRBC) mice (compared to un-infected controls) after transfusing them with fluorescent-labelled *Plasmodium berghei* ANKA-GFP (*Pb*G) donor pRBCs. Surprisingly, we observed that in acutely infected mice, Gen_0 pRBC were not cleared faster than in un-infected controls (despite elevated systemic cytokine responses) (Figure 3.6B & C), rather Gen_0 pRBC persisted longer in the circulation (Figure 3.6C). In addition, slower progression to Gen_1 pRBC was observed (Figure 3.6E). Flow cytometric assessment of life-stages using DNA/RNA dyes, Hoechst and Syto84, demonstrated surprisingly, that Gen_0 pRBCs exhibited slower maturation rates in previously-infected mice (Figure 3.6F). However, the mechanisms of slower maturation in acutely infected mice remained unclear. Subsequently, we investigated whether host responses were involved in impaired maturation. *Rag1*$^{-/-}$ mice which mount very weak systemic inflammatory responses during infection, including a weak production of TNF and IFNγ [135] were used. The data suggested that there was

little difference in the parasite clearance in naïve and infected *rag1*$^{-/-}$ mice (Figure 3.6C). Moreover, progression from Gen_0 to Gen_1 was substantially slowed in *rag1*$^{-/-}$ infected mice (Figure 3.6E), either in 5-d or 12-d infected *rag1*$^{-/-}$ mice (Figure 3.6F). Further, the data suggest that host innate-immune response can prevent parasite replication as well enhanced parasite clearance through production pro-inflammatory cytokines.

A.

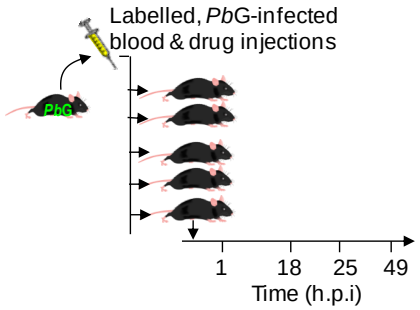
Labelled, PbG-infected
blood & drug injections
PbG
1
18
25
49
Time (h.p.i)

B.

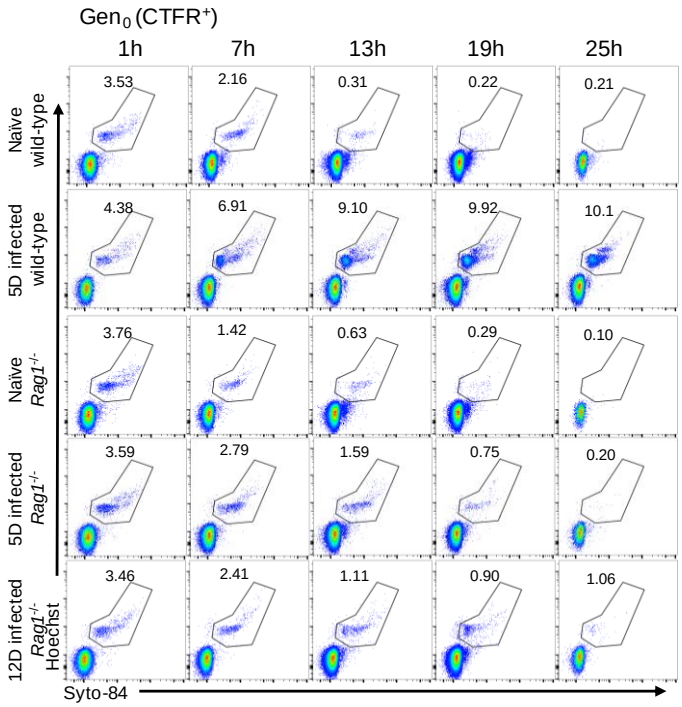
Gen0 (CTFR+)
1h
7h
13h
19h
25h
Naïve wild-type
5D infected wild-type
Naïve Rag1-/-
5D infected Rag1-/-
12D infected Rag1-/-
Hoechst
Syto-84
3.53
2.16
0.31
0.22
0.21
4.38
6.91
9.10
9.92
10.1
3.76
1.42
0.63
0.29
0.10
3.59
2.79
1.59
0.75
0.20
3.46
2.41
1.11
0.90
1.06

C.

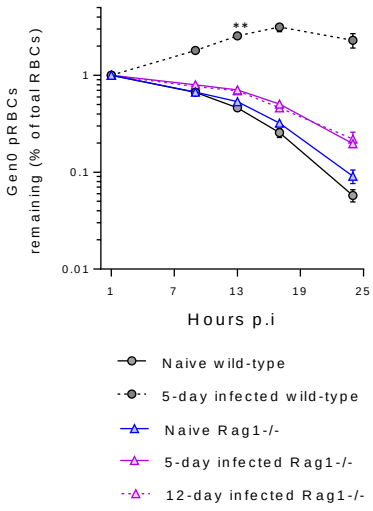
Gen0 pRBCs remaining (% of toal RBCs)
**
1
0.1
0.01
1
7
13
19
25
Hours p.i
Naive wild-type
5-day infected wild-type
Naive Rag1-/-
5-day infected Rag1-/-
12-day infected Rag1-/-

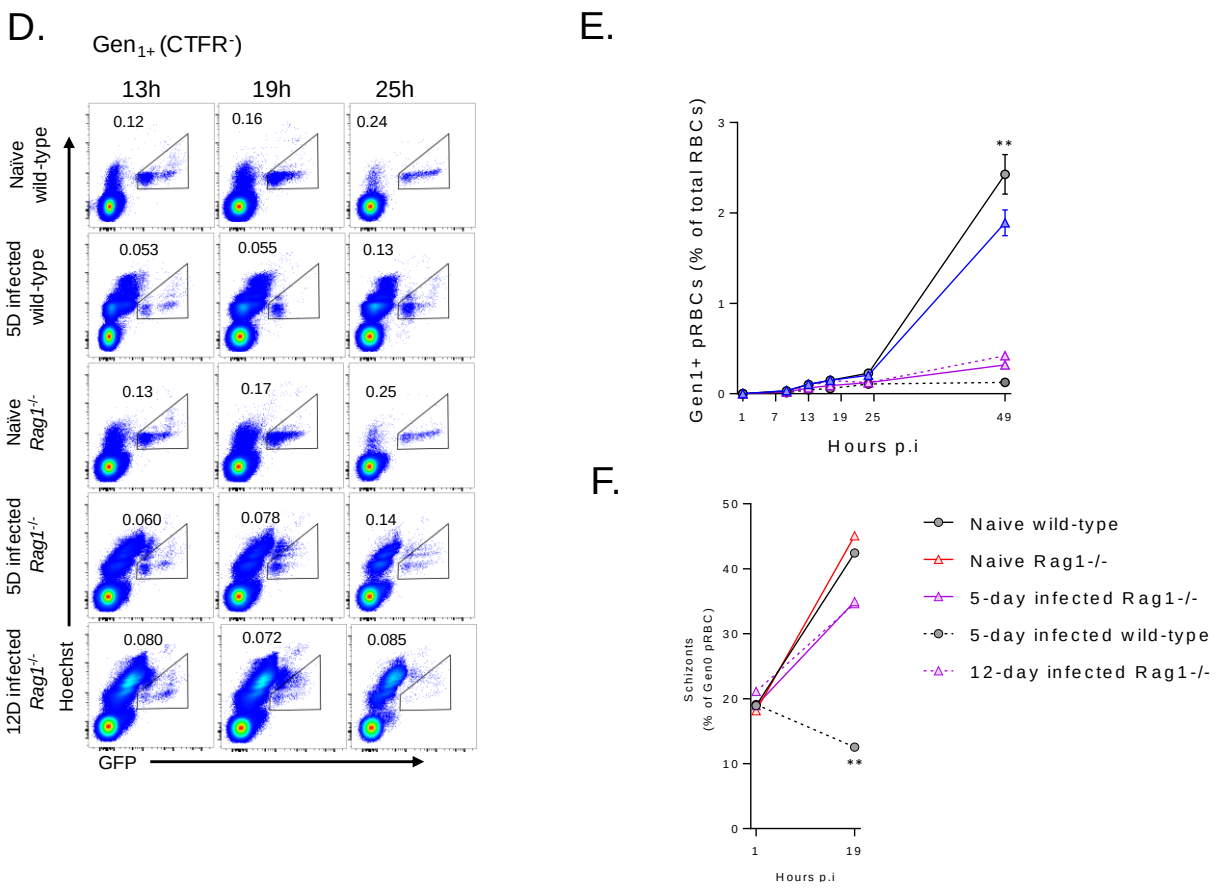

Figure 3.6 Acute infection impaired parasite development. ***(A)*** *Different groups of mice were infected with CTFR-labelled PbG infected donor blood. Tail bleed of recipient mice were done 1 - 97 h.p.i at different intervals and parasitaemia measured by flow cytometry.* ***(B)*** *Representative FACS plots for donor labelled RBC and* ***(C)*** *proportion of Gen_0 pRBCs remaining for 1-25 h.p.i.* ***(D)*** *FACS plots of Gen_1+ pRBCs are shown for 13-25 h.p.i. and* ***(E)****, Gen_1+ pRBCs were graphed* ***(F)*** *The proportion of G_0 pRBC that were schizonts in vivo. (n = 5 per group, error bars are SEM, p<0.01 = **, p<0.001 = ***). Data representative of two independent experiments showing similar results.*

3.4 Discussion

In these experiments, we examined the role of phagocytes in controlling parasite numbers, both the presence and in the absence of drugs. We observed a complex role of phagocytes that involved a clear capacity for removing a particular generation of pRBC, but no striking impact on total parasitemia. This may because of competing roles for phagocytes in both removal of pRBC and promoting parasite growth via pro-inflammatory responses or other unknown mechanisms.

It has also observed that the effects of anti-malarial drug on the parasite growth occurred in a dose-dependent manner, where the high dose of artesunate and mefloquine (1000µg and 250 mg/kg respectively) completely suppressed parasite growth in the first 48 h after treatment, whereas parasite growth was evident in mice treated after 24 h of treatment with lower doses and in the lowest dose of Mefloquine and in control mice (saline treated). We could not, however, characterise the status and proportion of parasites that contributed to further replication. As other studies have noted, survival of a sub-population could potentially lead to the rapid emergence of drug resistance to artemisinin monotherapy [182], the clinical use of combined therapy improves the cure rate and delays the development of parasite resistance to artemisinin [183-185].

In the combination therapy study, it was observed that artesunate plus mefloquine combined treatment was more effective in the controlling total parasitemia compared to artesunate treatment alone. Our findings are consistent with the effectiveness of ACT in controlling parasites, which has been observed in an ACT *ex vivo* efficacy study [186]. Moreover, mefloquine delayed the parasite maturation process but did not completely inhibit parasite maturation, allowing limited progression to the next generation of parasites.

Here, it was observed that artesunate treatment caused Gen_0 pRBCs to remain longer in circulation, which consequently lowered the numbers of pRBCs below detection level in the next generation (Gen_1+ pRBCs), by preventing parasite transition from one generation to the next. Therefore, it was interesting to study whether host factors were involved in this situation of parasite control; either by enhancing the removal of artesunate treated killed or damaged parasite or delaying parasite maturation. Previous *ex vivo* spleen perfusion studies suggested that the spleen more efficiently removes the mature trophozoites and schizonts stages parasites with an approximately 50% shorter half-life than the ring form [187]. In contrast, it has also observed that the depletion of phagocytes was associated with increased persistence of drug-affected young-stage parasites. This is consistent with the belief that artesunate-affected ring-stage parasites are usually removed actively from circulation via “pitting” [122, 126] - a mechanism in which the affected parasite is removed from the RBC and the cell is returned to the circulation, which is likely to involve phagocytic cells

[122, 126, 188]. Interestingly, our splenectomy experiments tend to suggest that the spleen is not essential for removing viable parasites from the bloodstream, as the removal of spleen did not alter the clearance of Gen_0 pRBC. This is an important point because it tends to be assumed that the spleen clears pRBC from the bloodstream effectively. However, the splenectomy experiments should be interpreted with caution because compensatory mechanisms likely exist, such as liver macrophages taking up more parasites in splenectomised mice [189]. Nevertheless, we propose that the spleen is not a major organ for pRBC removal. It is, however, the main site for priming pathological immune response, which are not easily compensated for in splenectomise mice. Given that splenic T-cell responses actually promote parasite numbers in this model, the overriding effect of splenectomy is to block gen1 without having major effects on Gen_0. The limitation of this study is that it could not explore possible roles of different polymorphonuclear cells in the observed reduced clearance of parasites by using clodronate liposomes that acts broadly on many phagocytic cells including macrophages, dendritic cells, and granulocytes [128, 190].

Finally, we have shown that in acutely infected mice G_0 pRBC persists longer in the circulation by delaying parasite maturation. Delayed parasite maturation was also observed in association with artesunate treatment, where parasites could not develop into schizonts. Other studies in *P. falciparum* also suggested that drug treatment was able to slow or halt (dormancy) the life-cycles, which is thought to be a parasite stress response allowing parasites to survive treatment [155, 182, 191, 192]. Therefore, it seems likely that delayed maturation is a parasite survival mechanism, which occurs in response to environmental stress, perhaps as a result of its efforts to mitigate damage caused by some form of stress, whether exerted by a drug or by the host environment. It thus appears that delayed maturation could be a parasite survival strategy, although the mechanism of delayed maturation remains unclear. However, in our experimental approach, transfusion of identical infected donor cells from a single donor mice into naïve and acutely infected mice enabled us to examine the ability of the host environmental factors to act on pre-infected cells and thereby influencing the parasite life-cycle development. Moreover, it is evident here that sensing of the environment by the parasite is a rapid response since the persistence of Gen_0 pRBcs was evident after the first time point. In addition, we have identified a key role of host factors in this process. Parasite maturation was not delayed in *rag1*$^{-/-}$ mice, which lack both T and B cells and other abnormalities of lymphoid architecture. This does not imply that antigen-specific immunity is required for delayed maturation, as T and B cells are known to also contribute to the early innate immune response through the production of cytokines [193-195].

Moreover, in the *Pb*ANKA model, a pathogenic immune response generate in the spleen depends on dendritic cells priming of pathogenic CD4+ and CD8+ T-cells. In particular, it is known that CD8+ T cells migrate to the brain where they cause fatal pathology via expression of molecules such as granzyme B [196]. It is also known that this CD8+ T cell response promotes parasite growth via as yet undefined mechanisms. Therefore, while the spleen might be regarded as the site for clearance of pRBC by host inflammatory response, it also is the site for a pathogenic pro-inflammatory and T-cell response. Spleen thus plays a complex role in *Pb*ANKA infections, in that there may be a balanced inflammatory and host clearance mechanisms occurring in the same organ.

In order to observe parasite life-stage development using our approach, we specifically chose to transfer semi-synchronous ring-stage Gen_0 pRBCs, which facilitated us in examining the process of parasite maturation and development. Although we did not observe faster removal pRBCs from the circulation by the host, we could not entirely exclude the role of the spleen in the clearance of pRBC during infection; however, it was evident that slow maturation exerts a major impact on the overall parasite growth in acute infection [144]. Further studies are needed to identify the exact molecular mediators of delayed maturation. Importantly, we have shown that this experimental approach is a powerful tool for dissecting host-parasite interactions during blood-stage *Plasmodium* infection *in vivo*.

Using the clearance /growth assay in mice has allowed measuring the clearance of parasite under a number of conditions including drugs, the presence of spleen, the role of phagocytes, and the influence of host pro-inflammatory responses. To definitively examine the role of phagocytes in removing pRBC, we had to focus on the effect of phagocytes on a defined population of pRBC, in this case Gen_0. We observed the kinetics of loss of Gen_0 pRBC in mice treated with clodronate liposomes to untreated mice, as well as repeating this comparison in mice treated with artesunate. We noted a profound reduction in the rate of loss of Gen_0 in mice treated with clodronate. This indicates that phagocytes play an important role in clearing pRBC from mice. The effct of clodronate on Gen_1, is complex because phagocytes not only clear pRBC, but also preserve the integrity of immune tissues such as the spleen.in the absence of phagocytes, T /B cells are not retained well in the spleen,and as a result pathogenic immune responses are abrogated. However, our experimental design did not allow examining whether or not phagocytes interfere with the maturation rates of parasites. We hypothesize that other mechanisms might play a role in supporting parasite growth, e.g. phagocytes in the spleen might facilitate rupture of schizonts as they pass through the organ, or pro-inflammatory responses might alter the micro-architecture of the spleen in some way to facilitate their rupture. These would be further explored in humans infected with *Plasmodium* by developing new techniques.

Chapter Four:

Exploring mechanisms of antibody-mediated parasite control during blood-stage *Plasmodium* infection

4.1 Abstract

Plasmodium-specific antibodies can play an important role in immunity to malaria, as exemplified by the fact that their passive transfer can control infection [197]. However, the exact *in vivo* mechanisms of action for these antibodies remain unclear. Using murine models of immunity to blood-stage malaria, *P. yoelii* 17XNL, and *P. chabaudi chabaudi* AS infection, I have studied the effect of parasite-specific antibodies in controlling malaria parasites *in vivo*. Data revealed that passive transfer of serum from immune animals did not lead to faster clearance of parasitized red blood cells (pRBCs), despite being effective at preventing parasite growth. Next, it was observed, via clodronate liposome treatment, that phagocytic cells played a partial role in the efficacy of antibody-mediated control. In contrast, cobra venom factor treatment suggested no role for C3/C5 complement factors. Finally, it was noted that parasite-specific IgG from these two mouse models bound poorly to the surface of pRBC *in vivo* and *in vitro*, and instead were capable of recognising parasite structures found in asexually replicative forms of the parasite, that we reason to be merozoites. Thus, in mouse models of humoral immunity to malaria, parasite-specific antibodies bind poorly to pRBC and consequently protect against infection by preventing parasite transition from one generation of pRBC to the next, most likely via phagocyte-dependent control of free merozoites.

4.2 Introduction

Antibodies are an important component of acquired immunity against malaria, as demonstrated in the passive transfer of immune serum, firstly in rhesus monkey [101], and later in malaria-infected children which resulted in a reduction of parasite load and improved clinical status [102-104]. These findings provided the understanding that parasite-specific antibodies are able to effectively control parasite numbers in humans and *in vivo* animal models.

In endemic populations, naturally-acquired immunity to malaria takes 10-15 years of exposure to develop, as individuals experience repeated exposures to malaria parasites [30]. Efforts have been made to identify potential antigenic targets of protective antibodies [105, 106]. The mechanism by which they control parasite numbers *in vivo* has also been reviewed [105, 107-109]. Protection against malaria likely depends on the functionalities of antibodies produced against parasite proteins exported to the surface of pRBC and/or to those expressed on the surface of merozoites [105], However, the mechanism by which antibodies protect against malaria remains unclear.

A number of possible *in vivo* antibody-mediated mechanisms have been reported and revealed in elegant *in vitro* assays targeting *Plasmodium* proteins on pRBC. These include Growth Inhibition Assays (GIAs) [110, 111], which assess if antibodies can reduce parasite growth in the RBC over a few replication cycles; opsonic phagocytosis assays and antibody-dependent cellular inhibition (ADCI) assays [112-114], which assess whether antibodies facilitate uptake and/or inhibition by phagocytes; and complement-fixing and killing assays [115, 116], which assessed how well antibodies facilitate C1q deposition and complement-dependent direct killing. The correlation between the functional efficacy in GIAs and immunity to malaria remains unclear [117-120]; however, in recent years, methods to assess opsonic phagocytosis or C1q-fixation *in vitro* (mostly of merozoites), have demonstrated its correlation with protection against *P. falciparum* malaria symptoms and high-density parasitemia [114-116]. These reports suggested that antibody-mediated immunity to the blood-stage of infection can be mediated by their binding to merozoites, but requires the engagement of host factors including phagocytes and the complement system. More recently, it was also suggested that antibodies against the pRBC surface protein, PfEMP1, which drove opsonic phagocytosis *in vitro*, demonstrated partial protection against malaria and that these antibodies were acquired slightly earlier in life compared to merozoite-targeting antibodies [121]. Thus, the epidemiological data in humans supports the notion that multiple co-existing mechanisms acting against merozoites and pRBC may contribute to antibody-mediated pRBC control during blood-stage infection. However, few if any of these mechanisms have been convincingly observed *in vivo*.

To explore *in vivo* mechanisms of action for protective antibodies acquired after blood-stage infection, I employed established models of blood-stage immunity in inbred C57BL/6J mice, and adapted the *in vivo* Clearance/Growth assay from Chapter 3, for use with *Py*17XNL and *Pc*AS parasites [134, 198, 199]. This allowed tracking of a cohort of labeled pRBC and direct estimation of how antibodies controlled infection with homologous parasites. Non-lethal *Py*17XNL and *Pc*AS infections were chosen due to their self-resolving nature and their well-documented production of parasite-specific antibodies, which are known for mediating immunity to re-challenge [200-202].

4.3 Results

4.3.1 Assessing *Py*17XNL model and Clearance /Growth assay

Prior to the exploration of *in vivo* mechanisms of action of antibodies, it was important to assess whether the use of immune serum and our Clearance/Growth assay was indeed effective to study the mechanisms of antibody function *in vivo*. A number of parameters such as the amount of immune serum and the antibody exposure time required to exert the optimal functional impact were optimised before investigating the mechanistic aspects of antibody action using our laboratory's *in vivo* Clearance/Growth assay.

4.3.1.1 Immune and non-immune murine serum was generated using non-lethal *P.yoelii 17XNL*

To study the mechanisms of antibody-mediated parasite control *in vivo*, we opted to use immune serum from inbred C57BL/6J mice that had resolved a blood-stage *P. yoelii* 17XNL infection or control non-immune serum from un-infected age-matched mice. *Py*17XNL expresses parasite-derived proteins on the surface of both pRBC and merozoites in a manner similar to human *Plasmodium* species [203-205]. It is a model characterised by robust humoral immunity, and the development of parasite-specific serum IgG and IgM. Previous data from our group and others have identified that *Py*17XNL-specific IgG and IgM was detectable by 14 d.p.i., that parasitemia was largely resolved by 30 d.p.i., and that peak parasite-specific IgG levels occurred at around 60-70 d.p.i. [206]. Thus, C57BL/6J mice were intravenously infected with $1x10^4$ *Py*17XNL-infected pRBCs, infection was confirmed on day 12 p.i., and resolution of infection confirmed on day 30 p.i. (Figure 4.1A). Mice were then monitored around day 60-70 p.i., to ensure that *Py*17XNL-specific IgG had been generated (Figure 4.1B). Serum containing parasite-specific IgG (and age-matched non-immune serum) was collected and stored for future experiments.

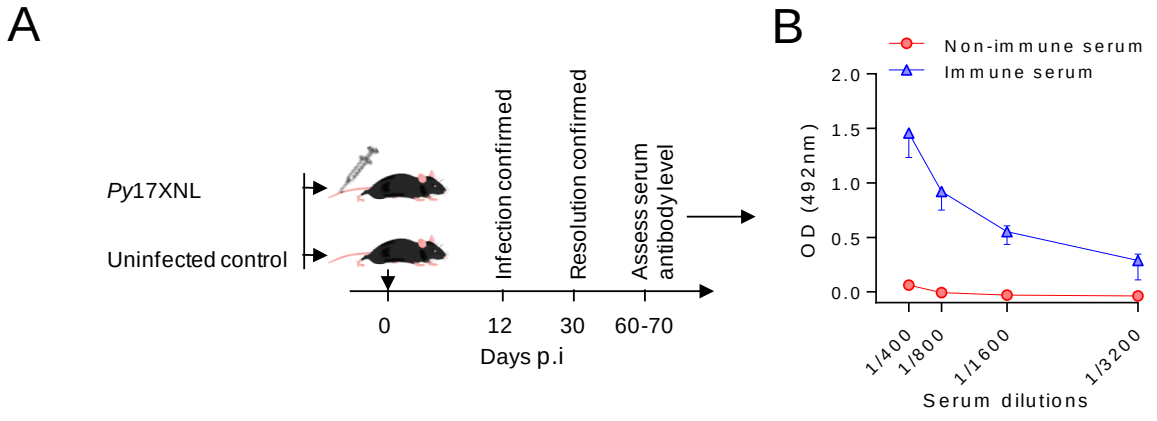

Figure 4.1 Generation of Py17XNL-immune serum using the self-resolving non-lethal Py17XNL rodent model. (A) *Immune mice were generated following blood-stage infection with P. yoelli 17XNL*

(Py17XNL). Infection was confirmed 12 d.p.i., and ***(B)*** *Py17XNL-specific IgG was measured 60-70 d.p.i in immune (blue) and age-matched non-immune (red) mice (n=5-30/group); data representative of more than five independent experiments, each with similar results.*

4.3.1.2 Immune serum restricts parasite growth during *Py*17XNL infection

After generation of immune and control non-immune serum from mice that had resolved primary *Py*17XNL infection and confirmation of the presence of parasite-specific IgG (Figure 4.1B), I next sought to determine if these antibodies could function *in vivo* to control infection, similar to the manner in which passive transfer of IgG was shown to protect malaria patients. This meant determining whether immune serum was able to control parasitemia when therapeutically administrated to mice infected with homologous parasites (Figure 4.2). At day 3 p.i. when parasitemia was ~0.05%, infected mice were transfused with a single dose (200µl) of immune serum, or non-immune control serum. Five out of 6 mice receiving immune serum partially controlled parasitemia over the subsequent 36 hours, compared to non-immune serum recipients (Figure 4.2). Interestingly, the mouse with the highest starting parasitemia (~0.1%) showed no evidence of parasitemia control when administered immune serum, suggesting that parasite load might influence the efficacy of immune serum treatment. Nevertheless, these data confirmed that immune serum, which contained parasite-specific IgG, was protective *in vivo*.

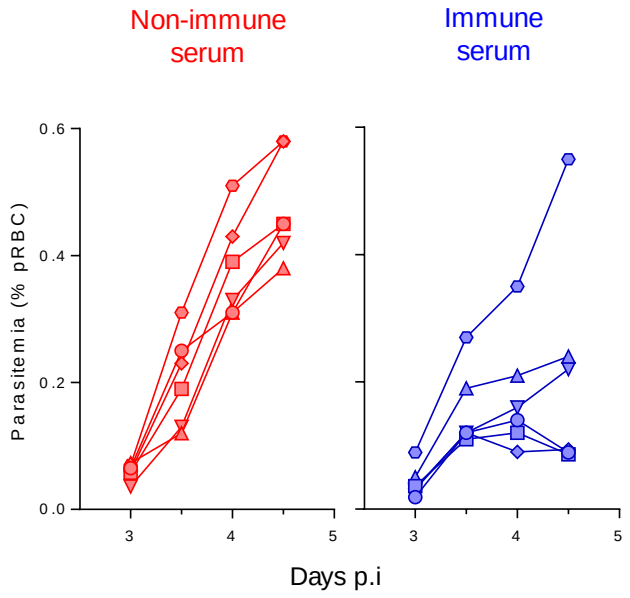

Figure 4.2 Efficacy of immune serum in restricting parasite growth in ongoing Py17XNL-infection. *Total parasitemia of individual Py17XNL-infected mice therapeutically treated at 3 d.p.i. with a single dose of Py17XNL-immune (blue) or non-immune (red) control serum (n=6 per group) and tracked for 36 hours thereafter; experiment conducted once.*

4.3.1.3 Assessing *in vivo* mechanisms of action for *Py*17XNL-specific immune serum

Having confirmed the *in vivo* protective capacity of *Py*17XNL-specific immune serum, it was next hypothesized that protection was mediated by accelerating the host-mediated removal of pRBC. To test this, I examined immune-serum mediated control of parasites using a modified version of our laboratory's *in vivo* Clearance/Growth assay. In Chapter 3 this assay was used to examine the dynamics of *P. berghei* ANKA parasites. Here, I employed the same labeling techniques with *Py*17XNL pRBC. Non-immune mice were administered immune serum, non-immune serum, or no serum intravenously 2 hours prior to infection with fluorescently-labelled (with CellTrace Far Red, CTFR) pRBCs from *Py*17XNL-infected passage mice. Parasitemia was monitored in recipient mice from 1-73h post infection by flow cytometry. Firstly, the data suggest that mice receiving immune serum exhibited significant control of parasitemia over the 3-day period, compared to mice treated either with non-immune serum or no serum (Figure 4.3A and B). Interestingly, there appeared to be no difference in parasitemia kinetics between non-immune serum recipients and those not receiving any serum, which suggested that there was little bystander/non-specific protection afforded by the administration of non-immune serum. Next, we made use of CTFR-labelling to define the first generation of transferred pRBC that were CTFR+ as Gen_0, and subsequent CTFR- generations as Gen_1+ pRBC. It was noted that immune serum recipients, efficiently impaired the transition of parasites from Gen_0 to Gen_1+ (Figure 4.3B), compared to non-immune recipients. Moreover, at earlier timepoints, most notably at 19h post-infection, Gen_0 parasites, though lower in number than at 1h, were present at the same frequency regardless of immune serum transfer (Figure 4.3C). Although this time point was not ideal for assessing removal of Gen_0, it was clear that immune serum was highly efficient at preventing parasites in Gen_0 pRBC from progressing to subsequent generations of pRBC. Further detailed assessment of earlier time points within the first 24 hours was required to examine pRBC clearance.

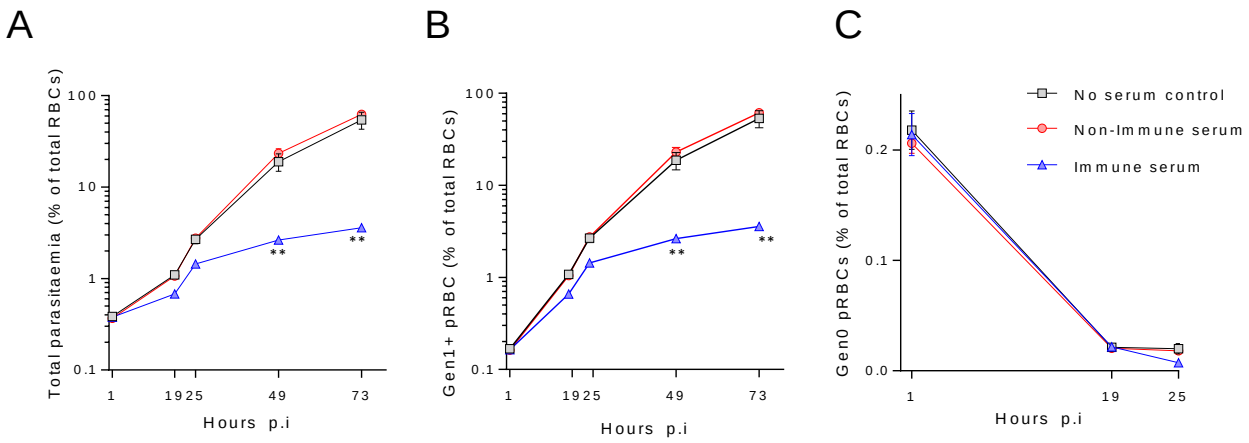

Figure 4.3 Control of parasite growth without accelerated parasite removal. (A) *Total parasitaemia,* ***(B)*** *growth of parasites (G_1+ parasites population) in recipient RBC; and* ***(C)*** *reduction in the*

*proportion of donor pRBCs (G_0 parasites population), called clearance; in WT mice pre-treated with 150 µl immune serum (blue) and non-immune serum (red) and no serum (black, n=5 per group) two hours before infection with fluorescently labelled Py17XNL infected blood (i.e., donor G_0 parasites population). Error bars represent SEM, p<0.01 = **. Data representative of two independent experiments showing similar results.*

4.3.1.4 Lack of *Py*17XNL-specific immune serum dose reponse in clearance of Gen_0 pRBC

Thus far, arbitrary volumes of serum (ranging from 100-200µl) had been used to determine *in vivo* efficacy of immune serum in controlling parasitemia and parasite growth. In addition, frequent sampling of Gen_0 pRBC had not been undertaken to test our hypothesis that immune serum accelerated host removal of pRBC from circulation. Therefore, to identify an appropriate dose of immune serum to be used in future experiments, and to study Gen_0 pRBC clearance, a range of serum doses (5, 20, 100 and 400µl of immune and 400µl of non-immune serum) were passively transferred 2h prior to infection with CTFR-labelled *Py*17XNL-infected pRBC. Detailed flow cytometric examination of Gen_0 and Gen_{1+} pRBC was conducted at 1, 6, 12, 18, 24, 48, 72 and 96 hours post-infection. It was striking, that while Gen_0 pRBC were lost from circulation in the absence of immune serum, likely via the normal process of maturation and RBC rupture, the rate of loss of Gen_0 pRBC was not accelerated by immune serum (Figure 4.4A). The data suggest that the animals immune system was adequate in removing the Go parasite population without requiring additional IgG. Importantly, however, immune serum when administered at the higher volumes of 400µl and to a lesser extent 100µl was highly effective at preventing progression to Gen_1 pRBC (Figure 4.4B). These data firstly showed that doses of immune serum above 100µl were required to control parasite growth in our models. Due to logistical issues of using high volumes of immune serum, it was decided that 200µl volumes (rather than 400µl) would ensure robust protection without having to generate excessively large batches of immune serum from *Py*17XNL-infected mice. Most importantly, detailed assessment of Gen_0 pRBC revealed that immune serum did not control parasite numbers by accelerating the rate of pRBC clearance from circulation. Instead, the data indicated that immune serum likely acted by preventing parasite transition from one generation pRBC to next. However, antibody in immune serum could possibly bind to the intra-erythocytic parasite to inhibit parasite development; but, we did not explore this in our study.

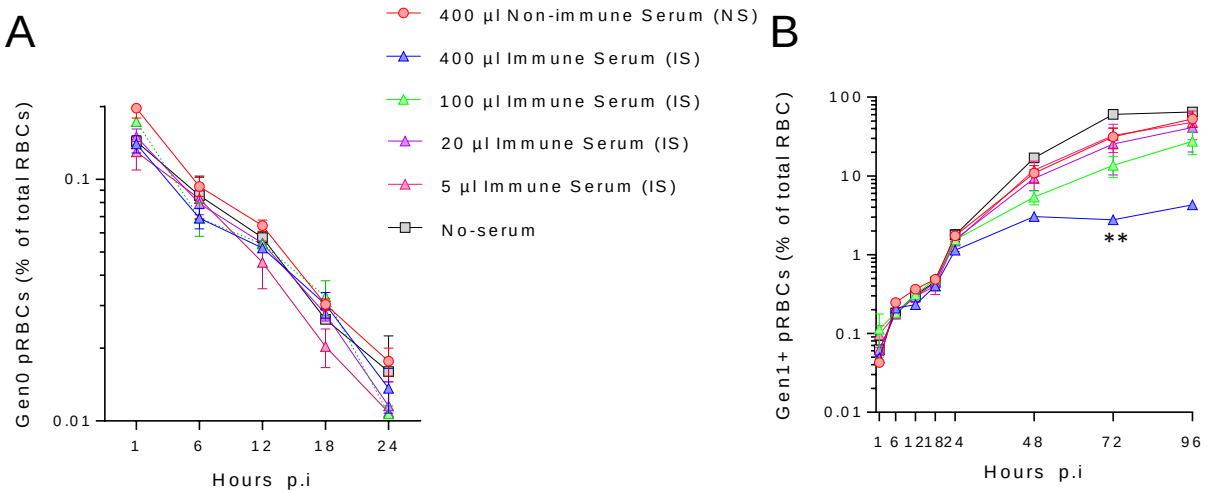

Figure 4.4 No dose-response in the clearance rate of pRBCs from circulation. (A) *The graph shows reduction in the proportion of pRBCs (Gen_0), called clearance; and* ***(B)*** *growth of parasites (G_{1+} parasites population) in recipient RBCs after rupturing from G_0 parasites in WT mice (n=3) pre-treated with 400, 100, 20 and 5µl of immune serum and 400µl non-immune serum at -2hrs to infection with fluorescently labelled Py17XNL infected blood (i.e., donor G_0 parasites population). Error bars represent SEM, p<0.01 = **. Experiment conducted once.*

4.3.1.5 Modification of the immune serum passive transfer protocol

Considering the reality of managing the experiment, it was essential to explore whether transferring serum into mice one day (24h) prior to infection was effective as 2h prior. In order to determine this, intravenous transfer of serum into mice was performed 2h and 24h prior to infection with fluorescently labeled pRBCs from *Py*17XNL infected passage mice. Tail bleeds of recipient mice were done at time intervals of 1-73h post-infection, and parasitemia monitored by flow cytometry. Data suggested that administration of non-immune serum to the recipient mice very close to the time of infection with pRBCs produced a similar, non-specific protection in the next generation of pRBCs (G_1+), which was not observed in the earlier two experiments. In an effort to simplify the implementation of the experiments, we felt it prudent going forward to administer serum 24 hours prior to parasite challenge with donor pRBCs (Figure 4.5) though the experiment done once.

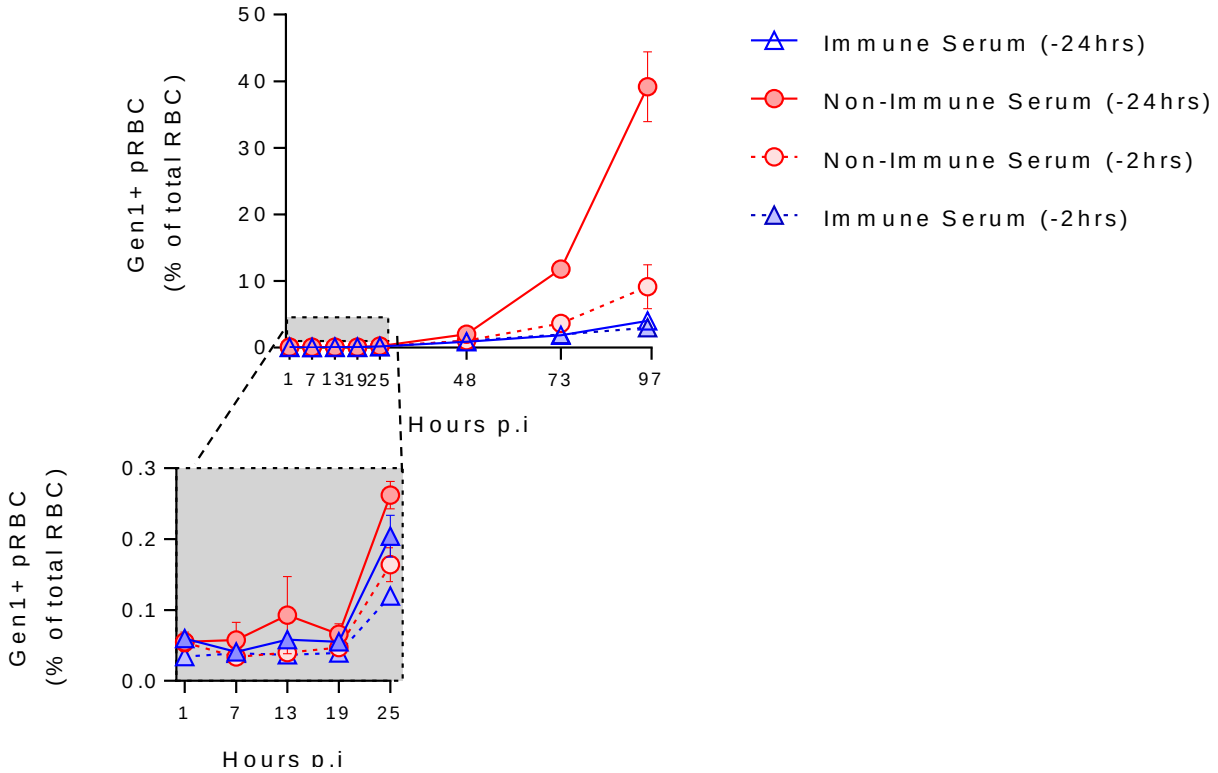

Figure 4.5 Administration of non-immune serum 2h prior to parasite challenge produces non-specific protection in Gen1 pRBCs. *Mice (n=5/group) were intravenously administered 200µl of Py17XNL immune serum (blue), or control non-immune serum (red) 2h (dotted lines) and 24h (solid lines) prior to receiving CTFR$^+$ Gen$_0$ pRBC containing Py17XNL. Gen$_{1+}$ pRBC analysed at time points indicated. Experiment conducted once.*

4.3.1.6 Cellular and humoral immunity do not increase parasite clearance *in vivo*

Although transferred antibodies inhibited parasite replication in naïve mice, it remained possible that additional immune mechanisms might operate in an intact immune mouse to accelerate Gen$_0$ clearance. To explore this, immune mice that had resolved a primary *Py*17XNL infection were intravenously injected with CTFR$^+$ pRBC (Figure 4.6A). As with passive antibody transfer, no changes were observed in Gen$_0$ pRBC removal compared to age-matched naïve controls (Figure 4.6B). In contrast, the emergence of Gen$_1$ pRBC was blocked in immune mice compared to naïve age-matched controls (Figure 4.6C), with PMR (the average number of Gen$_1$ pRBC generated at 25h from each transferred Gen$_0$ pRBC at 1h) substantially reduced from 17.3±7.7 in non-immune mice to 0.78±0.29 in immune mice. Together the data suggest that infection-induced, protective antibodies against *Py*17XNL parasites do not alter the rate of removal of pRBC *in vivo*. Instead, this data further confirms that these antibodies obstructed the progeny of pRBC from generating subsequent generations of pRBC.

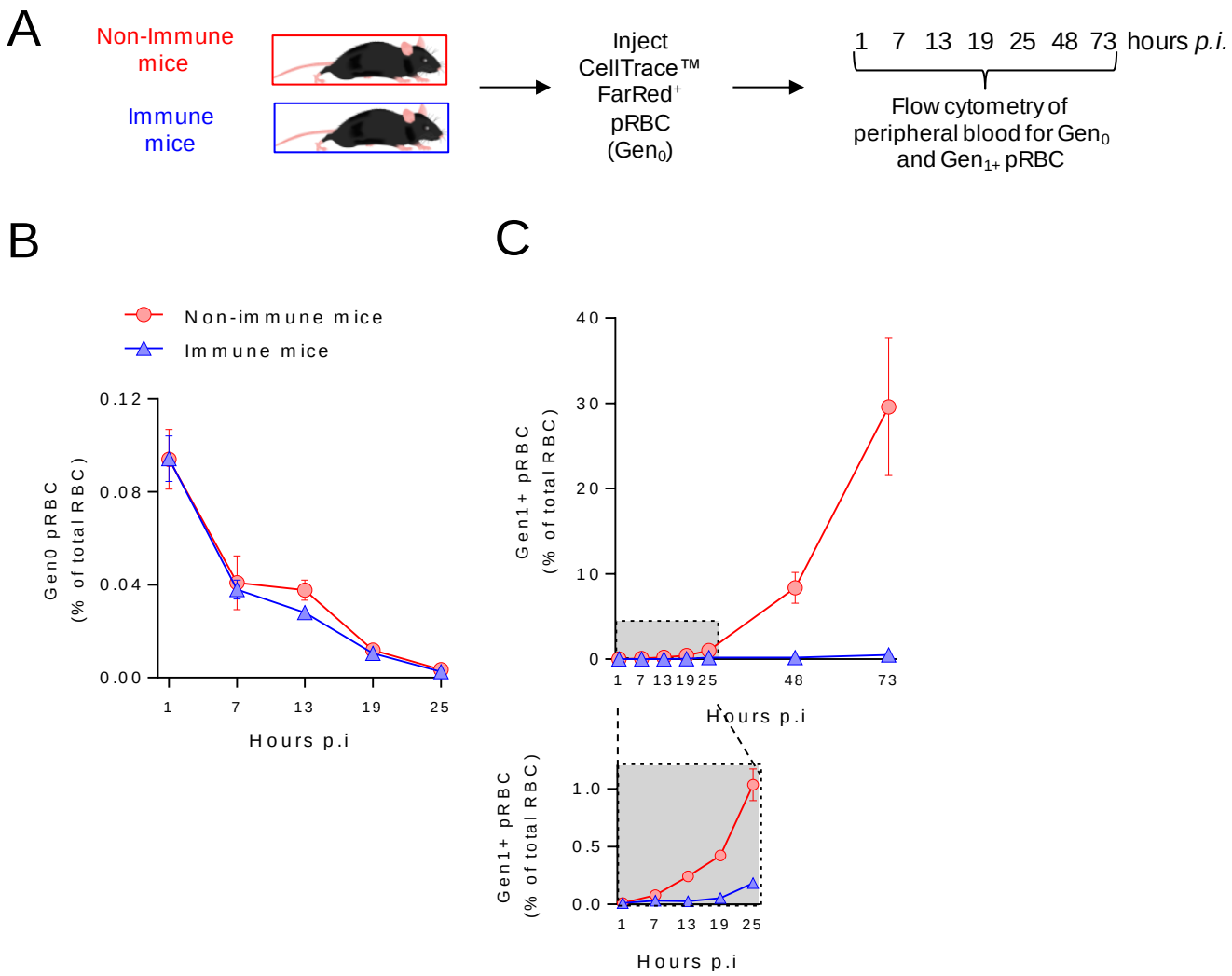

Figure 4.6 Combined cellular and humoral immunity do not accelerate pRBC clearance. (A) *Schematic showing that Py17XNL-immune (blue) and non-immune (red) mice (n=5/group) were challenged with CTFR$^+$ Py17XNL-infected pRBC, with peripheral RBC monitored at time points indicated for:* ***(B)*** *loss of Gen$_0$ (CTFR$^+$) pRBC over the first 25 hours, and* ***(C)*** *emergence over 3 days of Gen$_{1+}$ (CTFR$^-$) pRBC, with zoomed-in box showing the first 25 hours in more detail. Data representative of two independent experiments showing similar results.*

4.3.2 Exploring the mechanisms of antibody-mediated parasite control

A number of recent studies are in line with my observation that infection-induced antibodies were efficient at preventing *Py*17XNL parasite progression from one generation of pRBC to the next, without acceleration of parasite removal in the first 25h of p.i. Specifically, it has been suggested that antibody-mediated immunity to blood-stage infection can be effected by binding to merozoites, but with a necessary engagement of host factors including phagocytes and certain aspects of the complement system [114-116]. More recently, it was also suggested that antibodies against the pRBC surface protein, PfEMP1, which drove opsonic phagocytosis *in vitro*, afforded partial protection against malaria, and that these antibodies were acquired slightly earlier in life than merozoite-

targeting antibodies [121]. Thus, the epidemiological data in humans supports the concept that multiple co-existing mechanisms acting against merozoites and pRBC can contribute to antibody-mediated pRBC control during blood-stage infection. However, few if any of these mechanisms have been convincingly observed *in vivo*. Therefore, it was hypothesised that some of the antibodies elicited by *Py*17XNL infection would bind to pRBC and accelerate their clearance by the host.

4.3.2.1 Infection-induced, *Py*17XNL-specific antibodies do not accelerate pRBC clearance, but prevent parasites progressing to the next generation of RBC

After determining that passively transferred immune serum generated in inbred C57BL/6J mice against *Py*17XNL infection was effective in controlling parasitemia during challenge with CTRF labeled pRBCs, I next made use of the CTFR-labelling on pRBC to specifically study the progression from the initial generation (Gen_0) of pRBC to the next generation (Gen_{1+}) over the first 25 hours post-challenge. The experiment was carried out as previously detailed. Briefly, after collection of cardiac blood from *Py*17XNL-infected passage mice (typically exhibiting an age structure of 70% ring-stages), the blood was fluorescently labelled with CellTrace™ Far Red (CTFR) and transferred as the first generation, termed Gen_0 (including un-infected, CTFR-labelled RBC) into mice that had received *Py*17XNL-immune serum or non-immune control serum 24 hours earlier (Figure 4.7A). Here, a combination of Hoechst 33342 and Syto™ 84 nucleic acid dyes was used to identify parasite life-cycle stages of Gen_0 pRBC over the first 25 hours (Figure 4.7B).

As earlier, the data suggested that the loss of Gen_0 pRBC was equivalent between immune and non-immune serum recipients (Figure 4.7C), and allows the inference that pRBC clearance rates remained unaffected by passive transfer of protective immune serum. Similarly, Gen_0 parasite maturation occurred equivalently in immune and non-immune serum recipients over the 25-hour observation period (Figure 4.8). Next, while the rapid appearance of Gen_{1+} pRBC was observed in non-immune serum recipients, the immune serum substantially blocked the emergence of Gen_{1+} pRBC (Figure 4.7D). The PMR in mice that received control serum was 11.5±0.8, which was reduced to 3.7±0.1 in mice that received immune serum. Together, these data demonstrated that parasite-specific antibodies are able to control *Py*17XNL infection. This does not appear to be due to the accelerated removal of pRBC or impaired parasite maturation, but due to blocking the progeny of Gen_0 pRBC from establishing subsequent generations of pRBC.

A

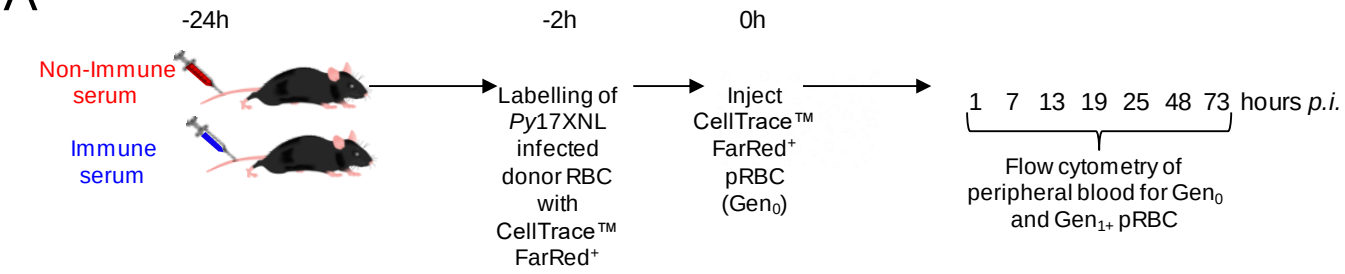
-24h
-2h
0h
Non-Immune serum
Immune serum
Labelling of Py17XNL infected donor RBC with CellTrace™ FarRed+
Inject CellTrace™ FarRed+ pRBC (Gen0)
1 7 13 19 25 48 73 hours p.i.
Flow cytometry of peripheral blood for Gen0 and Gen1+ pRBC

B

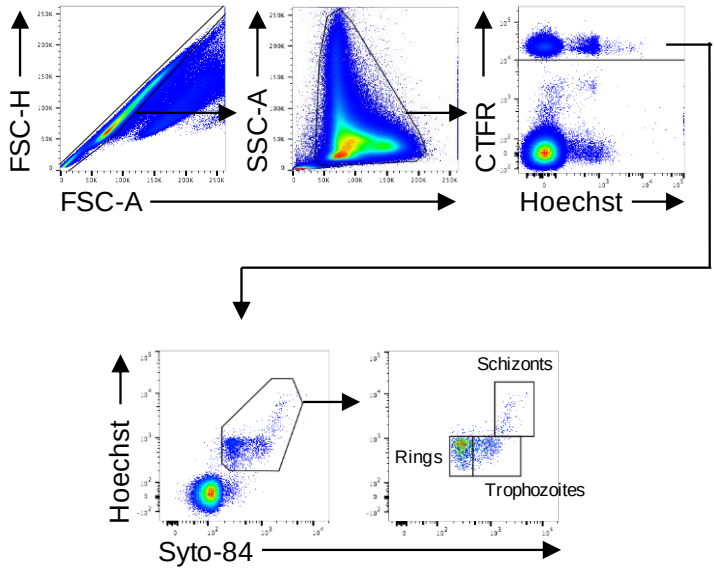
FSC-H
FSC-A
SSC-A
CTFR
Hoechst
Hoechst
Syto-84
Schizonts
Rings
Trophozoites

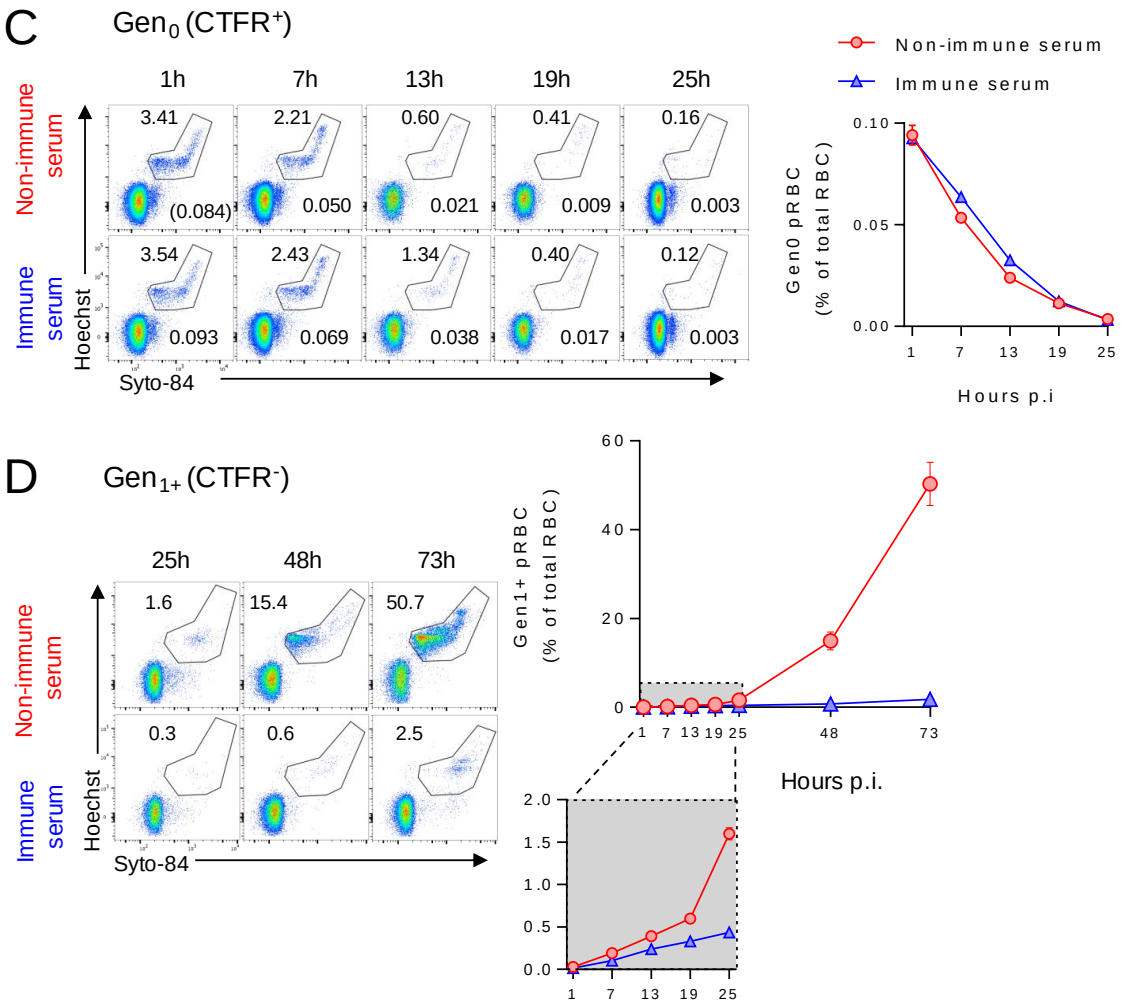

Figure 4.7 Infection-induced antibodies control Py17XNL parasite growth, not by accelerating pRBC clearance, but by blocking subsequent generations of pRBC. (A) *Schematic diagram showing mice (n=5/group) injected with serum from Py17XNL-immune (blue) or non-immune (red) mice 24h prior to challenge with CTFR-labelled Py17XNL-infected pRBCs, and the timing of tracking the infection progression by flow cytometry.* ***(B)*** *FACS gating strategy employed to analyze Gen_0 and Gen_{1+} pRBC: forward scatter area and height (FSC-A and FSC-H) used to identify single cells, and side scatter area (SSC-A)/FSC-A used to identify RBCs. $CTFR^+$ pRBCs were the initial generation (Gen_0), while Hoechst 33342/Syto 84 co-staining identified pRBCs and their life stages.* ***(C)*** *Representative FACS plots for time-course analysis of loss of Gen_0 ($CTFR^+$) pRBC with numbers showing % of $CTFR^+$ RBC containing parasites and the summary graph as a % of total RBC in recipient mice.* ***(D)*** *Representative FACS plots for time-course analysis of Gen_{1+} ($CTFR^-$) pRBC, and summary graph showing emergence of Gen_{1+} pRBCs over time. Data are representative of six independent experiments, each showing similar results.*

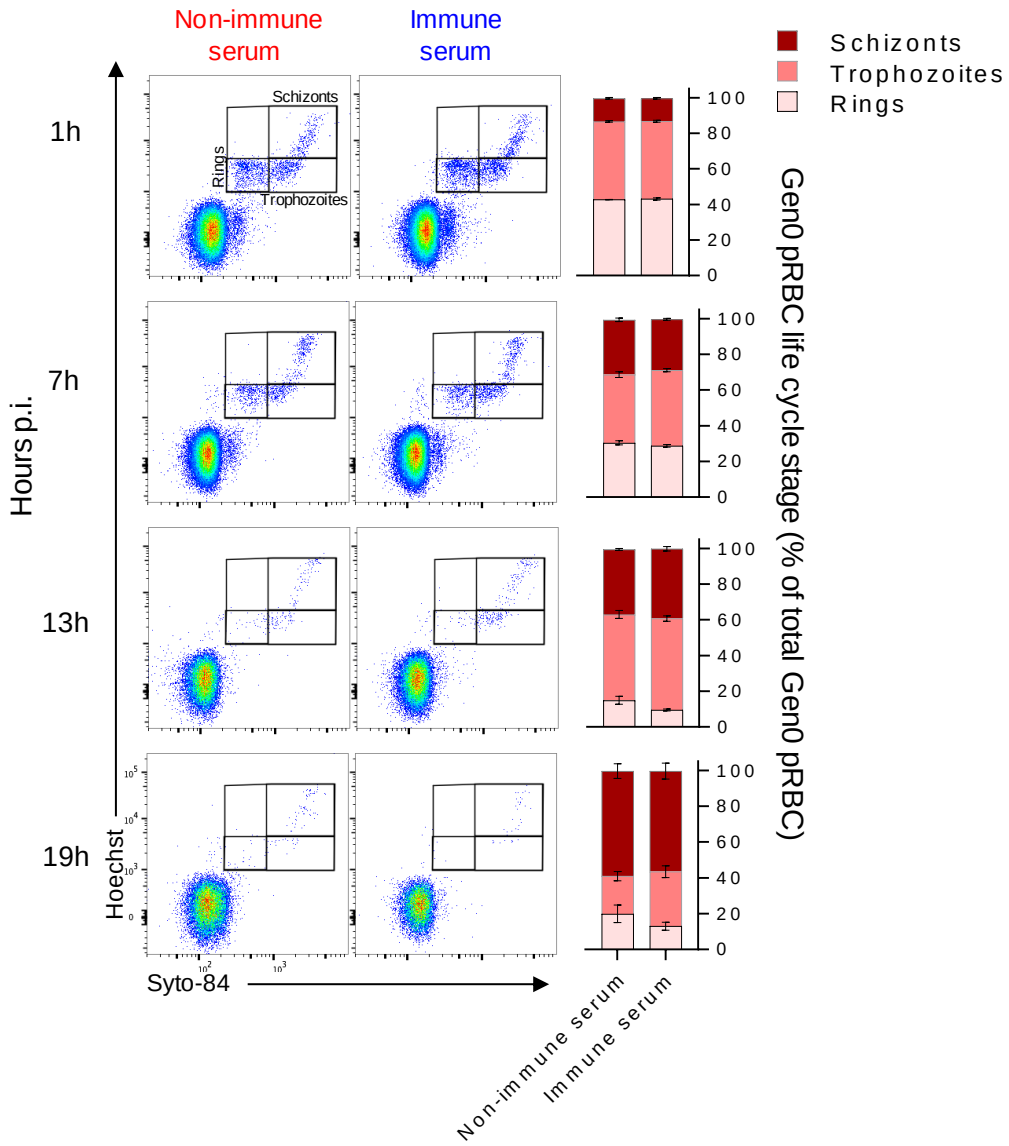

Figure 4.8 In vivo maturation of Gen0 Py17XNL-infected pRBC is unaffected by exposure to Py17XNL-immune serum. *Representative FACS plots gated on Gen$_0$ (CTFR$^+$) RBC in mice (n=5/group) at indicated time points after transfer into mice that had received either Py17XNL-immune or non-immune control serum 24h previously, showing parasite life-stages based on Hoechst and Syto 84 profiles. Graphs show percentage of Gen$_0$ pRBC in each life stage. Data are representative of >5 independent experiments, each showing similar results.*

4.3.2.2 *Py*17XNL-specific antibodies require phagocytic cells for optimal function *in vivo*

Antibodies may provide protection against malaria in different ways, including inhibition of the blood-stage replication preventing high-density parasitemia. A number of possible mechanisms have been proposed based on *in vitro* assays. Protection against *P. falciparum* infection may be mediated by binding of antibody to the merozoites thereby limiting the number of parasites, a process that involves host factors including the complement systems and phagocytes [207, 208]. A recent study has reported that anti-malarial antibodies in association with complement factor C1q-fixation inhibit invasion of erythocytes by merozoites, and facilitate complement deposition and lysis of merozotes [209]. Antibodies are also involved in the phagocytosis of *P. falciparum* merozoites, and in the activation of monocytes to producepro-inflammatory cytokines [114]. Phagocytic cells constitute an effective mechanism for reducing parasitemia. In this process, antibody acts as an opsonin and binds to infected erythrocytes (IE) or merozoites for phagocytosis. However, the exact *in vivo* mechanism(s) remains unknown. Thus, we wanted to determine the mechanisms involved in antibody-mediated parasite control.

Before investigating whether antibody control of parasite growth *in vivo* requires help from host factors such as phagocytic cells and complement or both, a control experiment was performed to understand the role of phagocytic cells in controlling parasites *in vivo*. Mouse phagocytic cells were depleted using a crude Clodronate-liposome (Clod-Lip, Netherland) treatment 3 days before administering donor pRBCs (Figure 4.9A). In the event of clearance by phagocytic cells following artesunate treatment, it might be expected that clodronate depletion could help parasites persist even longer in the circulation. In the event of no clearance by macrophages, it might be expected there would be exactly the same clearance in the artesunate-treated group with and without clodronate. Indeed, results of this experiment suggested an important role of phagocytic cells since the removal of the phagocytic cells resulted in the persistence of pRBCs in the circulation during the first 24 hours of infection compared to the control group (Figure 4.9B). However, there was no significant difference in parasite growth in the next cycle between the groups (Figure 4.9C).

cc

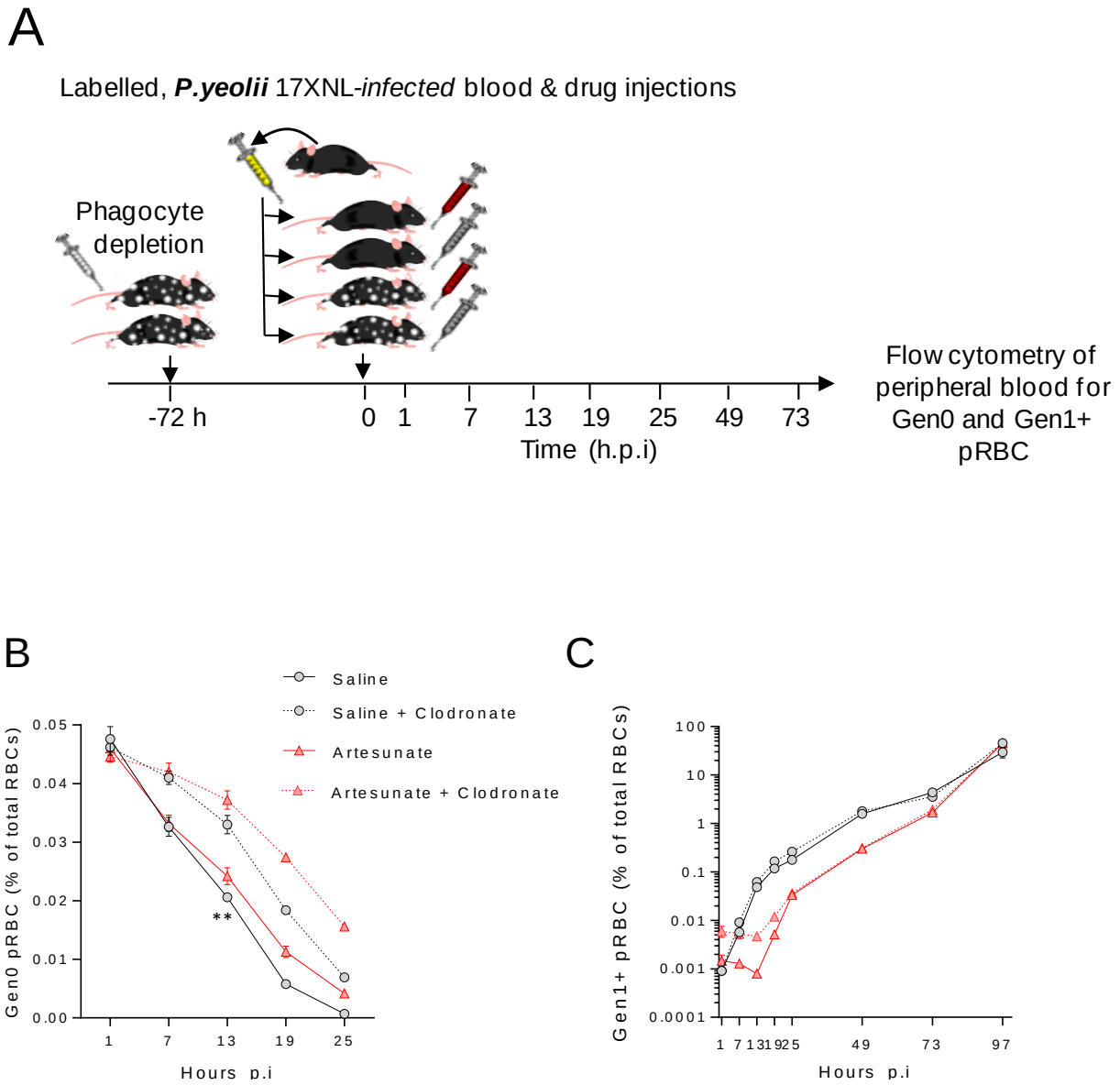

Figure 4.9 Phagocytes remove pRBC from circulation with and without artesunate treatment. ***(A)*** *Schematic diagram showing that mice treated with 200 µl of clodronate liposomes (dashed lines in B and C) 3 days prior to infection with fluorescently labelled Py17XNL-infected blood and immediately treated with saline (grey) or 1000 µg artesunate (red).* ***(B)*** *The graph shows reductions in the proportion of donor pRBCs (G_0 parasite population), called clearance and* ***(C)*** *growth of parasites (G_{1+} parasite population) in recipient RBCs after rupturing from G_0 parasites. Error bars represent SEM, p<0.01 = **. Data representative of two independent experiments showing similar resuts.*

Next, the role of phagocytes in the mechanism of anti-malarial antibody protection was assessed *in vivo* by pre-treating mice with clodronate liposomes before treatment with *Py*17XNL-immune serum (or control non-immune serum). Afterward, $CTFR^+$ labeled pRBC (Gen_0) were transferred and tracked as below (Figure 4.10A). Over the first 25 hours, phagocyte depletion slightly

reduced the rate of clearance of Gen_0 pRBC in both control and immune-serum treated mice (Figure 4.10B). When the effects of immune serum in clodronate-treated mice were examined, it was observed that clodronate treatment had reduced the protective effect of immune serum. That is, in phagocyte-intact mice, immune serum reduced PMR by 61.7% (range: 50-70) compared to control antibody-treated mice (Figure 4.10C). However, in phagocyte-depleted mice, immune serum reduced PMR by only 31.7% (range: 25-40) ($P<0.0096$, two-way ANOVA, significant interaction between serum administration and clodronate treatment, 5 mice/group, three independent experiments). Thus *Py*17XNL-immune serum was ~50% less effective in the absence of phagocytes over the first 25 hours. Nevertheless, at days 2 and 3 post-transfer, immune serum had limited the emergence of later generations (Gen_{1+}) of pRBC in both phagocyte-depleted and intact mice (Figure 4.10C). Therefore, *Py*17XNL-specific antibodies co-operated with phagocytic cells to optimally restrict parasites transitioning from Gen_0 to Gen_1 pRBC.

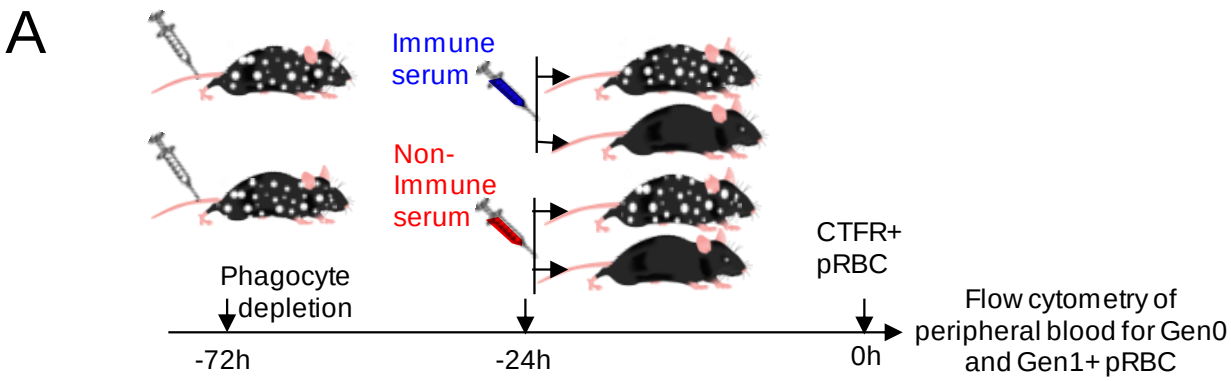

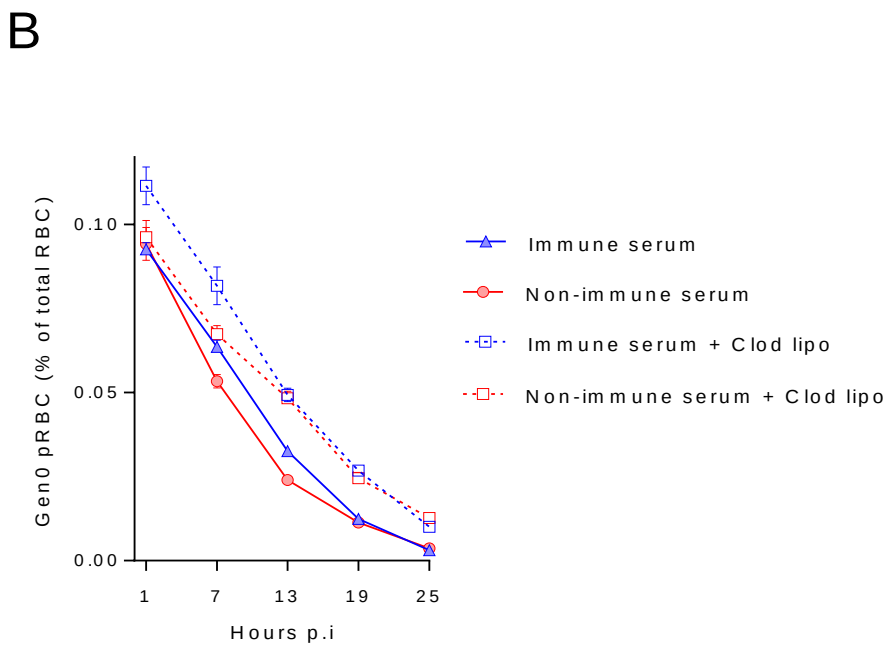

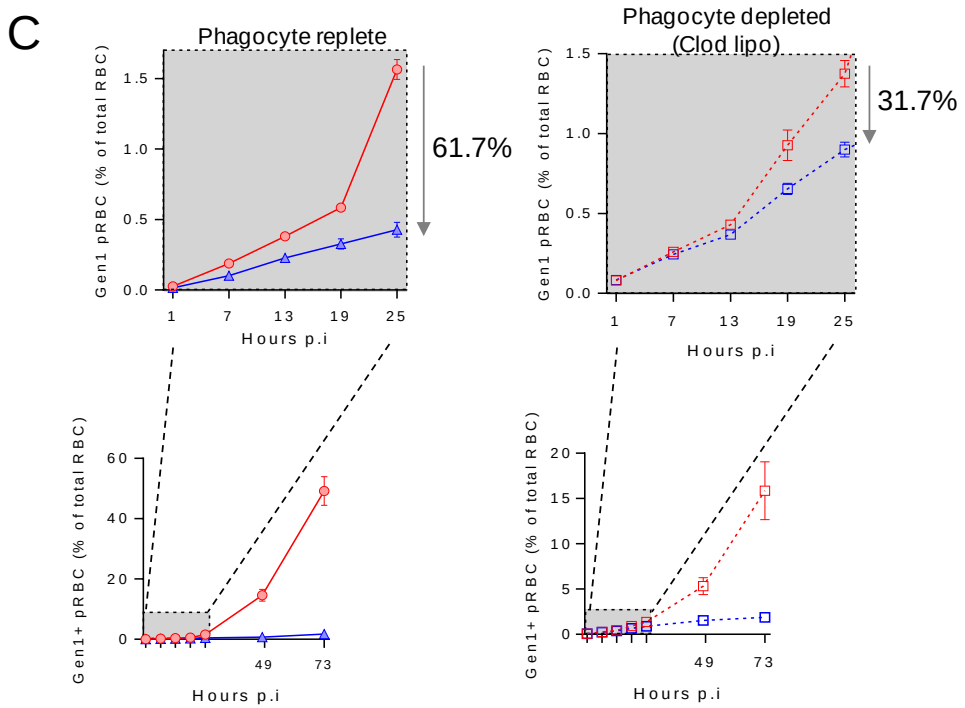

Figure 4.10 Py17XNL-specific antibodies require phagocytic cells for optimal in vivo function. (A) *Schematic showing 4 groups of mice (n=5/group) treated with clodronate liposomes (dashed lines) or left untreated (solid lines), and then given immune (blue) or non-immune (red) control serum prior to infection with CTFR$^+$ Py17XNL-infected pRBC, with peripheral blood assessed at different time points for:* ***(B)*** *loss of Gen$_0$ (CTFR$^+$) pRBC and* ***(C)*** *emergence of Gen$_{1+}$ (CTFR$^-$) pRBC in phagocyte replete (left), or clodronate liposome-treated (right) mice with the first 25h in detail. Percentages indicate the reduction in PMR elicited by immune serum compared to non-immune control serum. Data representative of three independent experiments showing similar results.*

4.3.2.3 *Py*17XNL-specific antibodies do not require complement mediated direct killing for optimal function *in vivo*

Next, phagocyte-independent mechanisms that antibodies might employ to prevent parasites transitioning from Gen$_0$ to Gen$_1$ were examined. Previous studies had reported two antibody-mediated, phagocyte-independent mechanisms: complement-dependent merozoite invasion blockade that requires C1q-deposition, and complement-mediated direct lysis of merozoites via the formation of membrane attack complexes (MAC). To test for the importance of MAC formation in the protective efficacy of *Py*17XNL-immune serum, we depleted mice of complement protein C3, using non-toxic cobra venom factor (CVF). Importantly, CVF-treatment does not target C1q, the upstream component of the complement cascade that can complex with antibodies to block merozoite invasion. CVF treatment leads to complement depletion by activating the alternative pathway of C3 activation [210]. To explore the role of complement in antibody-mediated parasite control, complement in WT mice was depleted by ~75-90% by continuous administration of 10 µg/mouse CVF (Quidel, San Diego, California) or saline control from days – 1 to + 3. Then *Py*17XNL-immune serum or non-

immune serum was transferred (day -1), and on the following day (day 0) CTFR^{+} labeled pRBCs were administered and tracked (Figure 4.11A). Firstly, it was confirmed that CVF treatment had substantially depleted C3 levels in the serum by measuring C3 levels every 24 hours post infection in CVF treated and saline-treated control mice (Figure 4.11B). As expected, the loss of Gen_0 pRBC was equivalent amongst all groups (Figure 4.11C). Finally, PMR reduction elicited by *Py*17XNL-immune serum (compared to non-immune serum) in mice either replete or CVF-treated were compared (Figure 4.11D). It was found that *Py*17XNL-immune serum effectively controlled PMR in both CVF-treated mice and saline controls ($P>0.12$, two-way ANOVA interaction between immune serum administration and CVF treatment, 5 mice per group, 2 independent experiments). Therefore our data could not define any clear role of antibody-dependent, complement membrane attack complex (MAC)-mediated direct lysis in the process of protection conferred by *Py*17XNL-immune serum antibodies. Taken together, our data suggests that infection-induced *Py*17XNL-specific protective antibodies co-operated with phagocytes, but did not engage complement-mediated direct killing to block parasite transition from one generation of RBC to another. However, we did not assess complement component C1q-mediated blocking of invasion of erythrocytes by merozoites, and we thus consider a possible role of complement.

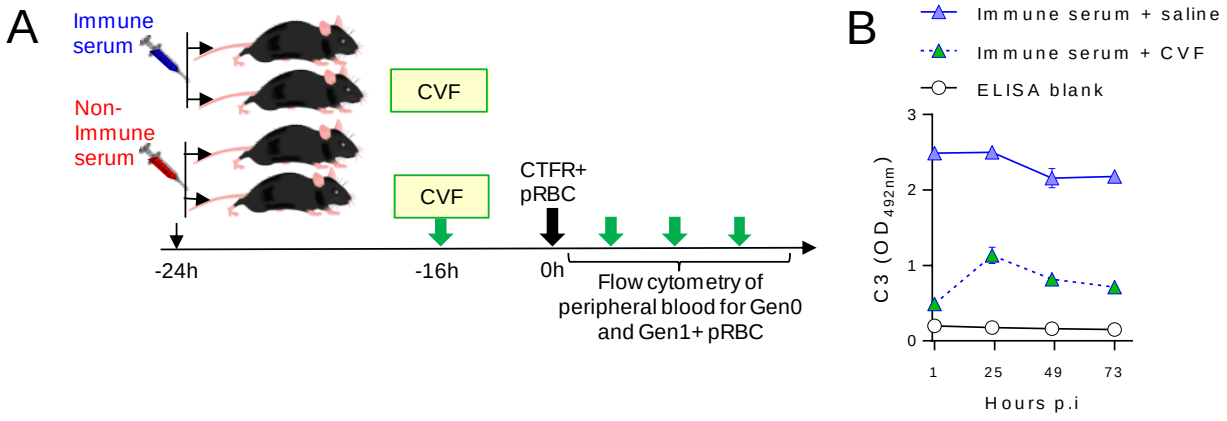

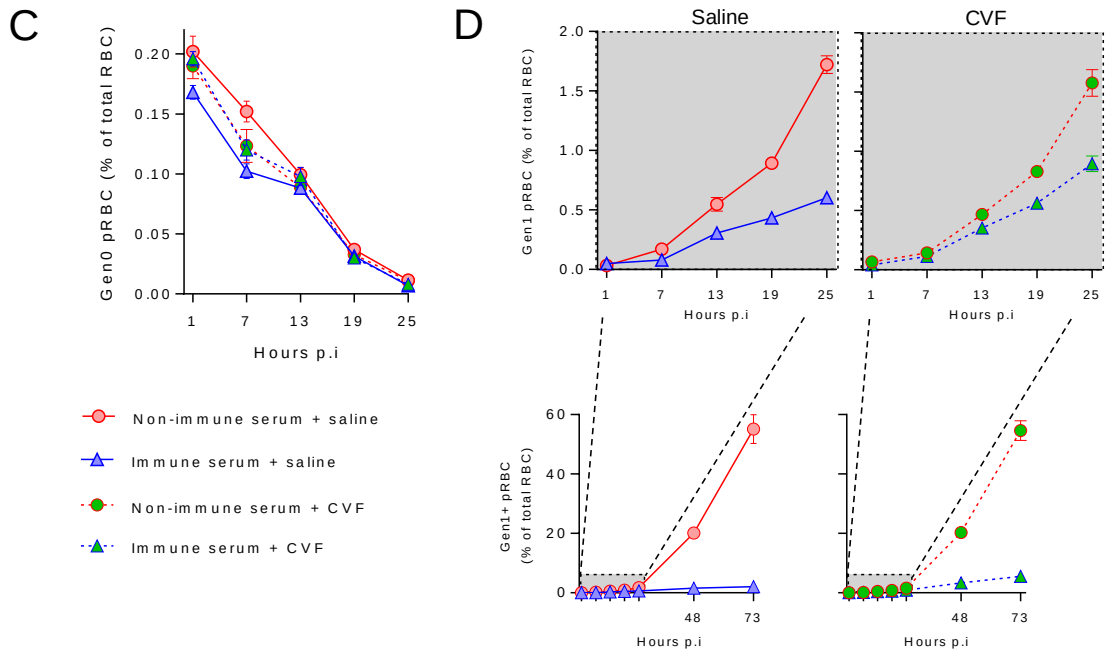

Figure 4.11 Py17XNL-specific antibodies do not require complement-mediated direct killing for in vivo function. (A) *Schematic showing 4 groups of mice (n=5/group) treated with immune (blue) or non-immune (red) control serum, and cobra venom factor (CVF, green) or control saline as indicated by green arrows, and challenged with CTFR$^+$ Py17XNL-infected pRBC.* ***(B)*** *Serum C3 levels assessed at various times post-challenge.* ***(C)*** *Loss of Gen$_0$ (CTFR$^+$) pRBC and* ***(D)*** *emergence of Gen$_{1+}$ (CTFR$^-$) pRBC in C3-replete, or CVF-treated mice with detail of the first 25h. Data represents two independent experiments showing similar results.*

4.3.2.4 *Py*17XNL-specific IgG binds poorly to intact pRBC, but strongly to permeabilised schizonts harbouring merozoites

Next, the life-cycle stage specificity of *Py*17XNL-specific antibodies was examined. Given that immune serum blocked parasite transition from one RBC to another, rather than accelerating pRBC clearance, we hypothesized that these antibodies might bind poorly to the pRBC surface but strongly to merozoite forms. To test whether immune serum antibodies bound to the surface of pRBC *in vivo*, *Py*17XNL-immune serum or non-immune control serum were passively transferred as before, and CTFR$^+$ pRBC transferred on the following day (Figure 4.12A). Then, Gen$_0$ pRBC was stained for cell-surface mouse IgG *ex vivo* after 1 or 4 hours (Figure 4.12B). As a positive control for mouse IgG-deposition on RBC, some samples were also incubated *in vitro* with a mouse monoclonal IgG (clone 34-3C) specific for murine RBC (Figure 4.12B). These analyses demonstrated firstly that this assay was capable of detecting mouse IgG bound to the surface of CTFR$^+$ RBC (Figure 4.12B). Secondly, after 1 hour of *in vivo* exposure to immune serum, less than 10% of pRBC had bound mouse IgG to levels above background (Figure 4.12B), a proportion that did not increase after another 3 hours of *in vivo* exposure (Figure 4.12B), or even following incubation with higher concentrations

of immune serum *in vitro* (Figure 4.13A). These data support the hypothesis that, compared to the 34-3C a positive control, *Py*17XNL-specific IgG bound only weakly to the surface of pRBC *in vivo* (Figure 4.12B). Noted that, the reduced antibody activity could be due to the variant nature of the variant surface antigens of pRBC. 34-3C, a RBC marker is much more abundant than variant surface antigens of pRBC, however, we have used 34-3C as a positive control in our experiments to assess the binding activity.

Next, to test whether parasite-specific IgG, present in immune serum, could potentially bind merozoites, parasites inside pRBC were exposed directly to immune serum *in vitro*, by RBC fixation and permeabilisation (Figure 4.13B). Interestingly, it was observed that although fixation and permeabilisation lysed all un-infected RBC and perhaps early-ring stage pRBC, as expected (Figure 4.13B compared to 4.13A), later-stage pRBC remained intact, permitting immune-staining and conducting flow cytometry (Figure 4.13B). In stark contrast to pRBC-surface IgG deposition, where the majority of pRBC did not bind IgG from immune serum (Figure 4.12B), it observed that ~90% of parasites within the intact, permeabilised pRBCs strongly bound IgG from immune serum, compared to <5% with control serum (Figure 4.13B). Additionally, pRBCs with the highest DNA content, indicative of progression through schizogony and generation of merozoites, exhibited the strongest *Py*17XNL-specific IgG staining (Figure 4.13C). These data were consistent with IgG in immune serum displaying stronger specificity for merozoites than for pRBC. Taken together, this *in vivo* and *in vitro* data supported the hypothesis that infection-acquired *Py*17XNL-specific IgG antibodies bind poorly to the surface of pRBC. However, this was not due to a lack of recognition of parasite antigens, since antibodies did bind to permeabilised pRBC (increasing binding with parasite maturation). These data suggest a specificity for merozoite forms, consistent with effects in blocking parasite replication. Moreover, keep in mind that the cells were fixed only after the binding assay was performed, it seems unlikely that fixation masked the presence of parasite antigen on the surface. Given that fixing was required for intracellular staining, it is possible though unlikely, that this process revealed antigens otherwise hidden on the cell surface. Further microscopical analysis of staining may be required in future experiments.

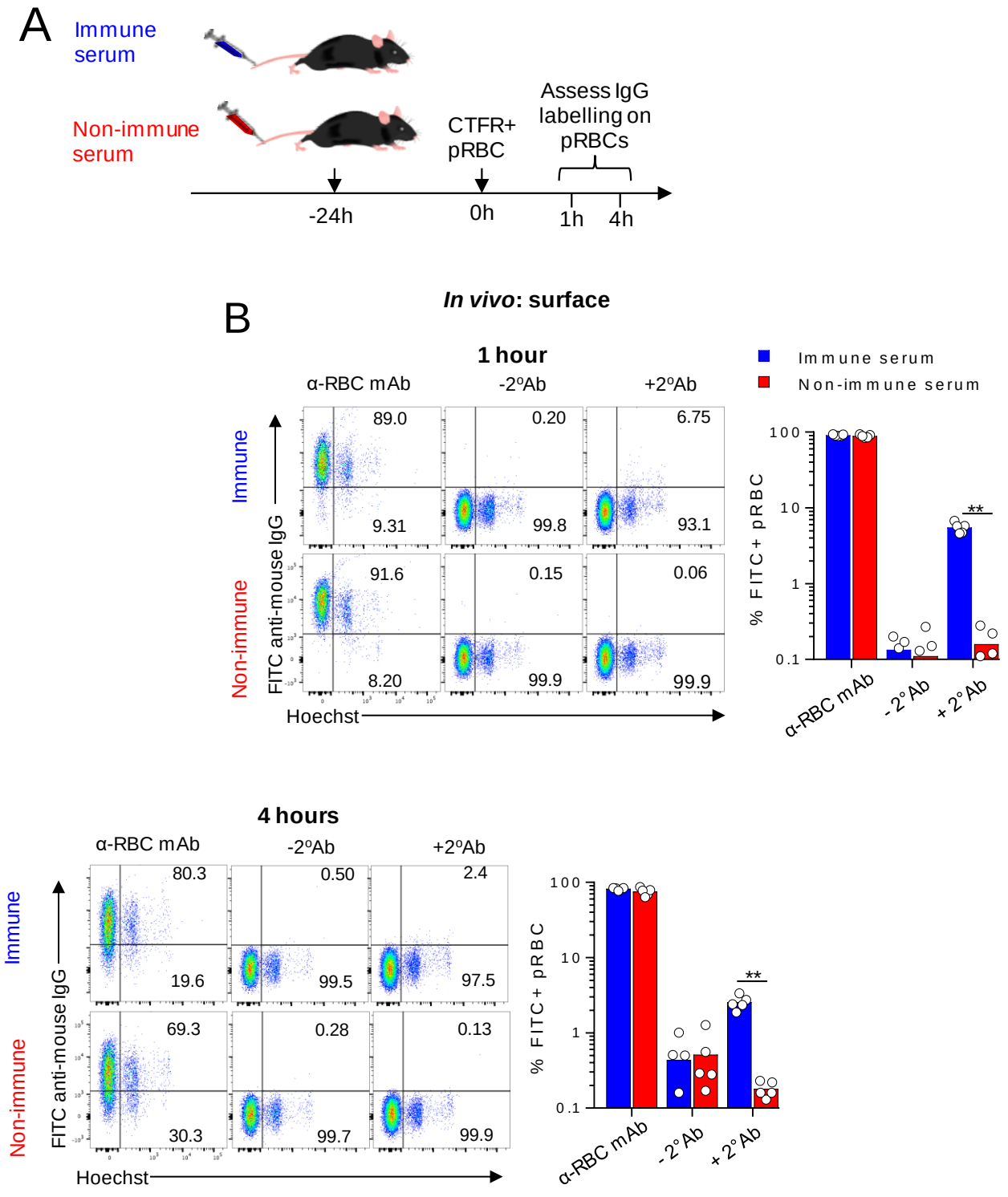

Figure 4.12 Py17XNL-specific IgG binds weakly to intact pRBCs. (A) *Schematic showing mice (n=5/group) injected with immune (blue) or non-immune (red) control serum 24h prior to infection*

with CTFR⁺ Py17XNL-infected pRBCs, with surface deposition of IgG on pRBC assessed 1h and 4h afterwards. ***(B)*** *Representative FACS plots showing detection of in vivo-deposited mouse IgG on the surface of CTFR⁺ RBC (after 1h & 4h in vivo exposure), with positive controls stained in vitro with RBC-specific mouse IgG (34-3C). Data represents two independent experiments showing similar results. Statistics: Mann-Whitney-test, **p<0.0.*

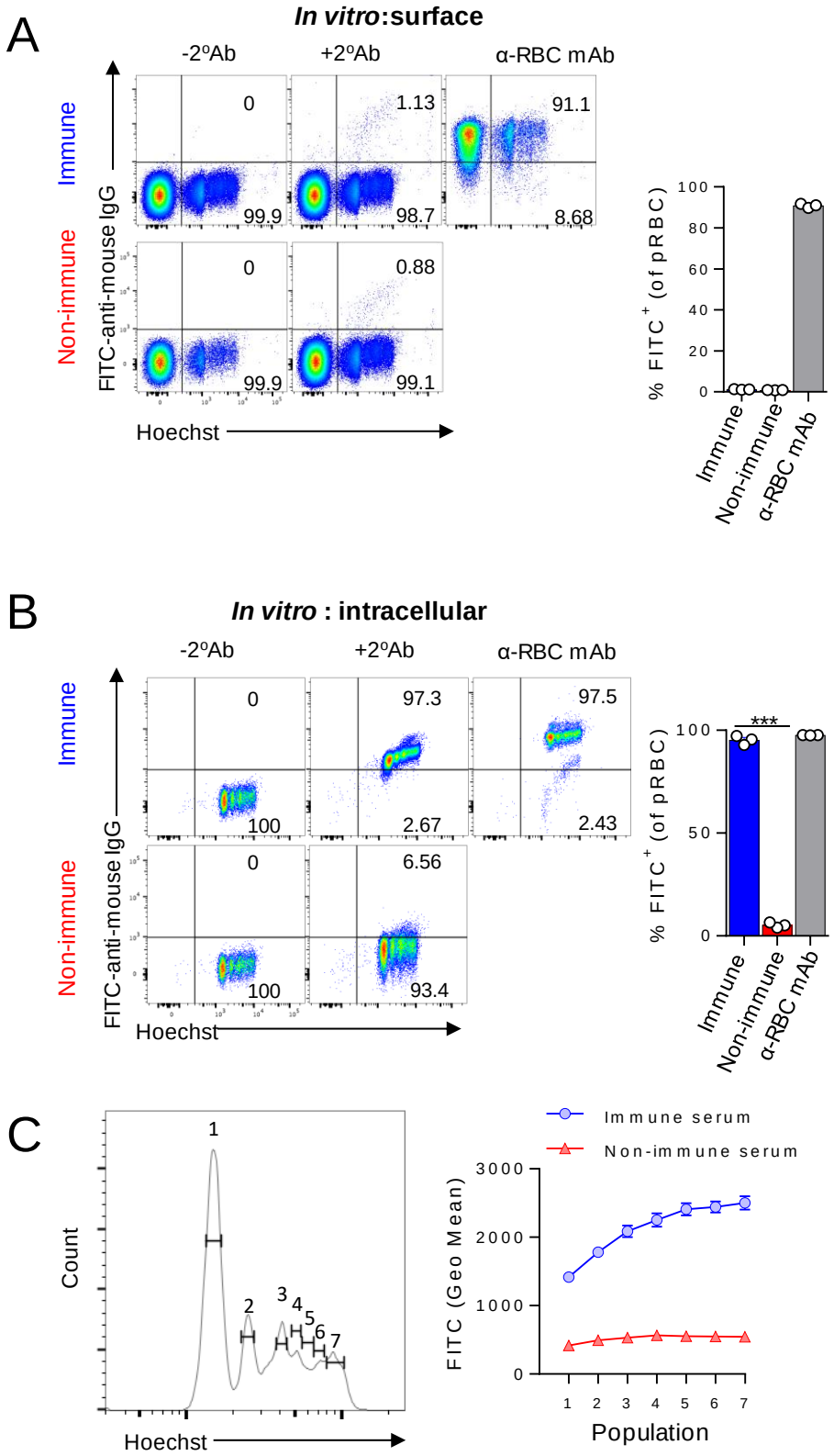

Figure 4.13 Py17XNL-specific IgG exhibits strong binding specificity for structures in schizonts. ***(A-B)*** *Detection of in vitro deposited IgG from immune (blue) or non-immune (red) control serum*

either: ***(A)*** *on the surface of RBC from Py17XNL-infected mice, or* ***(B)*** *inside RBC from Py17XNL-infected mice after fixation/ permeabilisation. Graphs show proportion of pRBCs bound.* ***(C)*** *Representative histogram showing gating for identifying Py17XNL pRBC containing different numbers of merozoites using Hoechst. Graph shows variations in the geometric mean fluorescence intensity of in vitro IgG deposition inside fixed and permeabilised pRBC according to DNA content, when incubated with immune or non-immune control serum (assessed in triplicate). Two-tailed Students T-test, p=0.0004. Data in (A-C) represents four independent experiments each with similar results.*

4.3.2.5 *P. chabaudi chabaudi* AS infection induced antibodies also protect by blocking the next generation of pRBC rather than accelerating pRBC clearance

Having explored the function of antibodies elicited during the primary blood-stage *Py*17XNL infection to protect against homologous re-challenge, next it was sought to determine whether such mechanisms might also act in a second common model of antibody-mediated immunity to malaria - *P. chabaudi chabaudi* AS infection of mice. Here, immune serum was harvested from *Pc*AS-infected wild-type C57BL/6J mice at 40 d.p.i. because earlier time course analysis had revealed this to be the peak period of parasite-specific IgG in this model [211]. First, it was confirmed that *Pc*AS-specific IgG was indeed present in immune serum preparations (Figure 4.14A). Next, the CTFR-labelling approach was used as above, using *Pc*AS-infected $CTFR^{+}$ pRBC, transferred into mice that also received *Pc*AS-immune serum or age-matched control serum 24 hours earlier (Figure 4.14B). Firstly, it was observed that the loss of Gen_0 pRBC was again not influenced by *Pc*AS-immune serum (Figure 4.14C) although the emergence of Gen_{1+} pRBC was clearly impaired (Figure 4.14D) with PMR reductions of ~50% for immune serum compared to control serum. Consistent with no effect on pRBC clearance, and strong effects on Gen_0 to Gen_1 transition, it also observed that *Pc*AS-specific IgG did not bind well to the surface of pRBC *in vitro* (Figure 4.15A), but was capable of binding to intracellular parasite antigens inside late-stage, permeabilised pRBC (Figure 4.15B). This data using a second model of antibody-dependent immunity exhibits striking similarities to the earlier observations with *Py*17XNL. Thus, in two independent models, infection-induced antibodies bound poorly to the surface of pRBC but provided robust protection, not by clearing pRBC but by blocking pRBCs from successfully generating daughter pRBCs.

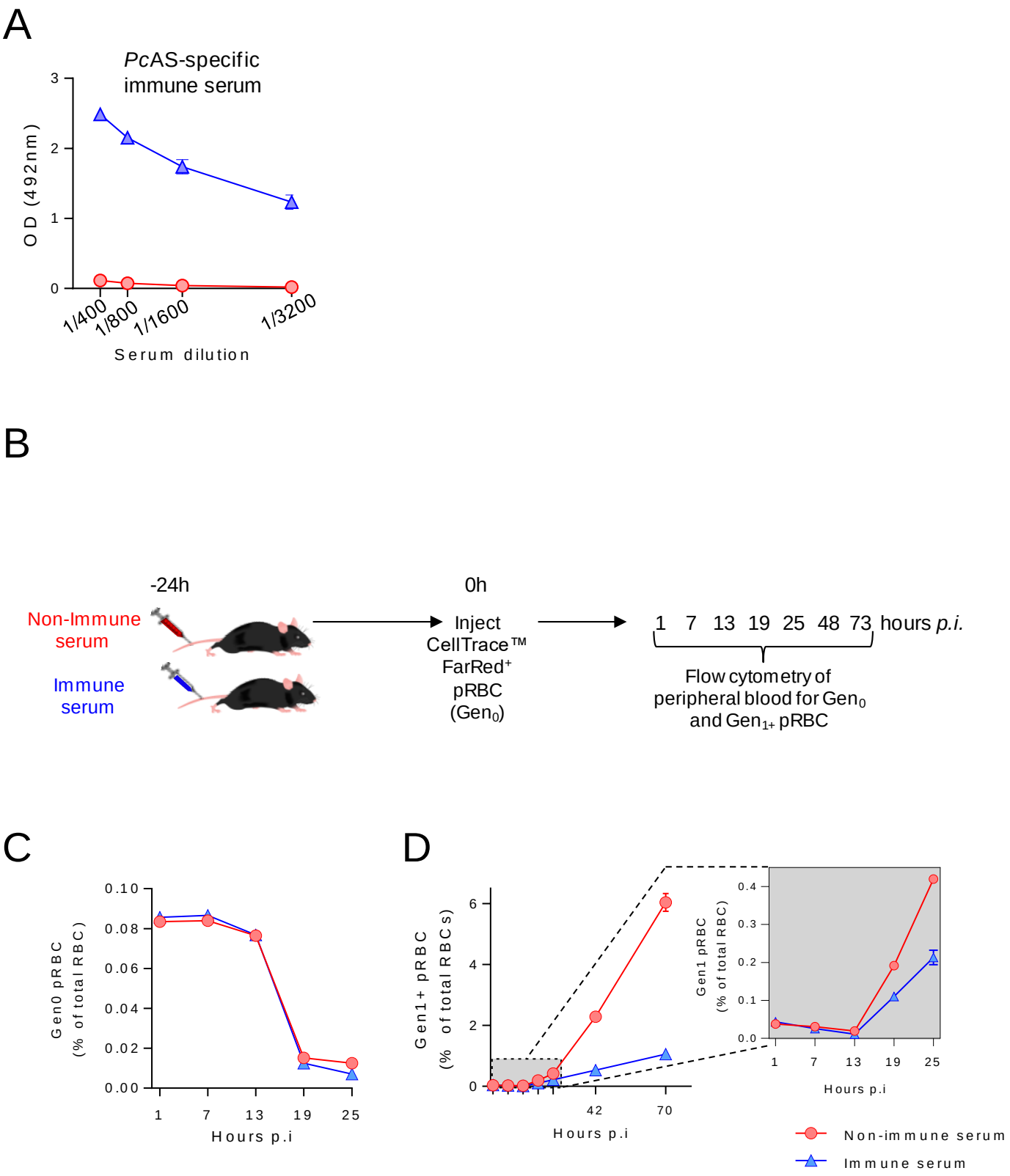

Figure 4.14 P. chabaudi chabaudi AS infection induced antibodies also protect by blocking transition of parasites between RBC, not by accelerating pRBC clearance. *(A) Assessment of PcAS-specific total IgG in diluted sera from infected or age-matched naïve mice (n=10/group), taken at day 40 p.i. with PcAS. (B-D) Mice (n=5/group) were injected with PcAS-immune serum (blue) or non-immune (red) control serum 24h prior to challenge with CTFR+ PcAS-infected pRBCs, with peripheral blood monitored at times indicated for: (C) loss of Gen0 (CTFR+) pRBC over the first 25h, and (D) emergence of Gen1+ pRBC over 73h, with the zoomed-in box showing the first 25h in more detail. Data representative of two independent experiments showing similar results.*

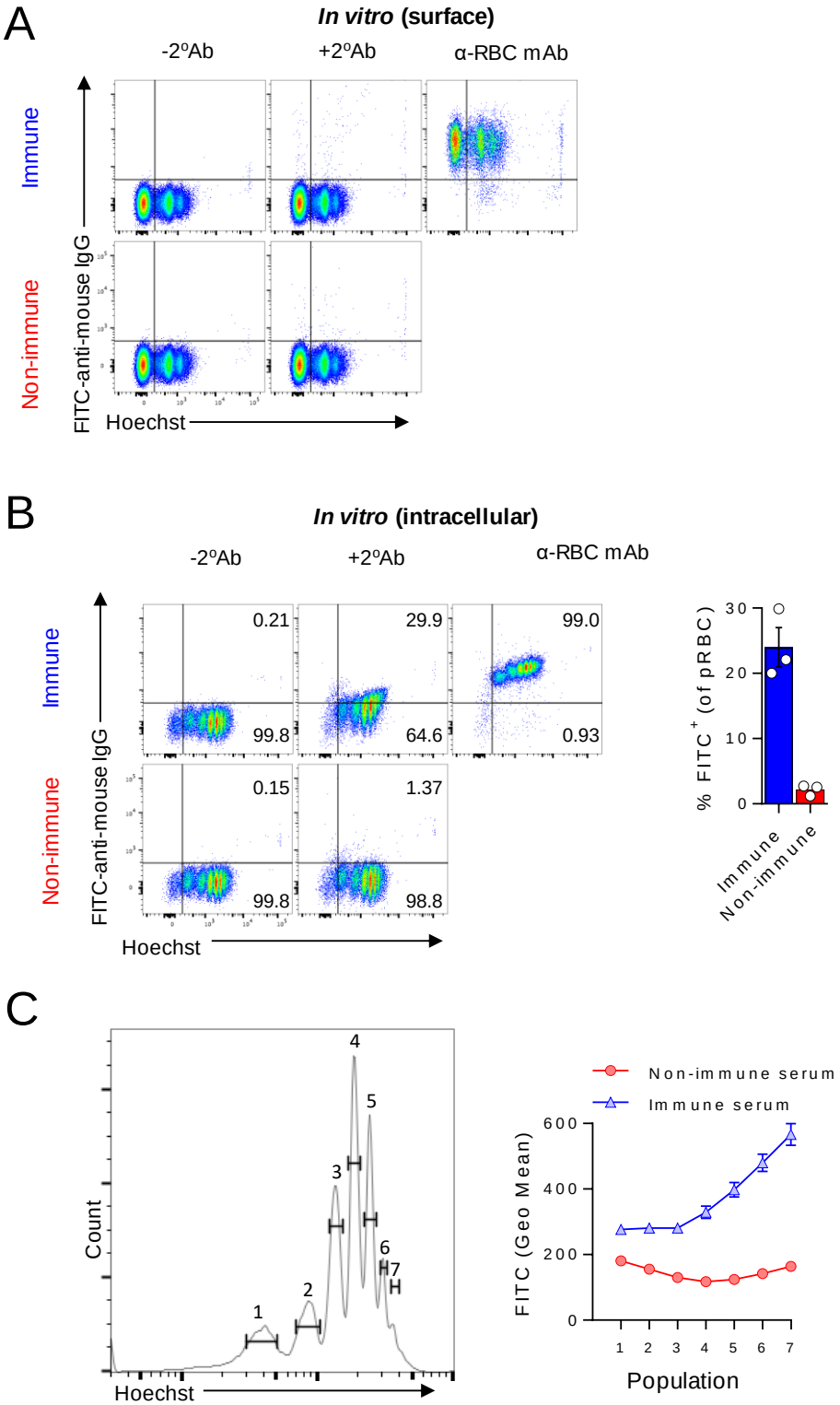

Figure 4.15 P. chabaudi chabaudi AS –specific antibody binds weakly to intact pRBC, yet exhibits substantial specificity for structures in schizonts. *Assessment of in vitro deposition of mouse IgG from PcAS-immune (blue) or non-immune (red) control serum performed in triplicate, either: (A) on the surface of RBC from PcAS-infected mice, or (B) inside RBC from PcAS-infected mice after fixation/permeabilisation. Graph shows percentage of pRBC binding to mouse IgG after fixation/permeabilisation. (C) Representative histogram shows gating for identifying PcAS-infected pRBC containing different amounts of parasite DNA using Hoechst. Graph shows variation in geometric mean fluorescence intensity of in vitro IgG deposition inside fixed and permeabilised pRBC*

according to DNA content. Data are representative of two independent experiments each with similar results.

4.4 Discussion

Antibodies play a key role in controlling parasite numbers during blood-stage malaria. However, the *in vivo* mechanisms of antibody-mediated parasite control are not well known. Several mechanisms have been proposed to explain how *Plasmodium*-specific antibodies may prevent or ameliorate malaria. Broadly speaking, these include three mechanisms: (i) antibodies act mostly alone without the need for other host processes; (ii) antibodies serve as triggers for phagocyte-dependent processes (opsonic phagocytosis and antibody-dependent cellular inhibition (ADCI)); or (iii) antibodies activate complement-mediated direct killing. All three mechanisms could theoretically act on pRBC or merozoites; however, assessing the importance of these *in vivo* has been challenging.

Here, the most common *in vivo* models of humoral immunity to malaria, *P. yoelii* 17XNL and *Pc*AS infection in C57BL/6 mice was used to dissect how parasite-specific antibodies elicited via primary infection, could control parasite numbers during a secondary challenge. This was combined with an RBC adoptive transfer technique to study parasite clearance and replication *in vivo* [134, 144, 212]. By tracking a single cohort of fluorescent-labeled pRBC, and their resultant progeny, it was evident that effective control of pRBC numbers by infection-induced antibodies in two models was mediated not by targeting clearance of pRBC by the host, but by preventing parasites transitioning from one generation of RBC to the next. Moreover, it provided *in vivo* evidence that phagocytes are necessary for these antibodies to optimally block transit of parasites between RBCs. Complement-mediated direct killing via formation of membrane attack complex (MAC) did not play any appreciable role; however, we did not examine C1q block in our study. Thus, data generated from these *in vivo* experiments supports the view that antibodies targeting merozoites for their phagocyte-dependent control play an important role in controlling blood-stage *Plasmodium* infection, although C1q complement mediated blocking may also play a role in parasite control.

Although the study demonstrated a role of phagocytes in preventing parasites transitioning from one generation of RBC to the next, it remains to be determined which of the two main phagocyte-dependent mechanisms - opsonic phagocytosis or ADCI was involved. Given that ADCI is mediated *in vitro* by a monocyte-derived cytokine, Tumor Necrosis Factor (TNF)[213], future studies could explore an *in vivo* requirement for TNF in our system. Another important question arising from the partial decline in antibody-efficacy after phagocyte depletion is whether the partial effect was due to incomplete depletion of phagocytes by clodronate liposomes, or it indicated the existence of multiple mechanisms of actions of antibodies. Although it is understandable that a single-dose of clodronate liposomes is not likely to completely deplete phagocytes for more than a few days, it nonetheless remains a very efficient way to remove phagocytes. For this reason, it is considered that other mechanisms likely contribute to pRBC control in these models, and blockade of merozoite

invasion is the most likely [214]. Future experiments and technological advances may be required to assess this mechanism since it is not currently possible to reliably visualise invasion of RBC by merozoites *in vivo*. A recent study has, however, reported successful isolation of viable merozoites from rodent malaria and demonstrated invasiveness of merozoites [215].

A recent study in human samples found that the capacity of merozoite-specific antibodies to facilitate deposition of the polymeric complement C1q complex strongly correlated with protection from high-density parasitemia [214]. Additionally, *in vitro* assays indicated that although C1q deposition could increase direct complement-mediated lysis of merozoites, C1q deposition alone, i.e. with no other components of the complement system present, was sufficient to enable antibodies to block the invasion of RBC by merozoites. The study thus concluded that merozoite-specific antibodies protected children against high-density parasitemia probably by blocking invasion, and not by direct complement-mediated lysis of merozoites. Our study in mice also supported a crucial role of merozoite-targeting IgG in blocking transition to the next generation of RBC, with no major role of complement-mediated direct lysis. However, we did not directly assess the role of antibody-mediated C1q deposition in our study. Thus, examining whether parasite-specific antibodies are impaired in their capacity to block Gen_0 to Gen_1 transit in $C1q^{-/-}$ mice would be important in future studies. Another important question is whether the complement system was adequately functional in the genetic background of C57BL/6J employed in our study, to compare similarities with human immunity to malaria. A previous assessment of complement in numerous inbred mouse strains focused on the capacity to directly lyse cellular targets [216]. In view of these earlier findings, it was perhaps surprising that in our system direct complement-mediated lysis was not an important mechanism in controlling infection. As the levels of C1 proteins are likely equivalent amongst most mouse strains [216], it remains to be determined whether C1q deposition contributes to antibody function in the *Py*17XNL and *Pc*AS systems. We hypothesised this to be the case since a previous report showed that genetic C1q deficiency in mice was associated with impaired immunity to re-challenge with blood-stage *Plasmodium* parasites [217].

Many, but not all of the suggested mechanisms by which antibodies could serve to control pRBC numbers *in vivo* can be explored during *Py*17XNL infection in mice. For example, it has been suggested that antibodies could prevent cyto-adherence, and thus sequestration of pRBC to endothelial surfaces in various tissues [218, 219]. Similarly, antibodies could prevent adherence of RBC to each other, also known as rosetting [218, 219]. Neither of these two phenomena is well-established in the *Py*17XNL model. Therefore, this data cannot be taken as complete assessment and understanding of all the mechanisms by which antibodies could prevent malaria in *P. falciparum* or *P. vivax*-infected humans. Instead, the findings of the study suggest that targeting pRBC by

antibodies through binding to the erythrocyte surface is not necessary for robust control, and that prevention of transit from one RBC to another, possibly by targeting merozoites, predominates in the two most commonly used mouse models of antibody-mediated immunity. It has previously been shown that *Py*17XNL parasites export variant surface proteins, *yirs*, to the surface of RBC during *in vivo* infection of mice. Moreover, *yirs* are clearly detected by the mouse immune system, and their variation is dependent upon the presence of adaptive immunity [220, 221] In our study, we observed that intact schizont stage pRBC did bind some parasite-specific IgG. It is possible that *yirs* proteins could be the target for such antibodies, in a similar way that *Pf*EMP1 appears to be a major target for pRBC binding antibodies in human samples [222]. However, an important question that emerges from our study is why the IgG response to infection was dominated by antibodies specific to the contents of permeabilised schizonts, most likely merozoites and proteins released into circulation during rupture, and not to pRBC surface proteins. The answer to this question remains currently unknown due to the facts that antigenic variations is a major feature of pRBC surface proteins, which could be related to the ability of antigen-presenting cells to access and process pRBC surface proteins compared to merozoite proteins and the cellular debris released by pRBC rupture.

The findings of this study also raise the question as to how antibody-mediated immunity might be boosted in a rational manner. For example, could increasing the plasma concentration of antibodies that recognise pRBC further improve protection? This may indeed be the case; however, since antigenic variation is a major feature of pRBC surface proteins, it will likely be challenging to induce pRBC-targeting antibodies that elicit long-lasting immunity to high-density parasitemia in humans. Nevertheless, the data using two major *in vivo* models of antibody-mediated immunity to blood-stage infection suggest that pRBC clearance is not a crucial mechanism for naturally-acquired antibodies in controlling parasitemia. Instead, this data is consistent with the suggestion that binding of affinity-matured IgG to the surface of merozoites could be highly protective against blood-stage *Plasmodium* infections *in vivo* via multiple mechanisms including those employing phagocytic cells. We could not infer whether these antibodies are merozoite binding; an Immune Fluorescent Assay (IFA) might be needed to explore the binding specificity in greater details. However, these pre-clinical *in vivo* data provide further insight into the types of antibody functions that might protect naturally-exposed and immunized humans against malaria. It is noted, due to time constrains during my PhD, I was unable to purify IgG from immune serum, and provide definitive proof that parasite specific IgG was indeed responsible for control of Gen_1 parasite numbers. Instead, individual batches of immune serum were quality controlled by performing parasite-specific IgG ELISA, and ensuring that each batch passed a threshold titre. Immune serum was not heat inactivated. It should be noted that subsequent to the submission of this thesis, IgG purification was completed, and confirmed as being productive in our models.

Chapter Five:

Developing a high-throughput *in vivo* screen for *Plasmodium* genes that mediate interaction with the host immune system

5.1 Abstract

The severity of malaria is often associated with the total number of *Plasmodium* parasites present in the body during infection. It is likely that both host and parasite genetic factors are involved in determining parasite dynamics *in vivo*. However, our understanding of parasite genes that control interactions with mammalian hosts is limited, particularly since a large portion of the *Plasmodium* genome still lacks functional annotation. Despite this, it is clear that *Plasmodium* genes mediate remodeling of host RBC, particularly via proteins exported out of the parasite itself. Hundreds of *Plasmodium* genes encode for exported genes, which are known collectively as the "exportome". While some of these have been well characterised, the precise functions of many remain completely unknown. Therefore, the aim of my work was to develop an *in vivo* methodology to screen parasite genes required for host interaction. Using *P. berghei* ANKA infection of wild-type and immune-deficient C57BL/6j and BALB/c mice, I screened 117 genes *in vivo* using an established high-throughput barcode-based sequencing approach. Of these genes, 32 were identified as essential for parasite growth regardless of host immune status. Importantly, 8 of the essential genes had no previous functional annotation. Most importantly, 10 mutants were out-competed from the pool of 117 knock-out parasites in wild-type mice, yet grew well in immune-deficient mice. One of these genes encodes PTEX88, a component of the molecular machinery that translocates parasite proteins out of the parasite itself [223]. Further analysis of inducible *ptex88* knockdown parasites suggested that PTEX88 might play a role in governing parasite maturation within RBCs. Thus, this study provided proof-of-concept that parasite genes do indeed exist that are important for blood-stage survival only in the presence of a fully functioning immune system.

5.2 Introduction

The emergence of resistance to anti-malarial drugs and the lack of an effective vaccine to prevent malaria highlight the urgent need for the development of targeted malaria intervention. During blood-stage malaria, the merozoite form of the *Plasmodium* parasite infects host RBCs and transports proteins to sub-cellular locations. These *Plasmodium*-exported proteins remodel the host RBC to enhance parasite virulence, thereby increasing the pathogenesis and severity of the disease.

During the remodelling process, many structural and biochemical changes occur throughout the parasite life-cycle that include development of a tubulovesicular network in the host cell that sorts and distributes exported proteins to target locations beyond its own plasma membrane (PM) and the parasitoporous vacuole membrane (PVM); and other membrane-bound structures formed during the development of this network, including Maurer's clefts (MCs) [61], electron-dense vesicles (~80 nm diameter) [62, 63], J-dots [64] and knob associated histidine-rich proteins (KAHRP) and PfEMP1 [66]. The PfEMP1 protein family is antigenically diverse as they are encoded by 60 *var* (variable) genes per haploid genome [67-70]. Several other exported parasite surface proteins, such as members of the RIFIN, STEVOR and SURFIN families, also exhibit antigenic variation [224, 225]. Some of these exported proteins, e.g. ring-infected erythrocyte surface antigen (RESA) and PfEMP3 are associated with the RBC cytoskeleton beneath the plasma membrane [226-228].

The genomes of Rodent Malaria Parasites (RMP) contain an average of 5,500 genes. A number of multi-gene families in RMP encode exported proteins, and these are mostly sub-telomeric [229]. However, more than 50% of *Plasmodium* genes have unknown function since their AT-rich genome was difficult to engineer in *E. coli* systems due to poor flanking sequences and the low rate of homologous recombination for reverse genetics studies. Reduced number of selection markers has also been a limiting factor, especially for *P.berghei* studies in which drug toxicity for the animals was an issue. Only a small percentage of genes that encode exported proteins have been previously investigated [230, 231].

Our collaborators (Dr. Oliver Billker, Wellcome Trust Sanger Institute) recently developed a method for reverse genetic screening of the *Plasmodium berghei* genome [138] by creating an open-access *Plasmodium* genetic modification resource, *Plasmo*GEM, which includes knock-out vectors that integrate efficiently along with gene-specific molecular barcodes [232]. Here, I studied export protein-related genes using *Plasmo*GEM resources.

Firstly, 1,818 genes coding for putative exported proteins were identified *in silico* prior to my project based on 1) export prediction, 2) putative transmembrane domain, 3) published sequence

phenotype, 4) PEXEL orthologue, 5) signal peptide, 6) translocon components, 7) Maurer's cleft/ sequestration genes, 8) Van Ooji conserved exportome or 9) rodent malaria parasite only synteny. Following score-based selection, 289 out of the total 1,818 genes coding for putative exported proteins were positive for at least 3 criteria and were selected for characterisation. Knock-out *Plasmo*GEM vectors for 117 genes were successfully generated from 289 candidates prior to the initiation of my project (refer to Flowchart 1).

Flowchart 1: Selection process of 117 genes

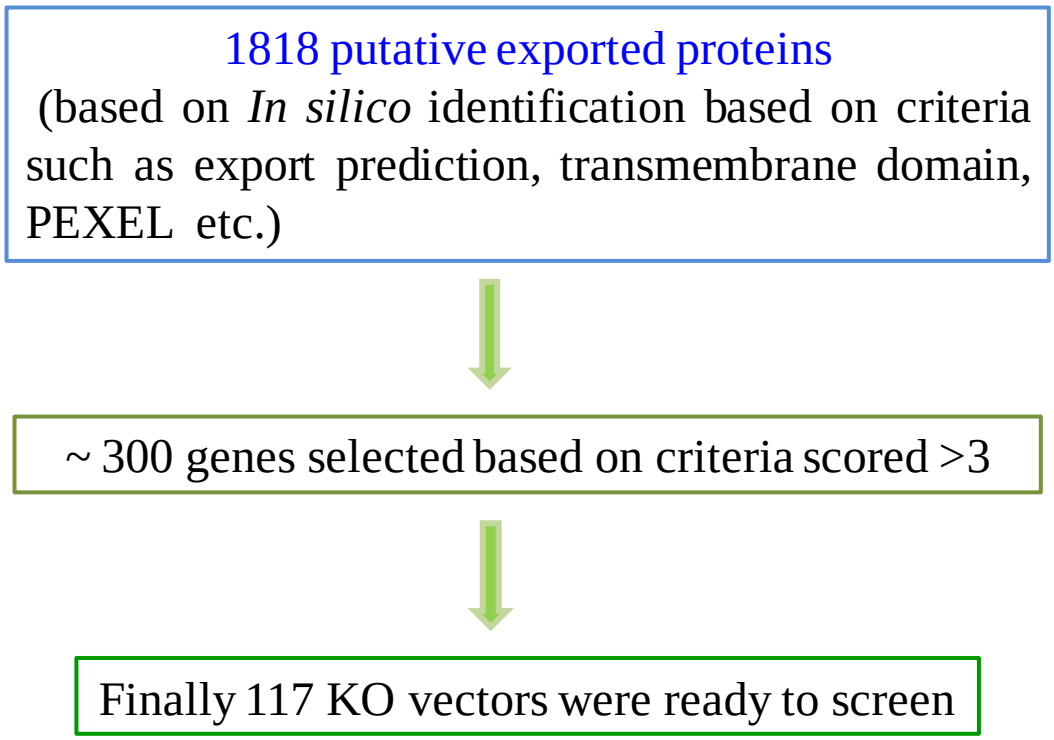

*Plasmo*GEM vectors were designed with long homology arms for efficient genome integration and carried gene-specific barcodes to identify individual mutants within a pool [232]. Vectors were generated from *Plasmodium berghei* ANKA (*Pb*A) genomic DNA libraries (*Pb*G) through a sequential, two-step process, which utilises recombinase-mediated engineering (recombineering) and Gateway technology [138]. The positioning of the recombineering primers determined the gene targeting strategy. A molecular barcode consisting of 11 variable nucleotides, flanked by 20 invariable nucleotides (that constituted primer annealing sites for PCR amplification), were introduced into each of the *Plasmo*GEM vectors. A common pair of PCR primers was used to amplify the barcode module from all *Plasmo*GEM constructs. The barcodes permitted identification of each vector, and therefore, each transgenic parasite by next-generation sequencing on an Illumina sequencer, a technique referred to as barseq. It has recently become possible to measure individual

growth rates within parasite pools composed of different mutants in the blood of a single mouse. Hence, analysis of mixed populations of mutants using barcode technology provides two major advantages: 1) acceleration of the *Plasmodium* genome screening process and 2) significant reduction in cost and animal usage.

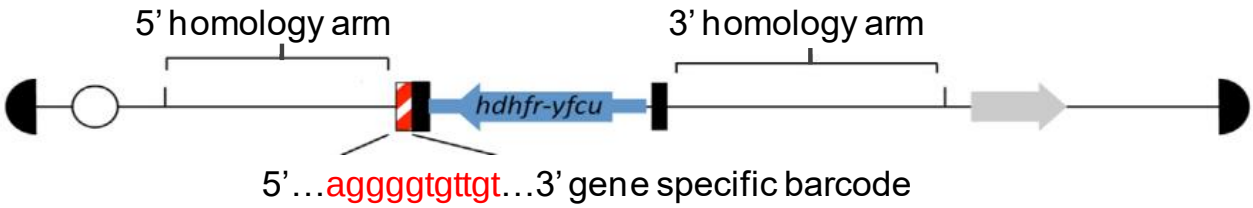

Figure 5.1 Schematic representation of knockout vector design.

Note: The design and preparation of the vectors was performed by the *Plasmo*GEM team at the Sanger institute.

5.3 Results

5.3.1 Detecting small numbers of bar-coded KO parasites in the blood and tissue of mice

5.3.1.1 Mutants can be detected in tissues using barseq analysis

One important aspect of parasite interaction with mammalian hosts, not only for *Plasmodium falciparum* in humans but also for *Pb*A in mice, is the potential for parasites to accumulate in microvasculature in various tissues. This process is termed "sequestration" in human malaria and is generally defined by the discovery of specific ligand/receptor interactions, such as chondroitin sulphate A/PfEMP1 interactions in pregnancy-associated placental sequestration. In my project, I hypothesized that certain exported proteins might be required not for growth in the blood-stream, but for accumulation in tissues. Therefore I predicted that certain KO parasites would be more abundant in the bloodstream than they would be amongst sequestered parasites in tissues. To test this hypothesis, it was first necessary to determine if parasite barcodes from *Plasmo*GEM vectors could be detected reliably in organs from infected mice since mutants had previously only been assessed in circulating blood [233]. Before screening large numbers of genes, I first investigated whether a small number of bar-coded mutants could be detected in various tissues of mice. Five mutants with known sequestration phenotypes were employed: 1) EMAP1 (erythrocyte membrane-associated protein), which is a member of the PEXEL-negative protein family, and has no known role in parasite sequestration [234]; 2) MIF (Macrophage migration inhibitory factor) is homologous to mammalian MIF, which modulates the immune response against blood-stage parasites, is located in the cytoplasm of the parasite, and has no known role in sequestration [235]; 3) TRX2 (Thioredoxin 2 protein), is a core component of the *Plasmodium* translocon of exported proteins (PTEX) and acts to unfold proteins for translocation [223]; 4) PTEX88 is another core component of PTEX involved in the sequestration of pRBC and cerebral malaria [223]; and 5) SBP1 (Skeleton Binding protein 1) is transmembrane protein that induces the formation of membranous structures within the pRBC cytoplasm called Maurer's Clefts (MC) and its main function is to position PfEMP1 on the RBC for cyto-adherence (i.e. protein-protein interaction) [236]. Given that PTEX88, TRX2, and SBP1 are all well-known exported proteins with published roles in disease severity in *Pb*A infections, these three KO parasites were hypothesized to be outcompeted in tissues compared to the blood-stream.

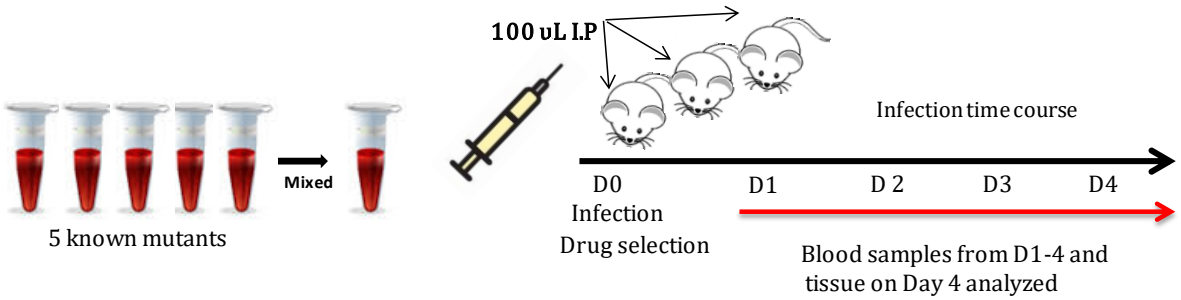

Figure 5.2 Detecting mixed populations of mutants in blood and tissues. *Mice (n= 3) were infected with 100 µl of 5 pooled PbA knock-out mutants and placed under pyrimethamine drug selection. Blood samples were collected on days 1- 4 p.i., and organs on day 4 p.i. after perfusion of CO_2 euthanised mice. Experiment conducted once.*

Mice were infected with 100µl of blood containing a pool of 5 mutants, each isolated from individual transfections and subsequently mixed together. On day 0 mice were placed under pyrimethamine drug selection and blood was collected on day 1- 4 p.i. and tissue samples were collected on day 4 p.i for DNA extraction (Figure 5.2). The samples were then processed for barcode sequencing and analysis.

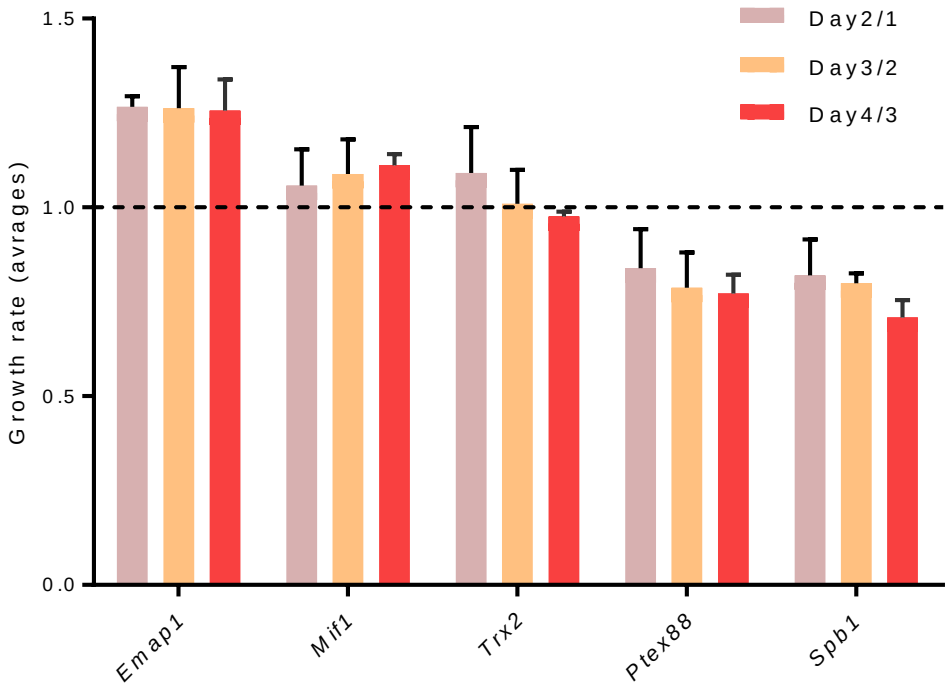

Figure 5.3 Mutants were present in blood as expected. *Average blood-stage growth rate of 5 known-phenotype barcoded PbA KO mutants (n=3).*

I first examined the ability of the 5 mutants in the pool to be detected in the blood. Having determined the relative abundance of each mutant within the pool, I next calculated a metric termed "growth rate" (Figure 5.3). I defined this to be the fold-change in the relative abundance of a mutant

from one day to the next (e.g from day 1 to day 2, or day 2 to day 3) (the calculation is given in methods section). *Emap1* and *Mif*, which were known to be non-essential for blood-stage growth, exhibited slightly higher growth rates than the other three mutants over the course of infection. In particular, *sbp1* and *ptex88* KO parasites had reduced growth rates compared to *Emap1* and *Mif*. This data first confirmed my own capacity to detect mutants within a pool, and furthermore confirmed reduced growth rate fitness, as expected, for parasites lacking *sbp1* or *ptex88.*

Having confirmed detection of KO parasites in the blood, I next determined whether KO parasites could be detected in tissues. In order to detect KO parasites in tissues, on day 4 p.i., multiple tissue samples (spleen, lung, heart, brain, liver, kidney and adipose tissue) were harvested from mice after removing circulating blood by perfusion of CO_2 euthanized mice. DNA was extracted from tissue samples and PCR used to amplify barcodes, prior to sequencing.

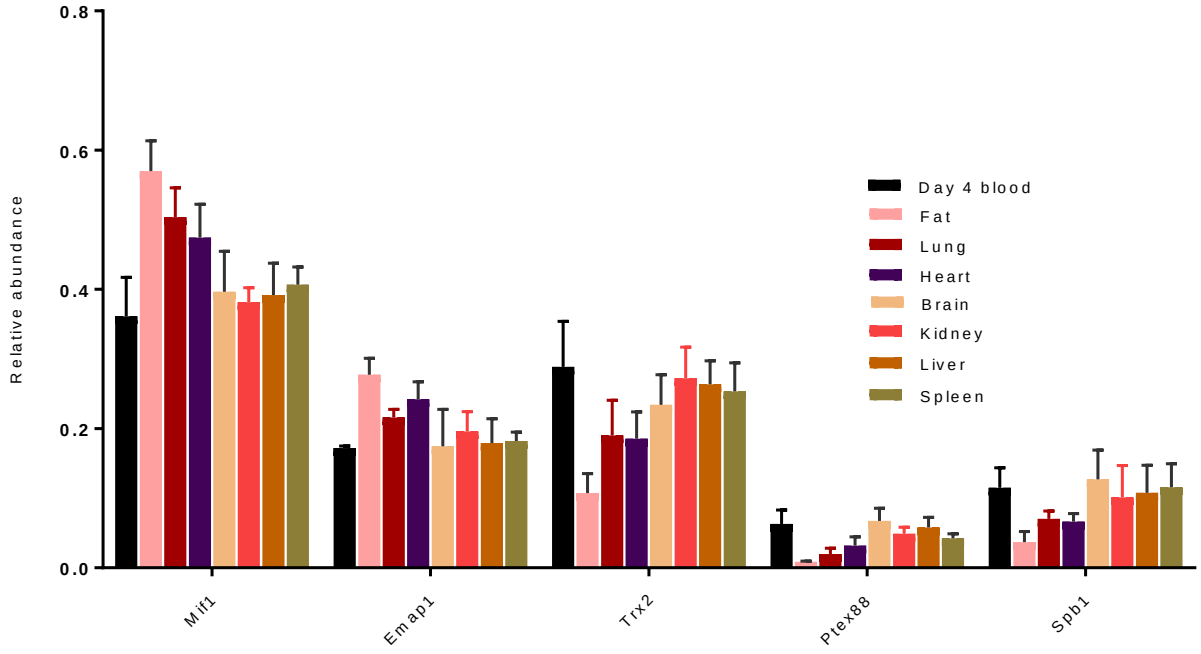

Figure 5.4 Mutants relative abundance of in blood and different tissues. *Mutants accumulate in tissues in accordance to blood relative abundance.*

The relative abundance of a mutant in different tissues showed the same pattern for the relative abundance of that mutant in the blood (Figure 5.4). As the relative abundance of *Mif* and *Emap1* were high in the blood, their relative abundance was also high in the tissues. Furthermore, tissues that are associated with parasite accumulation demonstrated increased relative abundances of most mutants in comparison to other tissues. For example, we found that adipose tissue had a high relative abundance of a mutant when the relative abundance was also high in the blood. However, adipose tissue showed low relative abundances when the mutant demonstrated a low abundance in the blood and this similar phenomenon was observed for *ptex88,* and *sbp1*. Therefore, our findings

demonstrated that the barcode based sequencing approach is indeed capable of detecting KO mutants in tissue as well as blood and that the relative growth rates and abundance of KO mutants is consistent with known phenotypes.

5.3.2 Screening 117 genes to explore their role in blood-stage infection

Here, it was hypothesised that parasite genes that encoded for exported proteins might be required for blood-stage growth, and interact with host factors. If a particular gene is important for interacting with the host immune system, then a KO mutant for that gene will be lost from the pool of mutants in the immune-competent host. Therefore, the wild-type mice C57BL/6J and BALB/c and their corresponding immune-deficient mice *rag1*$^{-/-}$ and SCID, which are mainly deficient of T and B cells, were used for screening of 117 genes. The detailed experimental procedure has been described in the material and methods (sub-section 2.4.14) and schematic representation (Figure 5.5). Briefly, the pool of KO vectors DNA was transfected into purified schizonts using the Lonza 4D-Nucleofactor system. Then the transfection mixture was immediately injected intravenously into the tail veins of 6-8 week old C57BL/6J, *rag1*$^{-/-}$, Balb/c, and SCID mice. After 24 hours of infection, mice were placed under drug selection. Blood samples were collected on days 4-7 p.i. and organs on day 7 p.i. after perfusion of CO_2 euthanized mice. Blood and tissue DNA was used for PCR amplification of barcodes, with an index primer used to tag each sample for individual identification, and then samples were sequenced by next-generation sequencing for barcode counting analysis.

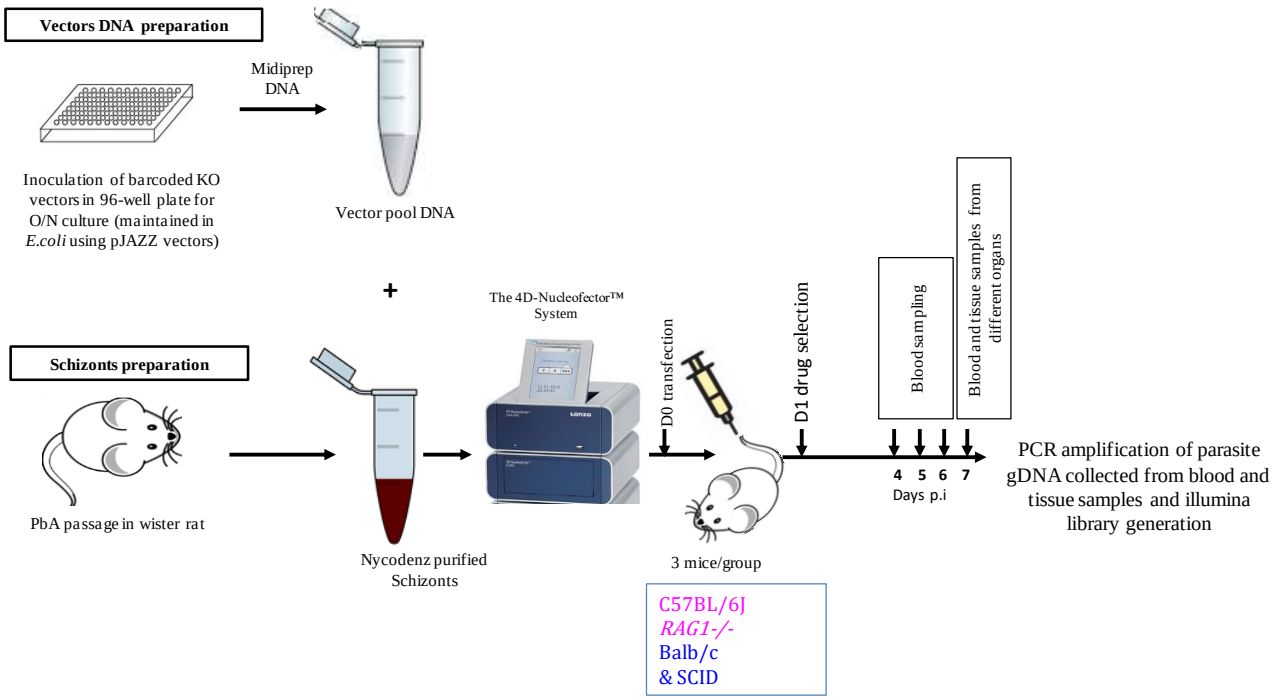

Figure 5.5 Schematic representation of screening of 117 KO vectors using barcode-based sequencing assay*. Trnasfetion was done once the pool of knock-out vectors DNA and schizonts were ready and mice were infected with transfected DNA via tail intravenously injection. Parasitemia monitored on day 4 p.i. and blood and tissue samples were analysed for barcode quantification.*

Table 1: List of *Plasmo*GEM identification numbers for vectors used in the experiments

Gene ID	Annotation	PBANKA_100060	erythrocyte membrane antigen 1
PBANKA_131800	serine/threonine protein kinase, putative	**PBANKA_120520**	conserved membrane protein, unknown function
PBANKA_133500	conserved Plasmodium protein, unknown function	**PBANKA_122090**	conserved Plasmodium protein, unknown function
PBANKA_062320	lysophospholipase, putative	**PBANKA_131150**	conserved Plasmodium protein, unknown function
PBANKA_052430	tryptophan/threonine-rich antigen, putative	**PBANKA_070070**	Plasmodium exported protein, unknown function
PBANKA_132380	conserved Plasmodium protein, unknown function	**PBANKA_050060**	fam-b protein
PBANKA_062310	Plasmodium exported protein, unknown function	**PBANKA_124380**	apicoplast TIC22 protein, putative
PBANKA_132800	serine/threonine protein phosphatase, putative	**PBANKA_041850**	Plasmodium exported protein, unknown function
PBANKA_041065	conserved Plasmodium protein, unknown function	**PBANKA_140040**	fam-b protein
PBANKA_133490	conserved Plasmodium protein, unknown function	**PBANKA_100850**	translocon component PTEX150
PBANKA_112510	3-oxoacyl-acyl-carrier protein synthase, putative	**PBANKA_060990**	Pbj4
PBANKA_101610	peptide chain release factor 1, putative	**PBANKA_135800**	thioredoxin 2
PBANKA_050260	conserved Plasmodium protein, unknown function	**PBANKA_102390**	glutathione S-transferase, putative
PBANKA_113970	conserved Plasmodium protein, unknown function	**PBANKA_094130**	translocon component PTEX88, putative
PBANKA_141030	M1-family alanyl aminopeptidase, putative	**PBANKA_122020**	lysophospholipase, putative
PBANKA_061580	exported serine/threonine protein kinase	**PBANKA_133220**	translation initiation factor IF-1, putative
PBANKA_140070	Plasmodium exported protein, unknown function	**PBANKA_133870**	plasmepsin V, putative
PBANKA_052320	serpentine receptor, putative	**PBANKA_134540**	ER lumen protein retaining receptor 1, putative
PBANKA_133090	conserved Plasmodium protein, unknown function	**PBANKA_110090**	fam-a protein
PBANKA_090790	conserved Plasmodium protein, unknown function	**PBANKA_110100**	fam-a protein
PBANKA_124660	fam-b protein cleft-like protein 1	**PBANKA_090270**	leucine-rich repeat protein
PBANKA_020760	asparagine-rich antigen, putative	**PBANKA_120790**	protein phosphatase, putative
PBANKA_133810	conserved Plasmodium protein, unknown function	**PBANKA_133430**	exported protein 2, putative
PBANKA_070100	tryptophan-rich antigen, putative, pseudogene	**PBANKA_104020**	BIR protein
PBANKA_140060	cytoadherence linked asexual protein, putative	**PBANKA_051900**	S-antigen, putative
PBANKA_031000	heat shock 40 kDa protein, putative	**PBANKA_140330**	phosphatase, putative
PBANKA_123820	DnaJ protein, putative	**PBANKA_030060**	Plasmodium exported protein, unknown function
PBANKA_083610	phosphatidylinositol N-acetylglucosaminyltransferase subunit P, putative	**PBANKA_020890**	conserved Plasmodium protein, unknown function
PBANKA_071420	ClpB protein, putative	**PBANKA_062350**	fam-a protein
PBANKA_061060	peripheral plastid protein 1, putative	**PBANKA_083680**	erythrocyte membrane associated protein 1 fam-a protein
PBANKA_093120	heat shock protein 101, putative	**PBANKA_100120**	conserved Plasmodium protein, unknown function
PBANKA_093830	heat shock protein, putative	**PBANKA_070120**	conserved Plasmodium protein, unknown function
PBANKA_082630	thioredoxin-like protein 2, putative	**PBANKA_080040**	conserved Plasmodium protein, unknown function
PBANKA_132070	signal peptide peptidase, putative	**PBANKA_010220**	trophozoite exported protein 1, putative
PBANKA_010780	citrate synthase-like protein, putative	**PBANKA_120710**	Plasmodium exported protein, unknown function
PBANKA_052480	early transcribed membrane protein small exported protein	**PBANKA_010720**	conserved Plasmodium protein, unknown function
PBANKA_031660	reticulocyte binding protein, putative	**PBANKA_120820**	conserved Plasmodium protein, unknown function
PBANKA_110430	conserved Plasmodium protein, unknown function	**PBANKA_060880**	conserved Plasmodium protein, unknown function
PBANKA_120070	conserved Plasmodium protein, unknown function	**PBANKA_100860**	conserved Plasmodium protein, unknown function
PBANKA_100390	sexual stage-specific protein precursor, putative	**PBANKA_051080**	conserved Plasmodium protein, unknown function
PBANKA_133270	duffy-binding protein	**PBANKA_111210**	conserved Plasmodium protein, unknown function
PBANKA_050120	up-regulated in infective sporozoites early transcribed membrane protein	**PBANKA_041540**	conserved Plasmodium protein, unknown function, pseudogene
PBANKA_111760	conserved Plasmodium protein, unknown function	**PBANKA_041190**	conserved Plasmodium protein, unknown function
PBANKA_083210	conserved Plasmodium protein, unknown function	**PBANKA_061310**	conserved Plasmodium protein, unknown function
PBANKA_110140	rhoptry-associated protein 2/3	**PBANKA_051810**	conserved Plasmodium protein, unknown function
PBANKA_110500	conserved Plasmodium protein, unknown function	**PBANKA_132420**	conserved Plasmodium protein, unknown function
PBANKA_092770	conserved Plasmodium protein, unknown function	**PBANKA_082420**	perforin-like protein 3
PBANKA_100010	reticulocyte binding protein, putative	**PBANKA_102910**	conserved Plasmodium protein, unknown function
PBANKA_091510	LEM3/CDC50 family protein, putative	**PBANKA_082530**	conserved Plasmodium protein, unknown function
PBANKA_134910	merozoite surface protein 7	**PBANKA_143540**	conserved Plasmodium protein, unknown function
PBANKA_070440	alpha/beta hydrolase, putative	**PBANKA_132960**	conserved Plasmodium protein, unknown function
PBANKA_133690	conserved Plasmodium protein, unknown function	**PBANKA_113870**	conserved Plasmodium protein, unknown function
PBANKA_021460	Plasmodium exported protein, unknown function	**PBANKA_083660**	fam-b protein
PBANKA_100760	conserved Plasmodium protein, unknown function	**PBANKA_144790**	conserved Plasmodium protein, unknown function
PBANKA_104030	fam-b protein	**PBANKA_135130**	conserved Plasmodium protein, unknown function
PBANKA_021550	erythrocyte membrane associated protein 2	**PBANKA_110130**	Putative SBP1
PBANKA_120060	Plasmodium exported protein, unknown function	**PBANKA_114590**	Putative MAHRP1b
PBANKA_050100	reticulocyte binding protein, putative	**PBANKA_131910**	Haemolysin 3
PBANKA_051700	early transcribed membrane protein	**PBANKA_010060**	schizont membrane associated cytoadherence protein (SMAC)

5.3.2.1 Validation of vectors

To confirm that all the selected vectors were present during transfection, a small aliquot of the transfection mixture was collected after electroporation by washing the electroporation wells of the 16-strip Amaxa 4D. This wash was then used as an input sample, thus acting as a positive control for the presence of vectors in the vector pool and also as an internal control for sample cross-contamination.

Vectors for seven control mutants (4 normal growing and 3 slow growing) were spiked into the pooled DNA of 117 KO vectors, making up the total of 124 transfected vectors in the pool. However, we only recovered 117 vectors (94%) in the input sample (depicted in Flowchart 3). A small number of vectors were lost, possibly because of the insufficient DNA of those specific vectors.

Flowchart 3: Presence of vectors DNA in the input samples

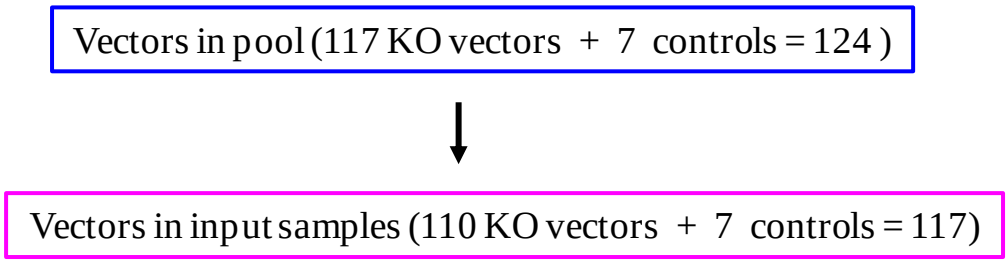

Vectors were not present in the DNA pool

PBANKA_062350	fam-a protein
PBANKA_070100	tryptophan-rich antigen, putative, pseudogene
PBANKA_090790	conserved Plasmodium protein, unknown function
PBANKA_100390	sexual stage-specific protein precursor, putative
PBANKA_120070	conserved Plasmodium protein, unknown function
PBANKA_122090	conserved Plasmodium protein, unknown function
PBANKA_131800	serine/threonine protein kinase, putative
PBANKA_134910	merozoite surface protein 7
PBANKA_135130	conserved Plasmodium protein, unknown function

Further analysis of the vector-specific barcode counting of the input pool DNA revealed that 81% of the vectors present in the input samples had a relative barcode abundance of approximately

400-500 (Figure 5.6) with 10% above or below the average line (*note*: one mutant was considered an outlier). Importantly, most of the vectors were present in relatively constant proportions in each input sample indicating that the DNA preparation in a pooled midiprep did not overtly bias the experiment (Figure 5.6).

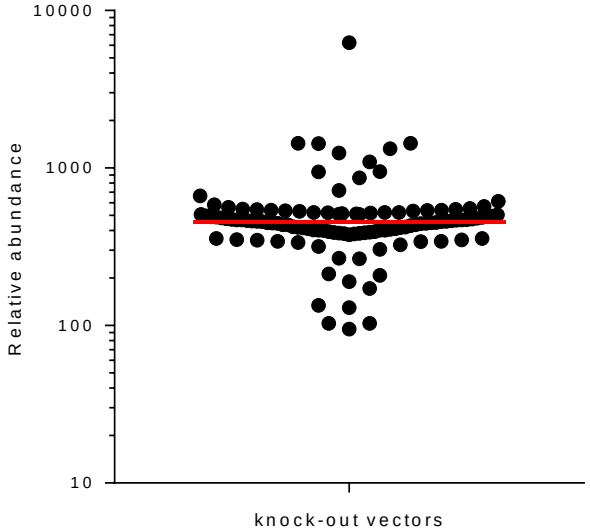

Figure 5.6 Relative abundance of vectors in the input sample. *The input sample was collected from the electroporation cuvette after transfection and measured the proportion of each vector present in the vector pool during transfection.*

5.3.2.2 Parasites grew normally in all mouse strains

Schizonts were transfected with the pool of vector DNA in twelve batches, and each batch was immediately injected intravenously into mice (n=3) of each four different mouse strains (i.e. C57BL/6J, *Rag1*$^{-/-}$, Balb/c, and SCID). After 24 h of infection, mice were placed under drug selection to eliminate wild-type parasites, and infections were monitored from day 5-7 p.i. using Giemsa-stained thin blood films. Data showed that overall parasites grew in a similar manner in all four groups of mice (Figure 5.7).

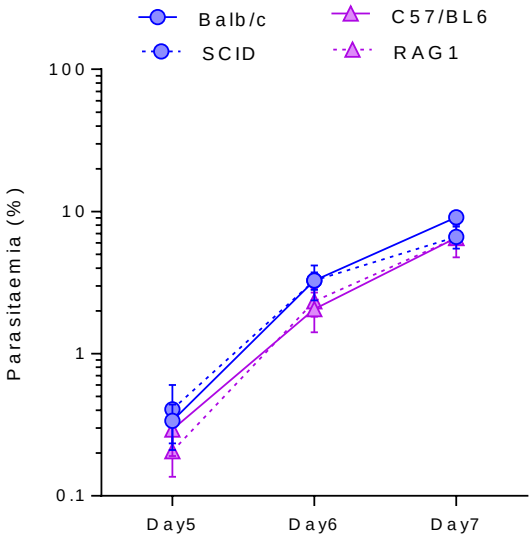

Figure 5.7 Mutant parasites grew similarly in all four mouse strains. *Transfected PbA schizonts were intravenously injected into C57BL/6J, rag1*$^{-/-}$*, Balb/c and SCID mice (n=3). Parasitemia was monitored on days 5-7 p.i. using Giemsa-stained thin blood films.*

5.3.2.3 Normal and slow growing control mutants had corresponding fitness values

Mutants of four genes known to be non-essential for asexual parasite growth were included in the pool of 117 genes "as reference genes" (normal growing controls) for comparing the growth rates of all other mutants. This reference set consisted of two knockout vectors for the major surface proteins of ookinetes, P25 and P28 [237]; another knockout vector for a secreted ookinete adhesive protein, *soap* [238]; and a C-terminal tagging vector for the redundant *p230* gene [239]. In addition, knock-out vectors of three genes of slow-growing controls, namely *plasmepsin* iv, *bckdh* (PBANKA_110420), and a putative *methyl transferase* (PBANKA_140160) were also included to identify mutants with reduced growth rates in a more accurate manner. Plasmepsin IV is an aspartic

protease involved in the degradation of hemoglobin. It has been reported that deletion of *plasmepsin IV* gene in the *P. berghei* genome resulted in attenuated growth [240]. PBANKA_110420 encodes the E1β subunit of the mitochondrial branched-chain α-ketoacid dehydrogenase (BCKDH) [241], and this was used because deletion of the E1α subunit of the same complex has a clear growth phenotype. The third attenuating knock-out vector targeted PBANKA_140160, a putative methyl transferase of unknown function, which demonstrated a slow-growing mutant phenotype [139]. Their growth phenotypes were quantified by calculating their mean relative fitness values as described in Materials and Methods (subsection 2.4.19). The normal growing control mutants were redundant for asexual blood-stage growth and grew over the course of infection with a mean relative fitness close to 1 (green line) as wild-type parasite fitness. The slow-growing control mutants showed reduced parasite fitness, with values between 0.60 and 0.73 (orange line) (Figure 5.8).

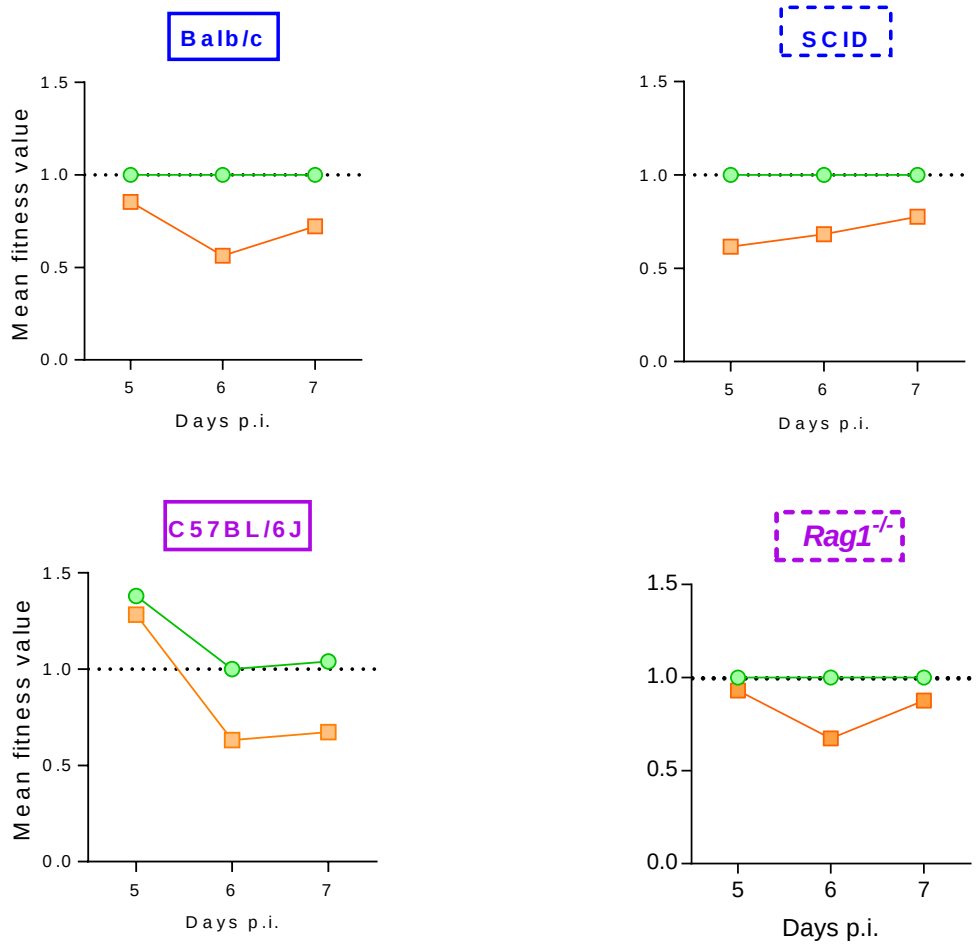

Figure 5.8 Fitness of normal and slow growing control mutants in blood. *The four mutants of normal growing control genes, which were redundant for asexual blood-stage growth, grew increasingly over the course of infection with a mean relative fitness close to 1 (green line) as wild-type parasite fitness. The attenuated slow growing control mutants showed a measureable reduction in parasite fitness, with values between 0.60 and 0.73 (orange line).5.3.2.4 Distribution of mutants in individual mouse strains.*

When a target gene is essential for blood-stage growth, mutant parasites will die and the corresponding barcodes will disappear from circulation either by lysis or by splenic clearance. Therefore, those genes with no barcode evidence on day 4 p.i. may be considered as essential genes for growth. However, there may be false negative results due to vectors that were unable to integrate into the parasite genome. Thus, to use more accurate terminology, genes with barcode levels that were below the detection threshold on day 7 p.i. were referred as "likely essential". Four mutant phenotypes were identified relative to the normal growing (fitness value = 1) and slow growing (fitness value = 0.6-0.7) control mutants: likely essential mutants - if there was no barcode for a specific mutant in any of the 3 mice on day 7 p.i.; slow growing with fitness values between 0.1 and 1.0; likely dispensable with fitness values of 1.0; and fast-growing with fitness values > 1.0. A mutant was included in this distribution analysis if it had a fitness value in at least two out of three infected mice (Figure 5.9).

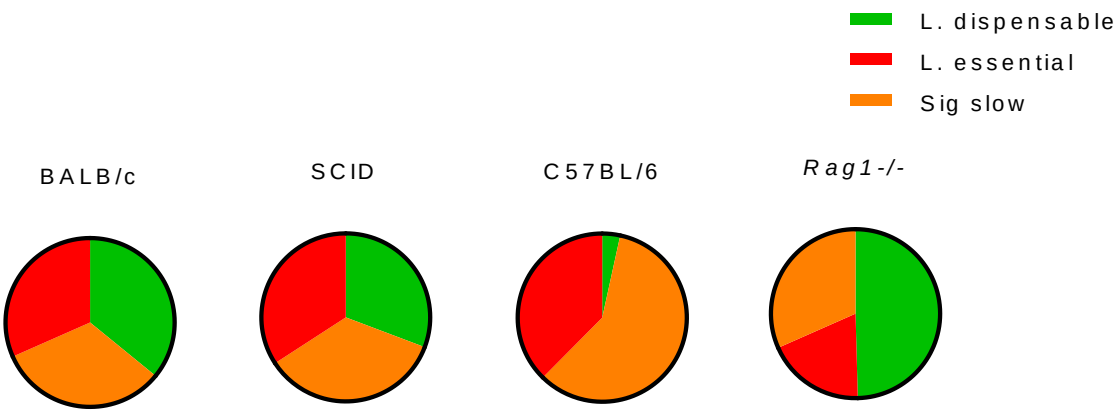

Figure 5.9 Distribution of mutants in 4 mouse strains (BALB/c, SCID, C57BL/6J and Rag1-/-) based on fitness value. *The fitness value for normal growing mutants is 1 and designated as likely dispensable genes (green), while slow growing mutants have fitness values between 0.1 and 1 (orange) and mutants for likely essential genes have fitness values less than 0.1(red).*

In the screening of 117 genes using this high through-put barcode sequencing approach, we found 32 genes were likely essential for parasite growth as there was no evidence of their corresponding barcodes in parasites circulating in the blood of any of the 4 groups of mice. Moreover, eight of these likely essential genes were completely novel because they were annotated only as conserved *Plasmodium* protein of unknown function. Therefore, these eight likely essential genes were selected for further study (boxed in Table 2). Interestingly, it has observed that the most of genes were either likely essential or were important for growth in the C57/Bl6 compared to Balb/c, which might be due to the differences in the immune responses between Balb/c and C57BL/6.

Table 2: Likely essential genes for blood-stage growth in malaria

Fitness value on day 7

Barcode	Gene ID	Annotation	C57BL/6J	*Rag1*$^{-/-}$	Balb/c	SCID
gcatttcatgt	PBANKA_010060	Schizont membrane associated cytoadherence protein (SMAC)	0	0	0	0
aagccaggacg	PBANKA_010780	Citrate synthase-like protein, putative	0	0	0	0
aggctctggct	PBANKA_020760	Asparagine-rich antigen, putative	0	0	0	0
gtcgcacccga	PBANKA_020890	StAR-related lipid transfer protein, putative	0	0	0	0
tgtgcaggtgc	PBANKA_030060	Plasmodium exported protein, unknown function	0	0	0	0
tgttgccataa	PBANKA_050260	Conserved Plasmodium protein, unknown function	0	0	0	0
cagccccatac	PBANKA_060990	Heat shock protein DNAJ homologue Pfj4, putative	0	0	0	0
gggtgggttga	PBANKA_061060	Peripheral plastid protein 1, putative (PPP1)	0	0	0	0
gactttaagaa	PBANKA_061310	Conserved Plasmodium protein, unknown function	0	0	0	0
caaagaaaaag	PBANKA_061580	Exported serine/threonine protein kinase (EST)	0	0	0	0
aaatgggcgcg	PBANKA_062310	Plasmodium exported protein, unknown function	0	0	0	0
ggtacgtagcc	PBANKA_071420	Chaperone protein ClpB1, putative (ClpB1)	0	0	0	0
tcaggcgtacc	PBANKA_082630	Thioredoxin-like protein 2, putative (TLP2)	0	0	0	0
acttgtgctgc	PBANKA_083610	Phosphatidylinositol N-acetylglucosaminyltransferase subunit P, putative	0	0	0	0
ctcttttgaat	PBANKA_093120	Heat shock protein 101 (HSP101)	0	0	0	0
ccaatcattat	PBANKA_093830	Heat shock protein, putative	0	0	0	0
gtctcttttcg	PBANKA_100850	Translocon component PTEX150 (PTEX150)	0	0	0	0
cgagattagtc	PBANKA_110130	Conserved rodent malaria protein, unknown function	0	0	0	0
ccgctcgttag	PBANKA_110500	Conserved Plasmodium protein, unknown function	0	0	0	0
acgggttcaac	PBANKA_113970	Conserved Plasmodium protein, unknown function	0	0	0	0
aaaatgatcgg	PBANKA_120820	Kinesin-4, putative	0	0	0	0
ggattccgcgt	PBANKA_132070	Signal peptide peptidase, putative (SPP)	0	0	0	0
ctggcctcgtt	PBANKA_132800	Serine/threonine protein phosphatase, putative (UIS2)	0	0	0	0
aaaccatcctc	PBANKA_133220	Translation initiation factor IF-1, putative (IF1)	0	0	0	0
tggactgagtc	PBANKA_133270	Duffy-binding protein	0	0	0	0
aggttctaccc	PBANKA_133430	Exported protein 2 (EXP2)	0	0	0	0
cgcggctgtct	PBANKA_133870	Plasmepsin V, putative (PMV)	0	0	0	0
tcggacggttg	PBANKA_134540	ER lumen protein retaining receptor 1, putative	0	0	0	0
agtgcgccact	PBANKA_140060	Cytoadherence linked asexual protein, putative	0	0	0	0
ttcatccccag	PBANKA_140330	NLI interacting factor-like phosphatase (NIF1)	0	0	0	0
attttcatctg	PBANKA_141030	M1-family alanyl aminopeptidase, putative (M1AAP)	0	0	0	0
ccaagacgcga	PBANKA_143540	Conserved Plasmodium protein, unknown function	0	0	0	0

Furthermore, we identified 10 mutants that did not grow in C57Bl/6J wild-type mice but grew well in immune-deficient mice *Rag1*$^{-/-}$ mice. Since mutants of these genes did not grow in immune-competent mice, this suggested that these genes were crucial for blood-stage parasite growth in the presence of an intact immune system, whereas they were redundant in immune-deficient mice. Therefore, we consider them an important group of genes for future studies into host-parasite interactions in malaria (Table 3). The differential growth capabilities of mutants indicate that parasite proteins may be involved in the progression and severity of the malarial disease. This is consistent with a recent study that showed that *ptex88*-deficient *P. berghei* parasites no longer sequestered within tissues and failed to cause cerebral malaria [230].

Table 3: Mutants that did not grow in C57BL/6J, but grew well in *rag1*$^{-/-}$ mice

Fitness value on day 7

Barcode	Gene ID	Annotation	C57BL/6J	*Rag1*$^{-/-}$	Balb/c	SCID
caaactacgca	PBANKA_070120	Conserved Plasmodium protein, unknown function	0	0.855675	0	0
ctgaatactcg	PBANKA_062320	Lysophospholipase, putative	0	0.8871839	0	0.767778
tagtcctttat	PBANKA_122090	Conserved Plasmodium protein, unknown function	0	0.914329	0.9275411	0.683944
ttctttgttat	PBANKA_080040	Conserved Plasmodium protein, unknown function	0	0.962981	0.7633314	0.723511
tgtgttttgtt	PBANKA_082530	Conserved Plasmodium protein, unknown function	0	1.0058039	0.9562367	0.750512
ttcggtatcgg	PBANKA_133810	Conserved Plasmodium protein, unknown function	0	1.082715	1.1004241	1.101753
ttcggtatcgg	PBANKA_133810	Conserved Plasmodium protein, unknown function	0	1.082715	1.1004241	1.101753
atccgcgtgta	PBANKA_094130	Translocon component PTEX88 (PTEX88)	0	1.1458119	0	0
tttccagaata	PBANKA_140070	Plasmodium exported protein, unknown function	0	1.183722	0	0.991461
ttgggtcaccc	PBANKA_113870	Conserved Plasmodium protein, unknown function	0	1.2555636	0.8756698	1.129106

5.3.2.6 No difference in the presence of mutants in blood and tissues of different mouse strains

Using my earlier work in applying barseq analysis to tissues, I next examined whether mutants accumulated in tissues in proportion to their presence in the blood and whether this was dependent on the immune status of the mice. Hence, linear regression analysis was performed on the abundance of each mutant in the blood and versus each tissue studied for each mouse strain on day 7 p.i. The abundance of normal growing (green triangle) and slow growing (orange rectangle) control mutants were aligned with the regression line (red line). Test mutants were similarly aligned with the regression line which suggested that the tissue accumulation of *P. berghei* mutants was related to the mutant's relative abundance in the blood, regardless of immune competency (5.10).

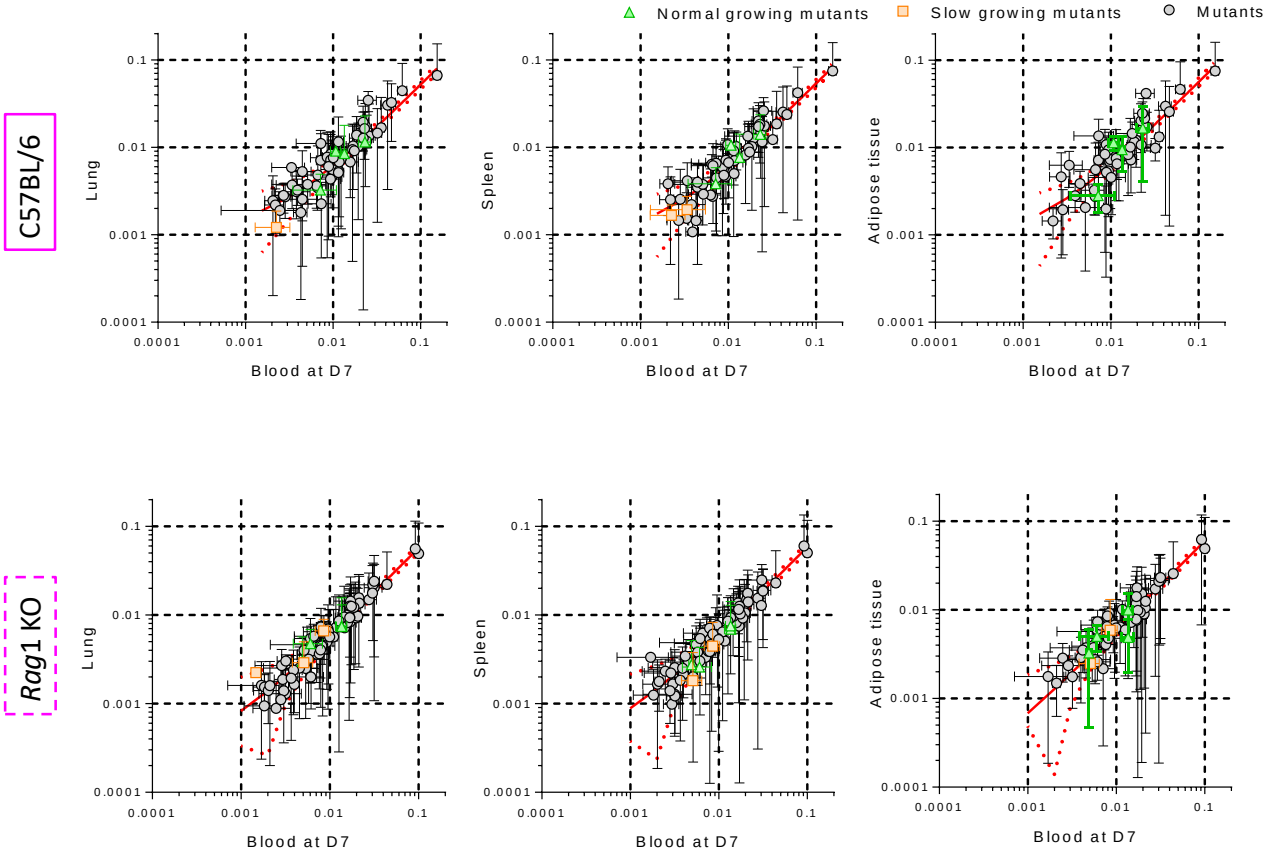

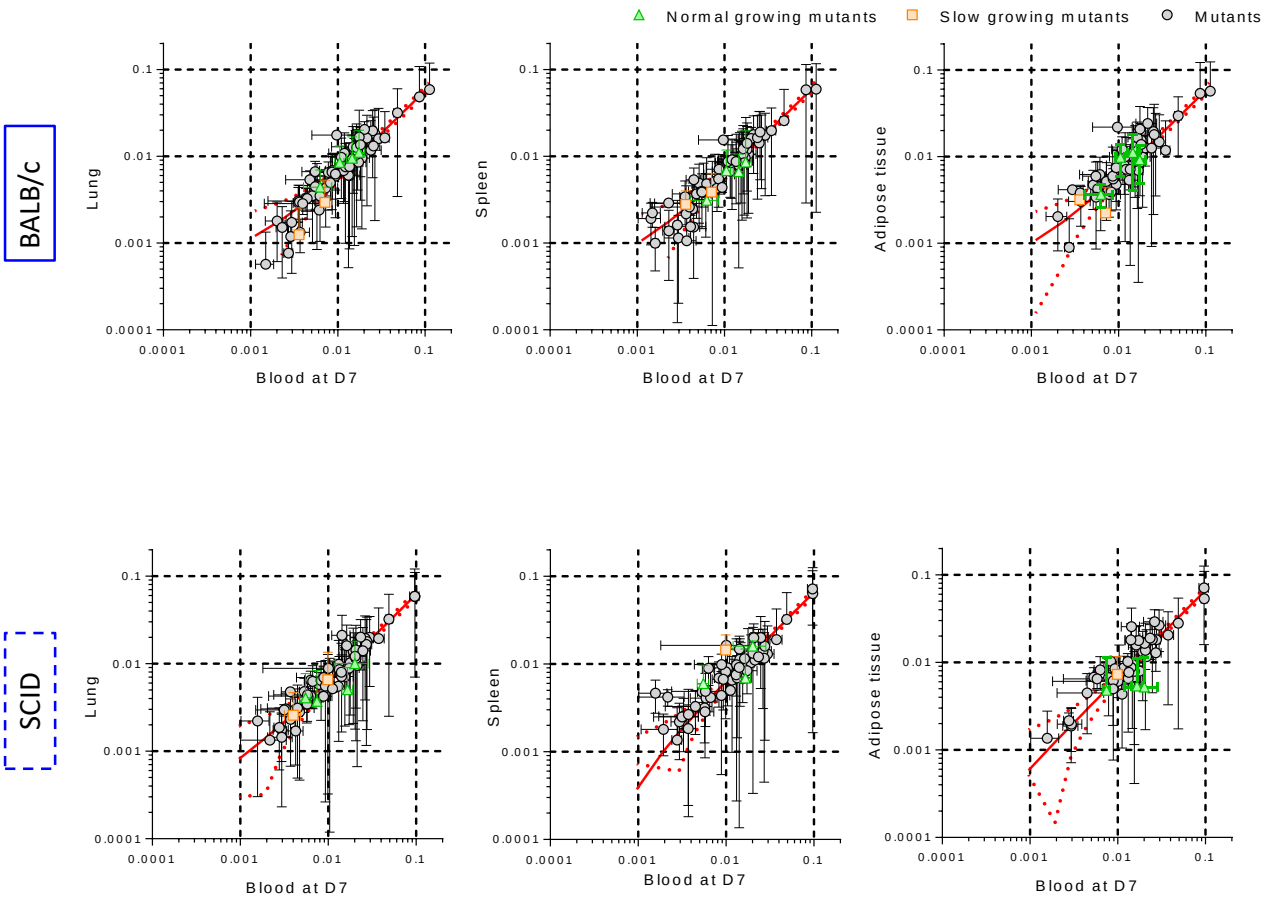

Figure 5.10 Comparison of the relative abundance of mutants in blood and tissue at day 7 p.i. *The relative abundance of a mutant on day 7 p.i. in the blood and tissue was plotted for 4 strains of mice (green = normal growing control mutants, orange = slow growing control mutants, and black/grey=test mutants).* ***The plot demonstrates correlation in mutants' abundance in blood and tissues regardless mouse strains.***

5.3.3 Exploring the role of PTEX88 proteins in during blood-stage malaria

The previous Barseq data suggested that PTEX88 was essential for parasite blood-stage growth in immune-competent C57BL/6J mice, but not in immune-deficient *rag1*$^{-/-}$ mice. This led us to further investigate how PTEX88 contributes to the *PbA* survival advantage in C57BL/6J mice – does it enable parasites to avoid clearance or does it support the development parasite life-cycle stages by enhancing maturation and replication rate. Thus, next, I sought to study the role of PTEX88 using a *Pb*PTEX88 inducible knock-down (iKD) parasites [242] and our *in vivo* Clearance/Growth assay.

5.3.3.1 Exploring the effect of PTEX88 knockdown on parasite growth *in vivo*

We used *Pb*PTEX88iKD parasites in which PTEX88 is knocked down via the administration of ATc in drinking water. We first investigated whether ATc has any non-specific effects on the growth of wild-type parasites. Mice were infected with wild-type *Pb* ANKA (luciferase) and *Pb*PTEX88iKD parasites and treated with either ATc (0.2mg/ml in 5% sucrose water) or control vehicle (5% sucrose water). Parasitemia was monitored daily from day 3 p.i., until mice developed clinical symptoms of cerebral malaria. We observed that ATc administration did not cause any non-specific effect on parasitemia in mice infected with wild *Pb*ANKA compared to the control group (Figure 5.11A). However, ATc administration in mice infected with mutant parasites *Pb*PTEX88iKD was associated with reduced parasite growth in comparison with the non ATc-treated control group (Figure 5.11B). The data suggested that ATc treatment had a specific effect on the growth of *Pb*PTEX88iKD parasites, consistent with previous studies [243].

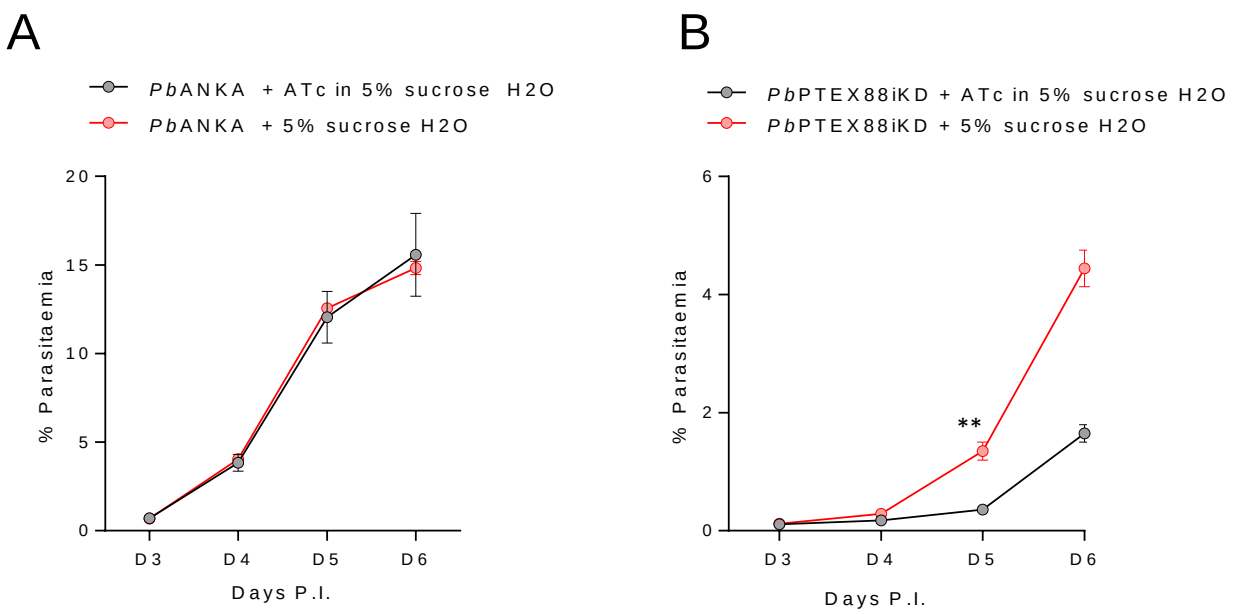

Figure 5.11 ATc treatment effect was specific to mutant PbPTEX88iKD in vivo. *Parasitemia in wild type (C57BL/6J) mice administered either ATc in 5% sucrose water (black line) or 5% sucrose (red line) after infection with PbANKA wildtype parasites* ***(A)*** *or PbPTEX88iKD parasites* ***(B).*** *Error bars represent SEM, p<0.01 = **. Experiment conducted once.*

5.3.3.2 Gen$_0$ parasites maturation impaired due to knock down of PTEX88

Next, it was hypothesised that PTEX88 might have a role in parasite clearance and maturation through life stages. This was studied by using *Pb*PTEX88iKD parasite and our in vivo Clearance/Growth assay. Here, after mice were infected with labeled pRBCs collected from a passage mouse infected with *Pb*PTEX88iKD parasites, they were treated either with ATc in drinking water or control vehicle. Mice were tail bled at intervals between 1 and 73h post-infection, and parasitemia monitored by flow cytometry. Initial analysis by measuring the proportion (%) of G_0 pRBCs (clearance) and G_1+ parasites population (parasite growth) in the recipient RBCs after transitioning from G_0 to G_1+ parasites demonstrated that knocking-down of PTEX88 resulted in more G_0 parasites to remain in circulation 25 hours after ATc treatment, as well lower numbers of Gen$_1$ parasites 48 hours after the knock-down (Figure 5.12). Our collaborator Rosemary Aogo and colleagues conducted further analyses using their mathematical model to ascertain whether the rate of parasite clearance or infectivity changed with PTEX88 knock down (personal communication) [244]. There was no significant difference in the rate of parasite clearance or infectivity between the controls and the ATc treatment groups. Since G_0 parasites persisted for longer with PTEX88 knock down, modellers employed the delayed maturation model [144] to find any evidence of delayed maturation, and the results suggested that PTEX88 knock-down caused *Pb*A parasites to mature at a slower rate (34-hour cycle) compared to controls (24-hour cycle), especially during the ring stage of the parasite life cycle. A recent study has reported that PTEX88 (the *Plasmodium* translocon of exported protein

88) facilitates entry of the trafficking proteins into the host cells, which is required for parasite development and survival. PTEX88 interacts closely with HSP101, but has weaker affinity with other core components of PTEX. PTEX88 is expressed during blood-stage life cycle; however, it is discretely found at the parasitophorous vacuole membrane during the ring stage [245]. This observation supports our data that PTEX88 is essential for parasite maturation, especially in the early stage of its life cycle and not for enabling the parasites to avoid clearance. Future experiment required to be conducted to understand the mechanisms involved in the slow maturation of parasites caused by PTEX88 knock-down, due to discrepant results in our initial and the repeat experiments. Moreover, delay in maturation in this model could be validated by injecting merozoites and tracking parasite life-stages for when next cycle of rings begins by isolation of viable merozoites.

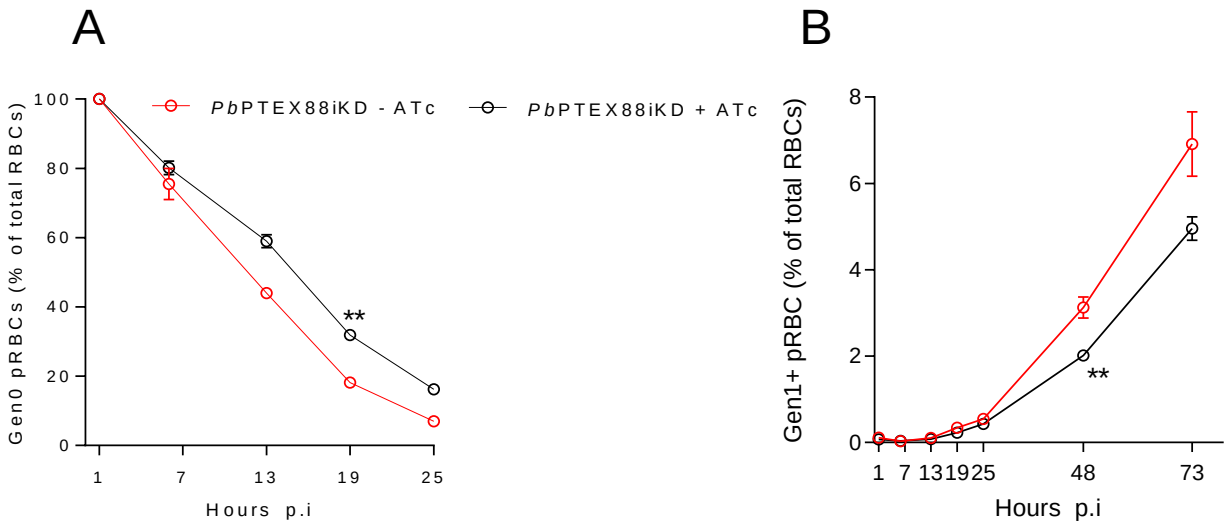

Figure 5.12 No influence of PTEX88 in the clearance and growth of parasite. *C57BL/6J mice (n=5) injected with labelled PbPTEX88iKD RBC were treated with either 0.2mg/ml ATC in 5% sucrose (black) or 5% sucrose vehicle (red).* ***(A)*** *The graph shows reductions in the proportion of percentage of G_0 pRBCs (Gen_0), called clearance and* ***(B)*** *growth of parasites (G_1+ parasites population) in recipient RBCs after rupturing from G_0 parasites in WT mice (n=5) treated with either 0.2mg/ml ATc in 5% sucrose or 5% sucrose vehicle. Error bars represent SEM, p<0.01 = **. Experiments conducted twice.*

5.4 Discussion

Here, first I confirmed that the barcode-based NGS sequencing approach [246] is indeed capable of detecting KO mutants in tissue as in blood. Then, I screened 117 exportome-associated genes to identify that in terms of infection outcome, particular exported parasite proteins interacted with the host using immune-competent and immune-deficient mice. The data revealed that 32 of these genes were essential for blood-stage growth regardless of mouse genetic background, including 8 with no previous functional annotation. Further analysis revealed that 10 genes were required for parasite growth in the presence of an intact immune system, but were not required for parasite growth in immune-deficient mice. Analysis of mutant abundance in tissues of different mouse strains indicated that mutants accumulated in tissues in proportion to their presence in blood, despite differences in immune competency.

On day 4, there was a difference between the proportions of barcodes for some mutants, despite similar input ratios of barcodes for those specific vectors, suggesting that some of the genes have roles in growth. However, it also is possible that different vectors may integrate into the parasite genome with different efficiency (integration efficiency depends on the length of vectors homology arms and recombination rate) [139]. Thus, there may be some false negative results in the data due to the vectors that were unable to effectively integrate into the parasite genome. Hence, we could not determine with confidence whether a lack of barcodes for a particular mutant was due to the inability of the resultant mutant to grow or due to the inability of the vector to integrate into the genome. Moreover, where barcode levels were below the detectable threshold by day 7, genes were referred to as “likely essential”, rather than essential. From the growth curve after day 4 p.i., we can monitor the dynamics of mutant growth within the host. Some mutants grew increasingly over the course of the infection and were thus inferred to be non-essential or redundant for blood-stage growth, while other mutants declined in growth over the course of the infection and were, therefore, considered to be slow growing mutants. A limitation of this analysis is that although some mutants were growing on day 4 and beyond, they were continually being outcompeted by redundant knockouts and, therefore, would ultimately drop below the detectable level of barseq (regardless of the actual number of parasites gradually growing). However, this limitation can be overcome by a second-pass screen that excludes most of the fast-growing (redundant) mutants [139].

Mutants which did not grow or had exhibited reduced growth in the model of cerebral malaria, C57BL/6J, but grew well in immune-deficient mice *rag1*$^{-/-}$ (T and B-cell deficient), represent one of the most interesting groups of genes for studying host-parasite interactions. Binding of parasite

proteins (presented on the surface of the iRBC following exportation from the parasite) to the host receptor of endothelial cells of the microvasculature leads to sequestration of iRBCs in organs and is responsible for severe complications in malaria, such as cerebral malaria caused by *Plasmodium falciparum* in humans. A previous study has shown that *P. berghei* iRBCs adhere to endothelial cells via binding to the receptor CD36 [129], which is also commonly used by other *Plasmodium* spp for binding iRBCs to host organs. This indicates that *P. berghei* may export proteins onto the surface of iRBCs to facilitate adherence to host tissues, e.g. the PfEMP1 protein expressed by *Plasmodium falciparum*. However, *P. berghei* does not contain any *Pfemp1* orthologues, nor does it contain any protein with domains that bear homology to the domains of PfEMP1 [247]. The *Plasmodium berghei* proteins that are responsible for cytoadherence, and other proteins involved in the transportation of these adherence proteins to the iRBC membrane remain largely unknown.

The existence of a correlation between the relative abundance of mutants in the blood and different tissues in 4 different strains of mice suggests that when *Plasmodium berghei* accumulates in the tissues, no mutants are lost in blood or vice versa. However, mutants of *ptex88* gene that was not grown in wild-type B6 mice but well grew in immune deficient *rag1*$^{-/-}$ mice mice (Table 3) is important for investigating host-parasite interaction further. Using our adoptive transfer protocol, we performed experiments to observe the effect of parasite proteins in the process of parasite clearance and growth. Initial analysis of the data for measuring parasite clearance (G_0) and growth (G_1+) suggested a role of PTEX88 (*Plasmodium* translocon of exportd protein 88) in the parasite clearance as more G_0 parasite remained in the circulation following ATc treatment compared to vehicle-treated mice infected with the *Pb*PTEX88-iKD parasite. Further analyses, using mathematical model, disclosed that although PTEX88 might have no role in the parasite clearance or infectivity, it caused delay in the maturation of parasite (34 hrs cycle for ATc treated compared vs. 24 h cycle for vehicle treated). A recent study has reported PTEX88 to facilitate entry of trafficking proteins, required for parasite development and survival, into the host cells. Moreover, it affects maturation in the early stage (ring stage) of the parasite life cycle compared to late stage. It has been shown that PTEX88 is involved in the sequestration and experimental cerebral malaria [223], and recently, Chisholm A *et. al* has found that PTEX88 interacts closely with HSP101 and discretely present in the parasitophorous vacuole membrane during ring stage of the parasite [245] [243]. Together, this experimental approach provided proof of concept that there may be genes that play a specific role for interacting with the host immune system. Future experiments required to follow larger numbers of genes, and begin the process of functionally testing candidates for immune-system dependent phenotypes, perhaps using competitive *in vivo* Clearance/Growth Assays in wild-type versus *rag1*$^{-/-}$ mice.

Chapter Six:

Final discussion

Malaria is a complex disease and its outcome depends on a wide variety of factors – including parasite species and strain, host immune responses, host and parasite metabolic pathways, and host and parasite genetic polymorphisms. Understanding the mechanisms by which host and parasite interact may be useful for developing novel therapeutic interventions in malaria [248, 249]. Therefore, this thesis has explored at organ-level, cellular-level and molecular level, various mechanisms by which infected hosts can control parasite growth in mouse models of blood-stage malaria. In addition, this thesis has also sought to define novel parasite factors, which enable the parasite to survive and grow within immune-competent hosts.

Using an *in vivo* RBC adoptive transfer protocol developed in our laboratory, referred to as the "*in vivo* Clearance/Growth" assay, I have explored host and drug-mediated control during blood-stage malaria. Although the prevailing view has been that host removal of pRBC is conducted by macrophages in the spleen and liver, *in vivo* evidence to support this is sparse. By following a single cohort of pRBC in the presence or absence of phagocytic cells, I revealed that these cells indeed play a partial role in removing pRBC from circulation. Furthermore, I showed that phagocytes in general, and the spleen in particular, are required to remove artesunate-affected parasites from circulation. Together, these data indicate that the mononuclear phagocytic system does function to remove pRBC, although its role in controlling parasite growth is rather modest. Previous reports showed that various host factors including the spleen and $CD8^+$ T-cells are paradoxically required to support high parasite burdens during *Pb*ANKA infection [250]. Unpublished data from my group has since also shown that the net role of phagocytes in this model is actually to support parasite growth, despite my data proving their role in removing some pRBC. This data raises the concept that organs like the spleen and cells such as phagocytes may play multiple competing roles in parasite control. For example, splenic phagocytes may serve to remove some pRBC, while simultaneously providing immune-mediated signals such as systemic inflammatory cytokines that trigger endothelial activation and parasite sequestration. Further experimentation is warranted to examine the complex roles that phagocytes play in malaria.

Next, I investigated in depth how anti-malarial drugs are so effective at controlling parasite numbers. Again, by following in detail a single cohort of pRBC, I showed that the anti-malarial drug artesunate prevented parasites from maturing in RBC. As a result of this, parasites lingered in the first generation of RBC in circulation, rather than maturing and rupturing. Although, it might be the case that these parasites were in fact killed, in thesis it was not possible to determine this definitively.

Further experiments may require an adoptive transfer or other methods to determine the degree to which anti-malarial drugs kill parasites, as opposed to impairing or arresting their maturation. This work may be useful given that parasite dormancy under drug control is an important area of research [155, 182, 191, 192].

Next, my data served to reveal a completely novel mechanism by which the host can control parasite growth, namely by directly slowing the maturation rate of parasites during acute infection. Prior to this work, the common view was that the duration of the blood-stage parasite life-cycle *in vivo* was fairly constant for a given species. Exposure of parasites in pRBC to an acute infection environment surprisingly slowed maturation, such that the life cycle was extended from 24 hours to 40 hours. Moreover, this appeared to be a host response-dependent phenotype, since infected *rag1*$^{-/-}$ mice could not elicit impaired maturation. Thus, the phenomena suggests that the impaired maturation may be consequent to some host factors, rather than the parasite factors: however, in the acute inflammatory environment parasites may survive by escaping their clearance from the circulation. Future studies could aim to discover what aspects of the host response to infection might mediate this effect. Moreover, it might be interesting to explore by transcriptomic studies, how the parasite senses and responses to the host environment.

In a subsequent chapter of this thesis, I focused on a molecular aspect of host-mediated parasite control, via parasite-specific antibodies. Although the *P. chabaudi* and *P. yoelii* 17XNL mouse models have been established as examples of robust antibody-mediated immunity, *in vivo* mechanisms of action for these antibodies have not been studied. My data suggested that in both models, parasite-specific IgG antibodies protected not by binding to the surface of infected RBC and accelerating their clearance from circulation, but by targeting the free form of the parasite, merozoites. By binding to merozoites, this prevented parasites from transitioning from one generation of RBC to the next, which had dramatic effects on parasite numbers. Moreover, we could demonstrate that phagocytes played a partial role in antibody efficacy, while the complement components C3 and C5 played no role in membrane attack complex (MAC)-mediated direct lysis of pRBCs. Previous *in vitro* studies have suggested that phagocytes are important for antibody-mediated parasite control either by opsonic phagocytosis or cellular inhibition [114, 251, 252] and my *in vivo* data is consistent with this. Recent data have suggested that C1q deposition [114] on the surface of antibody-coated merozoites might provide a mechanism by which antibodies function in human malaria. Future experiments are required to examine the role of C1q in antibody-mediated immunity *in vivo.*

While the main emphasis of this thesis has been to explore host and drug-mediated mechanisms of parasite control, in my final Results chapter, I changed focus to examine parasite factors, namely genes that encode for exported proteins that might be required for blood-stage growth,

and specific interaction with immune-competent hosts. I chose to work in this area because a large proportion of *Plasmodium* genes remained uncharacterized. During blood-stage malaria parasites export hundreds of proteins into the host erythrocyte [253, 254]. Many of these genes have unknown functions, partly due to difficulties in manipulating the AT-rich *Plasmodium* genome by reverse genetic technology. Here, using knock-out *Plasmo*GEM vectors and high throughput, barcode-based NGS sequencing approaches [246] I identified a number of genes which were important for blood-stage parasite growth. Importantly, I also revealed a number of genes that differentially in wild-type versus immune-deficient mice. For example, *ptex88* knockout parasites within a pool of 107 other mutants survived very poorly in immune-competent mice yet grew well in *rag1*$^{-/-}$ mice that lack a robust pro-inflammatory response to infection. Further analysis of *ptex88* knockdown parasites suggested a role for this gene in promoting parasite maturation rates in immune-replete mice. Most importantly, my experimental approach provided proof of concept that there may be genes that are crucial for interacting with the host immune system but are functionally redundant in immune-deficient environments. Future experiments should follow larger numbers of genes, and begin the process of functionally testing candidates for immune-system dependent phenotypes, perhaps using competitive *in vivo* Clearance/Growth Assays in wild-type versus *rag1*$^{-/-}$ mice.

Concluding remarks

By measuring parasite clearance and growth *in vivo* using the Clearance/Growth assay in mice, my thesis has explored the underlying mechanisms of host and drug-mediated control and parasite growth during blood-stage malaria *in vivo*. Most notably, acute responses in the host impaired parasite maturation rates and *Plasmodium*-specific antibodies prevented the transition from one RBC to the next. I also revealed that anti-malarial drugs generally do not accelerate pRBC clearance, but serve to impair or arrest maturation. Finally, a number of novel genes were discovered which are were essential for the blood-stage growth and interacting with the host immune system. Taken together, these data provide novel information on how malaria control might possibly be achieved in humans infected with *Plasmodium* species.

Chapter Seven:

References

1. Paul, R., *From Shakespeare to Defoe: Malaria in England in the Little Ice Age.* Emerging Infectious Disease journal, 2000. **6**(1): p. 1.
2. Tilley, L., *Rotational dynamics of the integral membrane protein, band 3, as a probe of the membrane events associated with Plasmodium falciparum infections of human erythrocytes.* Biochim. Biophys. Acta, 1990. **1025**: p. 135-142.
3. Ashley, E.A., A. Pyae Phyo, and C.J. Woodrow, *Malaria.* The Lancet, 2018. **391**(10130): p. 1608-1621.
4. Cowman, A.F., et al., *Malaria: Biology and Disease.* Cell, 2016. **167**(3): p. 610-624.
5. Vanderberg, J.P. and U. Frevert, *Intravital microscopy demonstrating antibody-mediated immobilisation of Plasmodium berghei sporozoites injected into skin by mosquitoes.* International Journal for Parasitology, 2004. **34**(9): p. 991-996.
6. Weiss, G.E., et al., *Revealing the Sequence and Resulting Cellular Morphology of Receptor-Ligand Interactions during Plasmodium falciparum Invasion of Erythrocytes.* PLOS Pathogens, 2015. **11**(2): p. e1004670.
7. Kirk, K., *Membrane Transport in the Malaria-Infected Erythrocyte*. Vol. 81. 2001. 495-537.
8. Bannister, L. and G. Mitchell, *The ins, outs and roundabouts of malaria.* Trends in parasitology, 2003. **19**(5): p. 209-213.
9. Garnham, P.C.C., *Malaria parasites of man: life-cycles and morphology (excluding ultrastructure).* in *Malaria: principles and practice of malariology*, W.H. Wernsdorfer and I. McGregor, Editors. 1988, Churchill Livingstone. p. 61-96.
10. Long, C.A. and F. Zavala, *Malaria vaccines and human immune responses.* Curr Opin Microbiol, 2016. **32**: p. 96-102.
11. Ramiro, R.S., S.E. Reece, and D.J. Obbard, *Molecular evolution and phylogenetics of rodent malaria parasites.* BMC evolutionary biology, 2012. **12**: p. 219-219.
12. Janse, C.J., J. Ramesar, and A.P. Waters, *High-efficiency transfection and drug selection of genetically transformed blood stages of the rodent malaria parasite Plasmodium berghei.* Nature Protocols, 2006. **1**: p. 346.
13. Amino, R., et al., *Imaging malaria sporozoites in the dermis of the mammalian host.* Nature Protocols, 2007. **2**: p. 1705.
14. World Health Organization, *World Malaria Report 2014.* WHO, 2014.

15. Stoute, J.A., et al., *A Preliminary Evaluation of a Recombinant Circumsporozoite Protein Vaccine against Plasmodium falciparum Malaria.* New England Journal of Medicine, 1997. **336**(2): p. 86-91.
16. Kester, K.E., et al., *Randomized, Double-Blind, Phase 2a Trial of Falciparum Malaria Vaccines RTS,S/AS01B and RTS,S/AS02A in Malaria-Naive Adults: Safety, Efficacy, and Immunologic Associates of Protection.* The Journal of Infectious Diseases, 2009. **200**(3): p. 337-346.
17. *Efficacy and safety of RTS,S/AS01 malaria vaccine with or without a booster dose in infants and children in Africa: final results of a phase 3, individually randomised, controlled trial.* The Lancet, 2015. **386**(9988): p. 31-45.
18. Theisen, M., et al., *A multi-stage malaria vaccine candidate targeting both transmission and asexual parasite life-cycle stages.* Vaccine, 2014. **32**(22): p. 2623-2630.
19. Seder, R.A., et al., *Protection Against Malaria by Intravenous Immunization with a Nonreplicating Sporozoite Vaccine.* Science, 2013. **341**(6152): p. 1359.
20. Trieu, A., et al., *Sterile Protective Immunity to Malaria is Associated with a Panel of Novel P. falciparum Antigens.* Molecular & Cellular Proteomics : MCP, 2011. **10**(9): p. M111.007948.
21. Carter, R., *Transmission blocking malaria vaccines.* Vaccine, 2001. **19**(17): p. 2309-2314.
22. Dondorp, A.M., et al., *Artesunate versus quinine in the treatment of severe falciparum malaria in African children (AQUAMAT): an open-label, randomised trial.* The Lancet, 2010. **376**(9753): p. 1647-1657.
23. *Artesunate versus quinine for treatment of severe falciparum malaria: a randomised trial.* The Lancet, 2005. **366**(9487): p. 717-725.
24. Organization, W.H., *Guidelines for the treatment of malaria*. 2015: World Health Organization.
25. Terkuile, F., et al., *Plasmodium falciparum: In Vitro Studies of the Pharmacodynamic Properties of Drugs Used for the Treatment of Severe Malaria.* Experimental Parasitology, 1993. **76**(1): p. 85-95.
26. Noedl, H., et al., *Artemisinin Resistance in Cambodia: A Clinical Trial Designed to Address an Emerging Problem in Southeast Asia.* Clinical Infectious Diseases, 2010. **51**(11): p. e82-e89.
27. Starzengruber, P., et al., *Current Status of Artemisinin-Resistant falciparum Malaria in South Asia: A Randomized Controlled Artesunate Monotherapy Trial in Bangladesh.* PLOS ONE, 2012. **7**(12): p. e52236.

28. Phyo, A.P., et al., *Emergence of artemisinin-resistant malaria on the western border of Thailand: a longitudinal study.* Lancet, 2012. **379**(9830): p. 1960-1966.
29. Dondorp, A.M., et al., *Artemisinin resistance in Plasmodium falciparum malaria.* The New England journal of medicine, 2009. **361**(5): p. 455-467.
30. Marsh, K. and S. Kinyanjui, *Immune effector mechanisms in malaria.* Parasite Immunol, 2006. **28**(1-2): p. 51-60.
31. Mbogo, C.N.M., et al., *Low-Level Plasmodium falciparum Transmission and the Incidence of Severe Malaria Infections on the Kenyan Coast.* The American Journal of Tropical Medicine and Hygiene, 1993. **49**(2): p. 245-253.
32. McElroy, P.D., et al., *Predicting Outcome in Malaria: Correlation between Rate of Exposure to Infected Mosquitoes and Level of Plasmodium falciparum Parasitemia.* The American Journal of Tropical Medicine and Hygiene, 1994. **51**(5): p. 523-532.
33. Okello, P.E., et al., *Variation in malaria transmission intensity in seven sites throughout Uganda.* The American journal of tropical medicine and hygiene, 2006. **75**(2): p. 219-225.
34. Rodriguez-Barraquer, I., et al., *Quantifying Heterogeneous Malaria Exposure and Clinical Protection in a Cohort of Ugandan Children.* The Journal of Infectious Diseases, 2016. **214**(7): p. 1072-1080.
35. Snow, R.W., et al., *Relation between severe malaria morbidity in children and level of Plasmodium falciparum transmission in Africa.* The Lancet, 1997. **349**(9066): p. 1650-1654.
36. Carneiro, I., et al., *Age-Patterns of Malaria Vary with Severity, Transmission Intensity and Seasonality in Sub-Saharan Africa: A Systematic Review and Pooled Analysis.* PLOS ONE, 2010. **5**(2): p. e8988.
37. Snow, R.W., et al., *Relation between severe malaria morbidity in children and level of Plasmodium falciparum transmission in Africa.* The Lancet, 1997. **349**(9066): p. 1650-1654.
38. Karnchanaphanurach, P., et al., *C3b deposition on human erythrocytes induces the formation of a membrane skeleton–linked protein complex.* The Journal of clinical investigation, 2009. **119**(4): p. 788-801.
39. Lingelbach, K. and K.A. Joiner, *The parasitophorous vacuole membrane surrounding Plasmodium and Toxoplasma: an unusual compartment in infected cells.* Journal of cell science, 1998. **111**(11): p. 1467-1475.
40. Baldwin, M., et al., *Human erythrocyte band 3 functions as a receptor for the sialic acid-independent invasion of Plasmodium falciparum. Role of the RhopH3–MSP1 complex.* Biochimica et Biophysica Acta (BBA) - Molecular Cell Research, 2014. **1843**(12): p. 2855-2870.

41. Gaur, D. and C.E. Chitnis, *Molecular interactions and signaling mechanisms during erythrocyte invasion by malaria parasites.* Current Opinion in Microbiology, 2011. **14**(4): p. 422-428.
42. Li, X., et al., *Identification of a specific region of Plasmodium falciparum EBL-1 that binds to host receptor glycophorin B and inhibits merozoite invasion in human red blood cells.* Molecular and Biochemical Parasitology, 2012. **183**(1): p. 23-31.
43. Lin, D.H., et al., *Crystal and Solution Structures of Plasmodium falciparum Erythrocyte-binding Antigen 140 Reveal Determinants of Receptor Specificity during Erythrocyte Invasion.* Journal of Biological Chemistry, 2012. **287**(44): p. 36830-36836.
44. Ord, R.L., et al., *Targeting Sialic Acid Dependent and Independent Pathways of Invasion in Plasmodium falciparum.* PLoS ONE, 2012. **7**(1): p. e30251.
45. Baldwin, M., et al., *Human erythrocyte Band 3 functions as a receptor for the sialic acid-independent invasion of Plasmodium falciparum. Role of the RhopH3-MSP1 complex.* Biochimica et biophysica acta, 2014. **1843**(12): p. 2855-2870.
46. Baum, J., et al., *Reticulocyte-binding protein homologue 5 – An essential adhesin involved in invasion of human erythrocytes by Plasmodium falciparum.* International Journal for Parasitology, 2009. **39**(3): p. 371-380.
47. Gaur, D., D.C.G. Mayer, and L.H. Miller, *Parasite ligand–host receptor interactions during invasion of erythrocytes by Plasmodium merozoites.* International Journal for Parasitology, 2004. **34**(13): p. 1413-1429.
48. Awandare, G.A., et al., *Plasmodium falciparum field isolates use complement receptor 1 (CR1) as a receptor for invasion of erythrocytes.* Molecular and biochemical parasitology, 2011. **177**(1): p. 57-60.
49. Crosnier, C., et al., *A Library of Functional Recombinant Cell-surface and Secreted P. falciparum Merozoite Proteins.* Molecular & Cellular Proteomics : MCP, 2013. **12**(12): p. 3976-3986.
50. Zenonos, Z.A., et al., *Basigin is a druggable target for host-oriented antimalarial interventions.* The Journal of Experimental Medicine, 2015. **212**(8): p. 1145-1151.
51. Douglas, Alexander D., et al., *A PfRH5-Based Vaccine Is Efficacious against Heterologous Strain Blood-Stage Plasmodium falciparum Infection in Aotus Monkeys.* Cell Host & Microbe, 2015. **17**(1): p. 130-139.
52. Patel, S.D., et al., *Plasmodium falciparum Merozoite Surface Antigen, PfRH5, Elicits Detectable Levels of Invasion-Inhibiting Antibodies in Humans.* The Journal of Infectious Diseases, 2013. **208**(10): p. 1679-1687.

53. Weaver, R., et al., *The association between naturally acquired IgG subclass specific antibodies to the PfRH5 invasion complex and protection from Plasmodium falciparum malaria.* Scientific Reports, 2016. **6**: p. 33094.
54. Srinivasan, P., et al., *Binding of Plasmodium merozoite proteins RON2 and AMA1 triggers commitment to invasion.* Proceedings of the National Academy of Sciences of the United States of America, 2011. **108**(32): p. 13275-13280.
55. Thomas, A.W., et al., *High Prevalence of Natural Antibodies against Plasmodium falciparum 83-Kilodalton Apical Membrane Antigen (PF83/AMA-1) as Detected by Capture-Enzyme-Linked Immunosorbent Assay Using Full-Length Baculovirus Recombinant PF83/AMA-1*. The American Journal of Tropical Medicine and Hygiene, 1994. **51**(6): p. 730-740.
56. Udhayakumar, V., et al., *Longitudinal study of natural immune responses to the Plasmodium falciparum apical membrane antigen (AMA-1) in a holoendemic region of malaria in western Kenya: Asembo Bay Cohort Project VIII.* The American journal of tropical medicine and hygiene, 2001. **65**(2): p. 100-107.
57. Thera, M.A., et al., *Safety and Immunogenicity of an AMA1 Malaria Vaccine in Malian Children: Results of a Phase 1 Randomized Controlled Trial.* PLoS ONE, 2010. **5**(2): p. e9041.
58. Thera, M.A., et al., *A Field Trial to Assess a Blood-Stage Malaria Vaccine.* The New England journal of medicine, 2011. **365**(11): p. 1004-1013.
59. Egan, E.S., et al., *A forward genetic screen identifies erythrocyte CD55 as essential for Plasmodium falciparum invasion ()*. Science (New York, N.Y.), 2015. **348**(6235): p. 711-714.
60. Haldar, K., et al., *Malaria: mechanisms of erythrocytic infection and pathological correlates of severe disease.* Annu Rev Pathol, 2007. **2**: p. 217-49.
61. G, M., *Die Malaria pernciosa.* Zentralbl. Bakteriol. Parasitenkd, 1902. **23**: p. 695–719.
62. Hanssen, E., et al., *Whole cell imaging reveals novel modular features of the exomembrane system of the malaria parasite, Plasmodium falciparum.* Int J Parasitol, 2010. **40**(1): p. 123-34.
63. Hanssen, E., *Electron tomography of the Maurer's cleft organelles of Plasmodium falciparum-infected erythrocytes reveals novel structural features.* Mol. Microbiol., 2008. **67**: p. 703-718.
64. Kulzer, S., et al., *Parasite-encoded Hsp40 proteins define novel mobile structures in the cytosol of the P. falciparum-infected erythrocyte.* Cell Microbiol, 2010. **12**(10): p. 1398-420.
65. Maier, A.G., *Exported proteins required for virulence and rigidity of Plasmodium falciparum-infected human erythrocytes.* Cell, 2008. **134**: p. 48-61.

66. Leech, J.H., et al., *Identification of a strain-specific malarial antigen exposed on the surface of Plasmodium falciparum-infected erythrocytes.* J Exp Med, 1984. **159**(6): p. 1567-75.
67. Gardner, M.J., et al., *Genome sequence of the human malaria parasite Plasmodium falciparum.* Nature, 2002. **419**(6906): p. 498-511.
68. Baruch, D.I., et al., *Cloning the P. falciparum gene encoding PfEMP1, a malarial variant antigen and adherence receptor on the surface of parasitized human erythrocytes.* Cell, 1995. **82**(1): p. 77-87.
69. Smith, J.D., *Switches in expression of Plasmodium falciparum var genes correlate with changes in antigenic and cytoadherent phenotypes of infected erythrocytes.* Cell, 1995. **82**: p. 101-110.
70. Su, X.Z., *The large diverse gene family var encodes proteins involved in cytoadherence and antigenic variation of Plasmodium falciparum-infected erythrocytes.* Cell, 1995. **82**: p. 89-100.
71. Arnot, D.E. and A.T. Jensen, *Antigenic Variation and the Genetics and Epigenetics of the PfEMP1 Erythrocyte Surface Antigens in Plasmodium falciparum Malaria.* Adv Appl Microbiol, 2011. **74**: p. 77-96.
72. Turner, L., et al., *Severe malaria is associated with parasite binding to endothelial protein C receptor.* Nature, 2013. **498**(7455): p. 502-505.
73. Kaul, D., et al., *Rosetting of Plasmodium falciparum-infected red blood cells with uninfected red blood cells enhances microvascular obstruction under flow conditions.* Blood, 1991. **78**(3): p. 812-819.
74. Leitgeb, A.M., et al., *Low Anticoagulant Heparin Disrupts Plasmodium falciparum Rosettes in Fresh Clinical Isolates.* The American Journal of Tropical Medicine and Hygiene, 2011. **84**(3): p. 390-396.
75. McMorran, B.J., et al., *Platelets Kill Intraerythrocytic Malarial Parasites and Mediate Survival to Infection.* Science, 2009. **323**(5915): p. 797-800.
76. Ahlborg, N., et al., *Plasmodium falciparum:Differential Parasite Growth Inhibition Mediated by Antibodies to the Antigens Pf332 and Pf155/RESA.* Experimental Parasitology, 1996. **82**(2): p. 155-163.
77. Raj, D.K., et al., *Antibodies to PfSEA-1 block parasite egress from RBCs and protect against malaria infection.* Science, 2014. **344**(6186): p. 871-877.
78. Pino, P., et al., *A multistage antimalarial targets the plasmepsins IX and X essential for invasion and egress.* Science, 2017. **358**(6362): p. 522-528.
79. Nasamu, A.S., et al., *Plasmepsins IX and X are essential and druggable mediators of malaria parasite egress and invasion.* Science, 2017. **358**(6362): p. 518-522.

80. Yazdani, S.S., et al., *Immune Responses to Asexual Blood-Stages of Malaria Parasites.* Current Molecular Medicine, 2006. **6**(2): p. 187-203.
81. Gomes, P.S., et al., *Immune escape strategies of malaria parasites.* Frontiers in microbiology, 2016. **7**: p. 1617.
82. Stevenson, M.M. and E.M. Riley, *Innate immunity to malaria.* Nature Reviews Immunology, 2004. **4**: p. 169.
83. Haque, A., et al., *Type I IFN signaling in CD8(–) DCs impairs Th1-dependent malaria immunity.* The Journal of Clinical Investigation, 2014. **124**(6): p. 2483-2496.
84. Artavanis-Tsakonas, K., J.E. Tongren, and E.M. Riley, *The war between the malaria parasite and the immune system: immunity, immunoregulation and immunopathology.* Clinical and Experimental Immunology, 2003. **133**(2): p. 145-152.
85. Kumaratilake, L., et al., *Effects of cytokines, complement, and antibody on the neutrophil respiratory burst and phagocytic response to Plasmodium falciparum merozoites.* Infection and immunity, 1992. **60**(9): p. 3731-3738.
86. Phillips, S., *Effector mechanisms against asexual erythrocytic stages of Plasmodium.* Immunology letters, 1994. **41**(2-3): p. 109-114.
87. Langhorne, J., et al., *Dendritic cells, pro-inflammatory responses, and antigen presentation in a rodent malaria infection.* Immunological reviews, 2004. **201**(1): p. 35-47.
88. Ing, R., et al., *Interaction of mouse dendritic cells and malaria-infected erythrocytes: uptake, maturation, and antigen presentation.* The Journal of Immunology, 2006. **176**(1): p. 441-450.
89. Lee, S., P. Crocker, and S. Gordon, *Macrophage plasma membrane and secretory properties in murine malaria. Effects of Plasmodium yoelii blood-stage infection on macrophages in liver, spleen, and blood.* Journal of Experimental Medicine, 1986. **163**(1): p. 54-74.
90. Deroost, K., et al., *Improved methods for haemozoin quantification in tissues yield organ-and parasite-specific information in malaria-infected mice.* Malaria journal, 2012. **11**(1): p. 166.
91. Krishnegowda, G., et al., *Induction of proinflammatory responses in macrophages by the glycosylphosphatidylinositols of Plasmodium falciparum cell signaling receptors, glycosylphosphatidylinositol (GPI) structural requirement, and regulation of GPI activity.* Journal of Biological Chemistry, 2005. **280**(9): p. 8606-8616.
92. Barrera, V., et al., *Host fibrinogen stably bound to hemozoin rapidly activates monocytes via TLR-4 and CD11b/CD18-integrin: a new paradigm of hemozoin action.* Blood, 2011: p. blood-2010-10-312413.
93. Su, Z., et al., *Opsonin-independent phagocytosis: an effector mechanism against acute blood-stage Plasmodium chabaudi AS infection.* The Journal of infectious diseases, 2002. **186**(9): p. 1321-1329.

94. Cramer, J.P., et al., *MyD88/IL-18-dependent pathways rather than TLRs control early parasitaemia in non-lethal Plasmodium yoelii infection.* Microbes and infection, 2008. **10**(12-13): p. 1259-1265.
95. Seixas, E., et al., *The interaction between DC and Plasmodium berghei/chabaudi-infected erythrocytes in mice involves direct cell-to-cell contact, internalization and TLR.* European journal of immunology, 2009. **39**(7): p. 1850-1863.
96. Arese, P., et al., *Recognition signals for phagocytic removal of favic malaria-infected and sickled erythrocytes,* in *Red Blood Cell Aging*. 1991, Springer. p. 317-327.
97. D'Ombrain, M.C., et al., *Association of Early Interferon-γ Production with Immunity to Clinical Malaria: A Longitudinal Study among Papua New Guinean Children.* Clinical Infectious Diseases, 2008. **47**(11): p. 1380-1387.
98. Angulo, I. and M. Fresno, *Cytokines in the Pathogenesis of and Protection against Malaria.* Clinical and Diagnostic Laboratory Immunology, 2002. **9**(6): p. 1145-1152.
99. Artavanis-Tsakonas, K., et al., *Activation of a Subset of Human NK Cells upon Contact with Plasmodium falciparum-Infected Erythrocytes.* The Journal of Immunology, 2003. **171**(10): p. 5396-5405.
100. Cruz, L.N., et al., *Tumor necrosis factor reduces Plasmodium falciparum growth and activates calcium signaling in human malaria parasites.* Biochimica et Biophysica Acta, 2016. **1860**(7): p. 1489-1497.
101. Coggeshall, L.T. and H.W. Kumm, *Demonstration of Passive Immunity in Experimental Monkey Malaria.* J Exp Med, 1937. **66**(2): p. 177-90.
102. Cohen, S., G.I. Mc, and S. Carrington, *Gamma-globulin and acquired immunity to human malaria.* Nature, 1961. **192**: p. 733-7.
103. McGregor, I.A., *The passive transfer of human malarial immunity.* Am J Trop Med Hyg, 1964. **13**: p. Suppl 237-9.
104. Langhorne, J., et al., *Immunity to malaria: more questions than answers.* Nat Immunol, 2008. **9**(7): p. 725-732.
105. Healer, J., C.Y. Chiu, and D.S. Hansen, *Mechanisms of naturally acquired immunity to P. falciparum and approaches to identify merozoite antigen targets.* Parasitology, 2017: p. 1-9.
106. Crompton, P.D., et al., *A prospective analysis of the Ab response to Plasmodium falciparum before and after a malaria season by protein microarray.* Proc Natl Acad Sci U S A, 2010. **107**(15): p. 6958-63.
107. Teo, A., et al., *Functional Antibodies and Protection against Blood-stage Malaria.* Trends Parasitol, 2016. **32**(11): p. 887-898.

108. Dobbs, K.R. and A.E. Dent, *Plasmodium malaria and antimalarial antibodies in the first year of life.* Parasitology, 2016. **143**(2): p. 129-38.
109. Fowkes, F.J., et al., *The relationship between anti-merozoite antibodies and incidence of Plasmodium falciparum malaria: A systematic review and meta-analysis.* PLoS Med, 2010. **7**(1): p. e1000218.
110. Reese, R.T. and M.R. Motyl, *Inhibition of the in vitro growth of Plasmodium falciparum. I. The effects of immune serum and purified immunoglobulin from owl monkeys.* J Immunol, 1979. **123**(4): p. 1894-9.
111. Stanley, H.A. and R.T. Reese, *In vitro inhibition of intracellular growth of Plasmodium falciparum by immune sera.* Am J Trop Med Hyg, 1984. **33**(1): p. 12-6.
112. Celada, A., A. Cruchaud, and L.H. Perrin, *Opsonic activity of human immune serum on in vitro phagocytosis of Plasmodium falciparum infected red blood cells by monocytes.* Clin Exp Immunol, 1982. **47**(3): p. 635-44.
113. Teo, A., et al., *A Robust Phagocytosis Assay to Evaluate the Opsonic Activity of Antibodies against Plasmodium falciparum-Infected Erythrocytes.* Methods Mol Biol, 2015. **1325**: p. 145-52.
114. Osier, F.H., et al., *Opsonic phagocytosis of Plasmodium falciparum merozoites: mechanism in human immunity and a correlate of protection against malaria.* BMC Med, 2014. **12**: p. 108.
115. Boyle, M.J., et al., *Human antibodies fix complement to inhibit Plasmodium falciparum invasion of erythrocytes and are associated with protection against malaria.* Immunity, 2015. **42**(3): p. 580-90.
116. Mugyenyi, C.K., et al., *Declining Malaria Transmission Differentially Impacts the Maintenance of Humoral Immunity to Plasmodium falciparum in Children.* J Infect Dis, 2017. **216**(7): p. 887-898.
117. Crompton, P.D., et al., *In vitro growth-inhibitory activity and malaria risk in a cohort study in mali.* Infect Immun, 2010. **78**(2): p. 737-45.
118. Dent, A.E., et al., *Antibody-mediated growth inhibition of Plasmodium falciparum: relationship to age and protection from parasitemia in Kenyan children and adults.* PLoS One, 2008. **3**(10): p. e3557.
119. Marsh, K., et al., *Antibodies to blood stage antigens of Plasmodium falciparum in rural Gambians and their relation to protection against infection.* Trans R Soc Trop Med Hyg, 1989. **83**(3): p. 293-303.
120. McCallum, F.J., et al., *Acquisition of growth-inhibitory antibodies against blood-stage Plasmodium falciparum.* PLoS One, 2008. **3**(10): p. e3571.

121. Chan, J.A., et al., *Patterns of protective associations differ for antibodies to P.falciparum-infected erythrocytes and merozoites in immunity against malaria in children.* Eur J Immunol, 2017.
122. Chotivanich, K., et al., *The Mechanisms of Parasite Clearance after Antimalarial Treatment of Plasmodium falciparum Malaria.* The Journal of Infectious Diseases, 2000. **182**(2): p. 629-633.
123. Djimde, A.A., et al., *Clearance of drug-resistant parasites as a model for protective immunity in Plasmodium falciparum malaria.* The American journal of tropical medicine and hygiene, 2003. **69**(5): p. 558-563.
124. White, N.J., *Malaria parasite clearance.* Malaria Journal, 2017. **16**: p. 88.
125. Khoury, D.S., et al., *Host-mediated impairment of parasite maturation during blood-stage Plasmodium infection.* Proceedings of the National Academy of Sciences, 2017. **114**(29): p. 7701-7706.
126. Chotivanich, K., et al., *Central role of the spleen in malaria parasite clearance.* J Infect Dis, 2002. **185**(10): p. 1538-41.
127. Engwerda, C.R., L. Beattie, and F.H. Amante, *The importance of the spleen in malaria.* Trends Parasitol, 2005. **21**(2): p. 75-80.
128. Couper, K.N., et al., *Macrophage-mediated but gamma interferon-independent innate immune responses control the primary wave of Plasmodium yoelii parasitemia.* Infection and immunity, 2007. **75**(12): p. 5806-5818.
129. Franke-Fayard, B., et al., *Murine malaria parasite sequestration: CD36 is the major receptor, but cerebral pathology is unlinked to sequestration.* Proc Natl Acad Sci U S A, 2005. **102**(32): p. 11468-73.
130. Stephens, R., R.L. Culleton, and T.J. Lamb, *The contribution of Plasmodium chabaudi to our understanding of malaria.* Trends in Parasitology, 2012. **28**(2): p. 73-82.
131. Amante, F.H. and M.F. Good, *Prolonged Th1-like response generated by a Plasmodium yoelii-specific T cell clone allows complete clearance of infection in reconstituted mice.* Parasite Immunol, 1997. **19**(3): p. 111-26.
132. Amante, F.H. and M.F. Good, *Prolonged Th1-like response generated by a Plasmodium yoelii-specific T cell clone allows complete clearance of infection in reconstituted mice.* Parasite Immunology, 1997. **19**(3): p. 111-126.
133. Su, Z., et al., *Vaccination with Novel Immunostimulatory Adjuvants against Blood-Stage Malaria in Mice.* Infection and Immunity, 2003. **71**(9): p. 5178-5187.

134. Khoury, D.S., et al., *Reduced erythrocyte susceptibility and increased host clearance of young parasites slows Plasmodium growth in a murine model of severe malaria.* Sci Rep, 2015. **5**: p. 9412.
135. Khoury, D.S., et al., *Effect of mature blood-stage Plasmodium parasite sequestration on pathogen biomass in mathematical and in vivo models of malaria.* Infect Immun, 2014. **82**(1): p. 212-20.
136. Aichele, P., et al., *Macrophages of the Splenic Marginal Zone Are Essential for Trapping of Blood-Borne Particulate Antigen but Dispensable for Induction of Specific T Cell Responses.* The Journal of Immunology, 2003. **171**(3): p. 1148-1155.
137. van Rooijen, N. and E. Hendrikx, *Liposomes for Specific Depletion of Macrophages from Organs and Tissues*, in *Liposomes: Methods and Protocols, Volume 1: Pharmaceutical Nanocarriers*, V. Weissig, Editor. 2010, Humana Press: Totowa, NJ. p. 189-203.
138. Pfander, C., et al., *A scalable pipeline for highly effective genetic modification of a malaria parasite.* Nat Meth, 2011. **8**(12): p. 1078-1082.
139. Gomes, A.R., et al., *A genome-scale vector resource enables high-throughput reverse genetic screening in a malaria parasite.* Cell Host Microbe, 2015. **17**(3): p. 404-13.
140. Ho, M., et al., *Splenic Fc receptor function in host defense and anemia in acute Plasmodium falciparum malaria.* Journal of Infectious Diseases, 1990. **161**(3): p. 555-561.
141. Looareesuwan, S., et al., *Dynamic alteration in splenic function during acute falciparum malaria.* New England Journal of Medicine, 1987. **317**(11): p. 675-679.
142. Chotivanich, K., et al., *Central role of the spleen in malaria parasite clearance.* Journal of Infectious Diseases, 2002. **185**(10): p. 1538-1541.
143. Angus, B.J., et al., *In Vivo Removal of Malaria Parasites From Red Blood Cells Without Their Destruction in Acute Falciparum Malaria.* Blood, 1997. **90**(5): p. 2037-2040.
144. Khoury, D.S., et al., *Host-mediated impairment of parasite maturation during blood-stage Plasmodium infection.* Proceedings of the National Academy of Sciences, 2017. **114**(29): p. 7701.
145. Renia, L., et al., *Cerebral malaria: mysteries at the blood-brain barrier.* Virulence, 2012. **3**(2): p. 193-201.
146. de Oca, M.M., C. Engwerda, and A. Haque, *Plasmodium berghei ANKA (PbA) infection of C57BL/6J mice: a model of severe malaria.* Methods in molecular biology (Clifton, N.J.), 2013. **1031**: p. 203-213.
147. Haque, A., et al., *High parasite burdens cause liver damage in mice following Plasmodium berghei ANKA infection independently of CD8(+) T cell-mediated immune pathology.* Infection and immunity, 2011. **79**(5): p. 1882-1888.

148. Chang, W.L., et al., *CD8(+)-T-cell depletion ameliorates circulatory shock in Plasmodium berghei-infected mice.* Infection and immunity, 2001. **69**(12): p. 7341-7348.
149. Lovegrove, F.E., et al., *Parasite burden and CD36-mediated sequestration are determinants of acute lung injury in an experimental malaria model.* PLoS pathogens, 2008. **4**(5): p. e1000068.
150. World Health Organization, *Severe falciparum malaria.* Transactions of the Royal Society of Tropical Medicine and Hygiene, 2000. **94**: p. S1-S90.
151. Dondorp, A.M., et al., *Estimation of the total parasite biomass in acute falciparum malaria from plasma PfHRP2.* PLoS medicine, 2005. **2**(8): p. e204.
152. Amaratunga, C., et al., *Artemisinin-resistant Plasmodium falciparum in Pursat province, western Cambodia: a parasite clearance rate study.* The Lancet infectious diseases, 2012. **12**(11): p. 851-858.
153. Ashley, E.A., et al., *Spread of artemisinin resistance in Plasmodium falciparum malaria.* New England Journal of Medicine, 2014. **371**(5): p. 411-423.
154. Group, W.P.C.S., *Baseline data of parasite clearance in patients with falciparum malaria treated with an artemisinin derivative: an individual patient data meta-analysis.* Malaria journal, 2015. **14**(1): p. 359.
155. Dogovski, C., et al., *Targeting the Cell Stress Response of Plasmodium falciparum to Overcome Artemisinin Resistance.* PLoS Biology, 2015. **13**(4): p. e1002132.
156. Hastings, I.M., K. Kay, and E.M. Hodel, *How robust are malaria parasite clearance rates as indicators of drug effectiveness and resistance?* Antimicrobial agents and chemotherapy, 2015. **59**(10): p. 6428-6436.
157. Wilson, D.W., et al., *Defining the Timing of Action of Antimalarial Drugs against Plasmodium falciparum.* Antimicrobial Agents and Chemotherapy, 2013. **57**(3): p. 1455-1467.
158. Dondorp, A.M., et al., *Artemisinin Resistance in Plasmodium falciparum Malaria.* New England Journal of Medicine, 2009. **361**(5): p. 455-467.
159. Nosten, F., et al., *Effects of artesunate-mefloquine combination on incidence of Plasmodium falciparum malaria and mefloquine resistance in western Thailand: a prospective study.* The Lancet, 2000. **356**(9226): p. 297-302.
160. Nosten, F. and N.J. White, *Artemisinin-based combination treatment of falciparum malaria.* The American journal of tropical medicine and hygiene, 2007. **77**(6_Suppl): p. 181-192.
161. Sowunmi, A. and A.M.J. Oduola, *Comparative efficacy of chloroquine/chlorpheniramine combination and mefloquine for the treatment of chloroquine-resistant Plasmodium*

falciparum malaria in Nigerian children. Transactions of The Royal Society of Tropical Medicine and Hygiene, 1997. **91**(6): p. 689-693.

162. Okoyeh, J.N., et al., *Responses of multidrug-resistant Plasmodium falciparum parasites to mefloquine in Nigerian children.* Tropical Medicine & International Health, 1997. **2**(4): p. 319-324.
163. Agomo, P.U., et al., *Efficacy, safety and tolerability of artesunate-mefloquine in the treatment of uncomplicated Plasmodium falciparum malaria in four geographic zones of Nigeria.* Malaria journal, 2008. **7**(1): p. 172.
164. Haque, A., et al., *High Parasite Burdens Cause Liver Damage in Mice following Plasmodium berghei ANKA Infection Independently of CD8(+) T Cell-Mediated Immune Pathology.* Infection and Immunity, 2011. **79**(5): p. 1882-1888.
165. Baptista, F.G., et al., *Accumulation of Plasmodium berghei-Infected Red Blood Cells in the Brain Is Crucial for the Development of Cerebral Malaria in Mice.* Infection and Immunity, 2010. **78**(9): p. 4033-4039.
166. Jauréguiberry, S., *Splenic pitting of the red blood cells during severe malaria treated with artemisinin*. 2015.
167. Portillo, H.A.d., et al., *The role of the spleen in malaria.* Cellular Microbiology, 2012. **14**(3): p. 343-355.
168. Looareesuwan, S., et al., *Malaria in Splenectomized Patients: Report of Four Cases and Review.* Clinical Infectious Diseases, 1993. **16**(3): p. 361-366.
169. Oster, C.N., L.C. Koontz, and D.J. Wyler, *Malaria in Asplenic Mice: Effects of Splenectomy, Congenital Asplenia, and Splenic Reconstitution on the Course of Infection**. The American Journal of Tropical Medicine and Hygiene, 1980. **29**(6): p. 1138-1142.
170. Grun, J.L., C.A. Long, and W.P. Weidanz, *Effects of splenectomy on antibody-independent immunity to Plasmodium chabaudi adami malaria.* Infection and Immunity, 1985. **48**(3): p. 853-858.
171. Sayles, P.C., D.M. Yanez, and D.L. Wassom, *Plasmodium yoelii: Splenectomy Alters the Antibody Responses of Infected Mice.* Experimental Parasitology, 1993. **76**(4): p. 377-384.
172. Patel, S.N., et al., *CD36 Mediates the Phagocytosis of Plasmodium falciparum–Infected Erythrocytes by Rodent Macrophages.* The Journal of Infectious Diseases, 2004. **189**(2): p. 204-213.
173. Day, N., et al., *Clearance kinetics of parasites and pigment-containing leukocytes in severe malaria.* Blood, 1996. **88**(12): p. 4694-4700.

174. Douglas, A.D., et al., *Comparison of Modeling Methods to Determine Liver-to-blood Inocula and Parasite Multiplication Rates During Controlled Human Malaria Infection.* The Journal of Infectious Diseases, 2013. **208**(2): p. 340-345.
175. Roca-Feltrer, A., et al., *The age patterns of severe malaria syndromes in sub-Saharan Africa across a range of transmission intensities and seasonality settings.* Malaria journal, 2010. **9**(1): p. 282.
176. Doolan, D.L., C. Dobaño, and J.K. Baird, *Acquired Immunity to Malaria.* Clinical Microbiology Reviews, 2009. **22**(1): p. 13-36.
177. Pinkevych, M., et al., *Decreased Growth Rate of P. falciparum Blood Stage Parasitemia With Age in a Holoendemic Population.* The Journal of Infectious Diseases, 2014. **209**(7): p. 1136-1143.
178. Molineaux, L., et al., *Malaria therapy reinoculation data suggest individual variation of an innate immune response and independent acquisition of antiparasitic and antitoxic immunities.* Transactions of The Royal Society of Tropical Medicine and Hygiene, 2002. **96**(2): p. 205-209.
179. Metcalf, C.J.E., et al., *Partitioning Regulatory Mechanisms of Within-Host Malaria Dynamics Using the Effective Propagation Number.* Science, 2011. **333**(6045): p. 984.
180. Khoury, D.S., et al., *Reduced erythrocyte susceptibility and increased host clearance of young parasites slows Plasmodium growth in a murine model of severe malaria.* Scientific Reports, 2015. **5**: p. 9412.
181. Quinn, T.C. and D.J. Wyler, *Intravascular Clearance of Parasitized Erythrocytes in Rodent Malaria.* Journal of Clinical Investigation, 1979. **63**(6): p. 1187-1194.
182. Cheng, Q., D.E. Kyle, and M.L. Gatton, *Artemisinin resistance in Plasmodium falciparum: A process linked to dormancy?* International Journal for Parasitology, Drugs and Drug Resistance, 2012. **2**: p. 249-255.
183. White, N.J., *Preventing antimalarial drug resistance through combinations.* Drug Resistance Updates, 1998. **1**(1): p. 3-9.
184. White, N., *Antimalarial drug resistance and combination chemotherapy.* Philosophical Transactions of the Royal Society B: Biological Sciences, 1999. **354**(1384): p. 739-749.
185. Giao, P.T., et al., *Artemisinin for treatment of uncomplicated falciparum malaria: is there a place for monotherapy?* The American journal of tropical medicine and hygiene, 2001. **65**(6): p. 690-695.
186. Frey, S.G., et al., *Artesunate-mefloquine combination therapy in acute Plasmodium falciparum malaria in young children: a field study regarding neurological and neuropsychiatric safety.* Malaria Journal, 2010. **9**: p. 291-291.

187. Safeukui, I., et al., *Retention of Plasmodium falciparum ring-infected erythrocytes in the slow, open microcirculation of the human spleen.* Blood, 2008. **112**(6): p. 2520.

188. Buffet, P.A., et al., *Ex vivo perfusion of human spleens maintains clearing and processing functions.* Blood, 2006. **107**(9): p. 3745.

189. Haque, A., et al., *High Parasite Burdens Cause Liver Damage in Mice following Plasmodium berghei ANKA Infection Independently of CD8+ T Cell-Mediated Immune Pathology.* Infection and Immunity, 2011. **79**(5): p. 1882-1888.

190. Terkawi, M.A., et al., *Depletion of Phagocytic Cells during Nonlethal Plasmodium yoelii Infection Causes Severe Malaria Characterized by Acute Renal Failure in Mice.* Infection and Immunity, 2016. **84**(3): p. 845-855.

191. Mok, S., et al., *Population transcriptomics of human malaria parasites reveals the mechanism of artemisinin resistance.* Science (New York, N.Y.), 2015. **347**(6220): p. 431-435.

192. Codd, A., et al., *Artemisinin-induced parasite dormancy: a plausible mechanism for treatment failure.* Malaria Journal, 2011. **10**(1): p. 56.

193. Bao, Y., et al., *Identification of IFN-γ-producing innate B cells.* Cell Research, 2014. **24**(2): p. 161-176.

194. Freeman, B.E., et al., *Regulation of innate CD8(+) T-cell activation mediated by cytokines.* Proceedings of the National Academy of Sciences of the United States of America, 2012. **109**(25): p. 9971-9976.

195. Kelly-Scumpia, K.M., et al., *B cells enhance early innate immune responses during bacterial sepsis.* The Journal of Experimental Medicine, 2011. **208**(8): p. 1673-1682.

196. Haque, A., et al., *Granzyme B Expression by CD8⁺ T Cells Is Required for the Development of Experimental Cerebral Malaria.* The Journal of Immunology, 2011. **186**(11): p. 6148-6156.

197. Cohen, S., I.A. McGregor, and S. Carrington, *Gamma-Globulin and Acquired Immunity to Human Malaria.* Nature, 1961. **192**: p. 733.

198. Khoury, D.S., et al., *Host-mediated impairment of parasite maturation during blood-stage Plasmodium infection.* Proc Natl Acad Sci U S A, 2017. **114**(29): p. 7701-7706.

199. Khoury, D.S., et al., *Characterising the effect of antimalarial drugs on the maturation and clearance of murine blood-stage Plasmodium parasites in vivo.* Int J Parasitol, 2017.

200. Butler, N.S., et al., *Therapeutic blockade of PD-L1 and LAG-3 rapidly clears established blood-stage Plasmodium infection.* Nat Immunol, 2012. **13**(2): p. 188-95.

201. Sebina, I., et al., *IL-6 promotes CD4+ T-cell and B-cell activation during Plasmodium infection.* Parasite Immunol, 2017. **39**(10).

202. Sebina, I., et al., *IFNAR1-Signalling Obstructs ICOS-mediated Humoral Immunity during Non-lethal Blood-Stage Plasmodium Infection.* PLoS Pathog, 2016. **12**(11): p. e1005999.
203. Cunningham, D.A., et al., *Host immunity modulates transcriptional changes in a multigene family (yir) of rodent malaria.* Mol Microbiol, 2005. **58**(3): p. 636-47.
204. Spencer Valero, L.M., et al., *Passive immunization with antibodies against three distinct epitopes on Plasmodium yoelii merozoite surface protein 1 suppresses parasitemia.* Infect Immun, 1998. **66**(8): p. 3925-30.
205. Hirunpetcharat, C., et al., *Complete protective immunity induced in mice by immunization with the 19-kilodalton carboxyl-terminal fragment of the merozoite surface protein-1 (MSP1[19]) of Plasmodium yoelii expressed in Saccharomyces cerevisiae: correlation of protection with antigen-specific antibody titer, but not with effector CD4+ T cells.* J Immunol, 1997. **159**(7): p. 3400-11.
206. Sebina, I., et al., *IFNAR1-Signalling Obstructs ICOS-mediated Humoral Immunity during Non-lethal Blood-Stage Plasmodium Infection.* PLOS Pathogens, 2016. **12**(11): p. e1005999.
207. Hodder, A.N., P.E. Crewther, and R.F. Anders, *Specificity of the Protective Antibody Response to Apical Membrane Antigen 1.* Infection and Immunity, 2001. **69**(5): p. 3286-3294.
208. Wilson, D.W., et al., *Quantifying the Importance of MSP1-19 as a Target of Growth-Inhibitory and Protective Antibodies against Plasmodium falciparum in Humans.* PLOS ONE, 2011. **6**(11): p. e27705.
209. Boyle, Michelle J., et al., *Human Antibodies Fix Complement to Inhibit Plasmodium falciparum Invasion of Erythrocytes and Are Associated with Protection against Malaria.* Immunity, 2015. **42**(3): p. 580-590.
210. Pepys, M.B., *Role of complement in induction of antibody production in vivo : effect of cobra factor and other c3-reactive agents on thymus-dependent and thymus-independent antibody responses.* The Journal of Experimental Medicine, 1974. **140**(1): p. 126-145.
211. James, K.R., et al., *IFN Regulatory Factor 3 Balances Th1 and T Follicular Helper Immunity during Nonlethal Blood-Stage Plasmodium Infection.* The Journal of Immunology, 2018. **200**(4): p. 1443.
212. Khoury, D.S., et al., *Characterising the effect of antimalarial drugs on the maturation and clearance of murine blood-stage Plasmodium parasites in vivo.* International Journal for Parasitology, 2017. **47**(14): p. 913-922.
213. Bouharoun-Tayoun, H., et al., *Mechanisms underlying the monocyte-mediated antibody-dependent killing of Plasmodium falciparum asexual blood stages.* The Journal of Experimental Medicine, 1995. **182**(2): p. 409.

214. Boyle, M.J., et al., *Human Antibodies Fix Complement to Inhibit Plasmodium falciparum Invasion of Erythrocytes and¬†Are Associated with Protection against Malaria.* Immunity, 2015. **42**(3): p. 580-590.

215. Boyle, M.J., et al., *Isolation of viable Plasmodium falciparum merozoites to define erythrocyte invasion events and advance vaccine and drug development.* Proceedings of the National Academy of Sciences of the United States of America, 2010. **107**(32): p. 14378-14383.

216. Ong, G.L. and M.J. Mattes, *Mouse strains with typical mammalian levels of complement activity.* Journal of Immunological Methods, 1989. **125**(1): p. 147-158.

217. Taylor, P.R., et al., *Complement Contributes to Protective Immunity against Reinfection by Plasmodium chabaudi chabaudi Parasites.* Infection and Immunity, 2001. **69**(6): p. 3853-3859.

218. Riley, E.M. and V.A. Stewart, *Immune mechanisms in malaria: new insights in vaccine development.* Nature Medicine, 2013. **19**: p. 168.

219. Teo, A., et al., *Functional Antibodies and Protection against Blood-stage Malaria.* Trends in Parasitology, 2016. **32**(11): p. 887-898.

220. Cunningham, D.A., et al., *Host immunity modulates transcriptional changes in a multigene family (yir) of rodent malaria.* Molecular Microbiology, 2005. **58**(3): p. 636-647.

221. Spencer Valero, L.M., et al., *Passive Immunization with Antibodies against Three Distinct Epitopes on Plasmodium yoelii Merozoite Surface Protein 1 Suppresses Parasitemia.* Infection and Immunity, 1998. **66**(8): p. 3925-3930.

222. Jo-Anne, C., et al., *Patterns of protective associations differ for antibodies to P. falciparum-infected erythrocytes and merozoites in immunity against malaria in children.* European Journal of Immunology, 2017. **47**(12): p. 2124-2136.

223. Matz, J.M., et al., *In Vivo Function of PTEX88 in Malaria Parasite Sequestration and Virulence.* Eukaryotic Cell, 2015. **14**(6): p. 528-534.

224. Cheng, Q., et al., *stevor and rif are Plasmodium falciparum multicopy gene families which potentially encode variant antigens.* Mol Biochem Parasitol, 1998. **97**(1-2): p. 161-76.

225. Winter, G., et al., *SURFIN is a polymorphic antigen expressed on Plasmodium falciparum merozoites and infected erythrocytes.* J Exp Med, 2005. **201**(11): p. 1853-63.

226. Culvenor, J.G., K.P. Day, and R.F. Anders, *Plasmodium falciparum ring-infected erythrocyte surface antigen is released from merozoite dense granules after erythrocyte invasion.* Infect Immun, 1991. **59**(3): p. 1183-7.

227. Pasloske, B.L., et al., *Cloning and characterization of a Plasmodium falciparum gene encoding a novel high-molecular weight host membrane-associated protein, PfEMP3.* Mol Biochem Parasitol, 1993. **59**(1): p. 59-72.

228. Kyes, S.A., et al., *Rifins: a second family of clonally variant proteins expressed on the surface of red cells infected with Plasmodium falciparum.* Proc Natl Acad Sci U S A, 1999. **96**(16): p. 9333-8.

229. Otto, T.D., et al., *A comprehensive evaluation of rodent malaria parasite genomes and gene expression.* BMC Biol, 2014. **12**: p. 86.

230. Matz, J.M., et al., *In Vivo Function of PTEX88 in Malaria Parasite Sequestration and Virulence.* Eukaryot Cell, 2015. **14**(6): p. 528-34.

231. Pasini, E.M., et al., *Proteomic and genetic analyses demonstrate that Plasmodium berghei blood stages export a large and diverse repertoire of proteins.* Mol Cell Proteomics, 2013. **12**(2): p. 426-48.

232. Schwach, F., et al., *PlasmoGEM, a database supporting a community resource for large-scale experimental genetics in malaria parasites.* Nucleic Acids Res, 2015. **43**(Database issue): p. D1176-82.

233. Gomes, Ana R., et al., *A Genome-Scale Vector Resource Enables High-Throughput Reverse Genetic Screening in a Malaria Parasite.* Cell Host & Microbe, 2015. **17**(3): p. 404-413.

234. Pasini, E.M., et al., *Proteomic and Genetic Analyses Demonstrate that Plasmodium berghei Blood Stages Export a Large and Diverse Repertoire of Proteins.* Molecular & Cellular Proteomics : MCP, 2013. **12**(2): p. 426-448.

235. Augustijn, K.D., et al., *Functional Characterization of the Plasmodium falciparum and P. berghei Homologues of Macrophage Migration Inhibitory Factor.* Infection and Immunity, 2007. **75**(3): p. 1116-1128.

236. De Niz, M., et al., *The machinery underlying malaria parasite virulence is conserved between rodent and human malaria parasites.* Nature Communications, 2016. **7**: p. 11659.

237. Tomas, A.M., et al., *P25 and P28 proteins of the malaria ookinete surface have multiple and partially redundant functions.* EMBO J, 2001. **20**(15): p. 3975-83.

238. Dessens, J.T., et al., *SOAP, a novel malaria ookinete protein involved in mosquito midgut invasion and oocyst development.* Mol Microbiol, 2003. **49**(2): p. 319-29.

239. van Dijk, M.R., et al., *Three members of the 6-cys protein family of Plasmodium play a role in gamete fertility.* PLoS Pathog, 2010. **6**(4): p. e1000853.

240. Spaccapelo, R., et al., *Plasmepsin 4-deficient Plasmodium berghei are virulence attenuated and induce protective immunity against experimental malaria.* Am J Pathol, 2010. **176**(1): p. 205-17.

241. Oppenheim, R.D., et al., *BCKDH: the missing link in apicomplexan mitochondrial metabolism is required for full virulence of Toxoplasma gondii and Plasmodium berghei.* PLoS Pathog, 2014. **10**(7): p. e1004263.

242. Chisholm, S.A., et al., *Contrasting Inducible Knockdown of the Auxiliary PTEX Component PTEX88 in P. falciparum and P. berghei Unmasks a Role in Parasite Virulence.* PLOS ONE, 2016. **11**(2): p. e0149296.

243. Elsworth, B., et al., *PTEX is an essential nexus for protein export in malaria parasites.* Nature, 2014. **511**(7511): p. 587-91.

244. Aogo, R.A., et al., *Quantification of host-mediated parasite clearance during blood-stage Plasmodium infection and anti-malarial drug treatment in mice.* International Journal for Parasitology, 2018.

245. A., C.S., et al., *The malaria PTEX component PTEX88 interacts most closely with HSP101 at the host–parasite interface.* The FEBS Journal, 2018. **285**(11): p. 2037-2055.

246. Schwach, F., et al., *PlasmoGEM, a database supporting a community resource for large-scale experimental genetics in malaria parasites.* Nucleic Acids Research, 2015. **43**(Database issue): p. D1176-D1182.

247. Hall, N., et al., *A comprehensive survey of the Plasmodium life cycle by genomic, transcriptomic, and proteomic analyses.* Science, 2005. **307**(5706): p. 82-6.

248. Acharya, P., et al., *Host–Parasite Interactions in Human Malaria: Clinical Implications of Basic Research.* Frontiers in Microbiology, 2017. **8**: p. 889.

249. Langhorne, J. and P.E. Duffy, *Expanding the antimalarial toolkit: Targeting host–parasite interactions.* The Journal of Experimental Medicine, 2016. **213**(2): p. 143-153.

250. Amante, F.H., et al., *Immune-Mediated Mechanisms of Parasite Tissue Sequestration during Experimental Cerebral Malaria.* The Journal of Immunology, 2010. **185**(6): p. 3632.

251. Celada, A., A. Cruchaud, and L.H. Perrin, *Opsonic activity of human immune serum on in vitro phagocytosis of Plasmodium falciparum infected red blood cells by monocytes.* Clinical and Experimental Immunology, 1982. **47**(3): p. 635-644.

252. Teo, A., et al, *A Robust Phagocytosis Assay to Evaluate the Opsonic Activity of Antibodies against Plasmodium falciparum-Infected Erythrocytes.* Methods Mol Biol, 2015(1325): p. p. 145-52.

253. Haase, S. and T.F. de Koning-Ward, *New insights into protein export in malaria parasites.* Cellular Microbiology, 2010. **12**(5): p. 580-587.

254. Batinovic, S., et al., *An exported protein-interacting complex involved in the trafficking of virulence determinants in Plasmodium-infected erythrocytes.* Nature Communications, 2017. **8**: p. 16044.